

DISSERTATION

**ECOLOGICAL RESPONSE OF LOWER TROPHIC LEVELS TO
EPISODIC TYPHOONS IN TEMPERATE COASTAL WATERS**

2014

SOKA UNIVERSITY

GRADUATE SCHOOL OF ENGINEERING

KENJI TSUCHIYA

ECOLOGICAL RESPONSE OF LOWER TROPHIC
LEVELS TO EPISODIC TYPHOONS IN TEMPERATE
COASTAL WATERS

MARCH 2014

KENJI TSUCHIYA

SOKA UNIVERSITY

Author: Kenji Tsuchiya

Title: Ecological response of lower trophic levels to episodic typhoons in temperate coastal waters

Department: Environmental Engineering for Symbiosis

Faculty: Engineering

Degree: Ph.D.

Convocation: March 2014

Permission is herewith granted to Soka University to circulate and copy for non-commercial purposes, at its discretion, the above title request of individuals or institutions.

We certify that we have read this dissertation and that, in our opinion, it is satisfactory in scope and quality as a dissertation for the degree of Doctor of Philosophy in Engineering.

February 2014

DISSERTATION COMMITTEE

Prof. Dr. Tatsuki Toda

Prof. Dr. Norio Kurosawa

Prof. Dr. Tomohiko Kikuchi

Contents

	page
ACKNOWLEDGEMENTS	i
ABSTRACT	ii
LIST OF TABLES	iv
LIST OF FIGURES	v
Chapter I General introduction	1
Table	7
Figure	9
Chapter II Responses of phytoplankton and bacteria to the passage of typhoons at inshore waters in Sagami Bay, Japan	10
2.1. Introduction	10
2.2. Materials and methods	12
2.2.1. Typhoons investigated in the present study	12
2.2.2. Study site, sampling procedures and analytical methods	13
2.2.3. Statistical analysis	16
2.3. Results	16
2.3.1. Meteorological and physical parameters, and nutrient stoichiometry	16
2.3.2. Primary production and bacterial production	19
2.3.3. Chl <i>a</i> concentration, ratio of POC to chl <i>a</i> concentration, bacterial abundance and ratio of bacterial abundance to chl <i>a</i> concentration	19
2.3.4. Phytoplankton assemblage	21
2.4. Discussion	22
Table	29
Figures	30

Chapter III	Vertical and temporal variations of phytoplankton, and microbial processes below the euphotic zone after the passage of typhoon at offshore waters in Sagami Bay, Japan	40
3.1.	Introduction	40
3.2.	Materials and methods	41
3.2.1.	Typhoon investigated in the present study	41
3.2.2.	Study site, sampling procedures and analytical methods	41
3.3.	Results	44
3.3.1.	Meteorological and optical parameters	44
3.3.2.	Physical and chemical parameters	44
3.3.3.	Bacterial abundance and bacterial production	45
3.3.4.	Chl <i>a</i> concentration, pheopigment concentration, POC and primary production	45
3.3.5.	Phytoplankton assemblage	46
3.4.	Discussion	47
	Figures	52
Chapter IV	General discussion	61
	Figures	66
REFERENCES		71

ACKNOWLEDGEMENTS

I am eternally grateful to my supervisor Professor Tatsuki Toda for his numerous support and guidance throughout the course of this study and for help rendered in the completion of this dissertation. I would like to gratefully acknowledge Professor Norio Kurosawa for his critical review, tremendous corrections and comments to improve and polish the dissertation. I am also deeply thankful to my co-supervisor Professor Tomohiko Kikuchi of Yokohama National University for his support to conduct this research in Sagami Bay and suggestions regarding the present study.

I express my sincere appreciation to Dr. Hideo Miyaguchi for his tremendous support and encouragement in countless ways throughout this study. I thank Drs. Norio Nagao, Tomoko Yoshiki and Ryota Nakajima for their valuable comments on this study and Professor Koji Hamasaki, Drs. Akio Imai, Tadafumi Ichikawa and Yuya Tada for their technical support. Thanks are also due to Izumi Funahashi, Tomoko Okashita, Masako Mitsudera and Sayaka Hirose, secretaries of Professor Toda, and all the colleagues of my laboratory for their supports throughout this study.

Finally, my deepest gratitude and appreciation goes to my parent, Teruyoshi Tsuchiya and Keiko Tsuchiya, for their encouragement and endless supports throughout my life. I am also grateful to the founder of Soka University: Dr. Daisaku Ikeda for his encouragement throughout my school life.

ABSTRACT

Variations of physical-chemical environments and responses of lower trophic levels accompanied by the passage of typhoons were examined at Manazuru Port (5 m depth) and Manazuru fixed offshore station (120 m depth) in the temperate coastal waters of Sagami Bay, Japan. Daily samplings were conducted at Manazuru Port during the passage of typhoons *Mawar* in 2005, *Sinlaku* in 2008, *Etau* in 2009 and *Malou* in 2010, and Manazuru fixed offshore station during the passage of typhoon *Malou* in 2010. After the passage of typhoons, salinity abruptly decreased, and inorganic macronutrient concentrations significantly increased. Nutrients were loaded by upwelling and terrestrial runoff during *Mawar*, and by terrestrial runoff during *Sinlaku*, *Etau* and *Malou*. Bacterial production showed a maximum just after the passage of typhoon, and exceeded 1.5-fold compared to primary production. On the other hand, primary production reached maximums three to five days after the passage of typhoons, and showed 10-fold value compared to bacterial production at the maximum of primary production. Relatively high dominances of dinoflagellates in phytoplankton communities just after the passage of typhoons, and then diatoms dominated the phytoplankton communities with increases in phytoplankton biomass. In the diatom communities, *Skeletonema* spp. during *Mawar* and *Chaetoceros* spp. during *Sinlaku*, *Etau* and *Malou* dominated. Dominances of *Skeletonema* spp. and *Chaetoceros* spp. were significantly correlated to N/P ratio positively and negatively, respectively ($p < 0.05$). The results suggest that the proportional contribution of nutrient sources, which determines nutrient stoichiometry, is an important factor in controlling phytoplankton community succession after the passage of typhoons. In the next study, temporal and vertical investigation at Manazuru fixed offshore station was conducted after the passage of *Malou* in order to clarify the mechanism of succession from dinoflagellates to diatoms and effects of typhoon passage on chemical-biological process below the euphotic zone. At the offshore station, dinoflagellates accumulated at the surface, while diatoms were distributed at the subsurface just after the passage of *Malou*. Four days after the passage of *Malou*, diatoms increased and dominated the phytoplankton community in the whole water column including below the euphotic zone,

verifying that dinoflagellates reflected swim strategy; diatoms reflected sink strategy. Below the euphotic zone, bacterial abundance and ammonium concentrations increased, and exhibited significantly positive correlation between them ($p < 0.001$), which suggested that bacterial ammonium regeneration progressed. Therefore, episodic typhoons play an important and significant role to enhance biological productions and the biochemical response within the water column is relatively fast after typhoon passage.

LIST OF TABLES

	page
Table 1-1 Summary of chlorophyll <i>a</i> (Chl <i>a</i>) concentration and primary production before and after typhoon passages	7
Table 1-2 Summary of bacterial abundance and bacterial production before and after typhoon passages	8
Table 2-1 Major phytoplankton species in the pre- and post-typhoon passage (B: Before typhoon, A: After typhoon)	29

LIST OF FIGURES

	Page
Figure 1-1 Number of typhoons approaching Japan excluding Okinawa Islands	10
Figure 2-1 Typhoon tracks and sampling area. Circles, triangles, squares and diamond shapes represents <i>Mawar</i> , <i>Sinlaku</i> , <i>Etau</i> and <i>Malou</i> passages, respectively, and each symbol shows the location at 3 am (Data obtained from the Japan Meteorological Agency). Solid lines and dashed lines show typhoons and tropical depression (including extratropical cyclone), respectively	30
Figure 2-2 Temporal variations in wind speed, precipitation, water temperature, salinity, NO_2+NO_3 , PO_4 , $\text{Si}(\text{OH})_4$ and N/P ratio in (a-h) <i>Mawar</i> , (i-p) <i>Sinlaku</i> , (q-x) <i>Etau</i> and (y-af) <i>Malou</i> . Dashed lines and gray shadows indicate the background data (non-typhoon) and the standard deviations, respectively	31
Figure 2-3 Temporal variations in (a) primary production and (b) ratio of primary production to chlorophyll <i>a</i> concentration (PP/Chl <i>a</i> ratio) during <i>Mawar</i>	33
Figure 2-4 Temporal variations in (a) primary production, (b) ratio of primary production to chlorophyll <i>a</i> (PP/Chl <i>a</i> ratio), (c) bacterial production, (d) ratio of bacterial production to bacterial abundance (BP/BA ratio) and (e) ratio of bacterial production to primary production (BP/PP ratio) during <i>Malou</i>	34
Figure 2-5 Temporal variations in chlorophyll <i>a</i> concentration (Chl <i>a</i>), ratio of particulate organic carbon to chl <i>a</i> (POC/Chl <i>a</i> ratio), bacterial abundance and ratio of bacterial abundance to chl <i>a</i> (BA/Chl <i>a</i> ratio) in (a-d) <i>Mawar</i> , (e-h) <i>Sinlaku</i> , (i-l) <i>Etau</i> and (m-p) <i>Malou</i> . Dashed lines and gray shadows indicate the background data (non-typhoon) and the standard deviations, respectively	35
Figure 2-6 Temporal variations in phytoplankton biomass, relative abundance, and relative diatom and dinoflagellate abundance in (a-c) <i>Mawar</i> , (d-f) <i>Sinlaku</i> , (g-i) <i>Etau</i> and (j-l) <i>Malou</i>	36
Figure 2-7 Temporal variations in residual of ratio of bacterial abundance to chlorophyll <i>a</i> concentration (BA/Chl <i>a</i> ratio) between observed and estimated BA/Chl <i>a</i> ratios in (a) <i>Mawar</i> , (b) <i>Sinlaku</i> , (c) <i>Etau</i> and (d) <i>Malou</i> . The estimated	

BA/Chl *a* ratio was calculated using the equation ($\log [\text{BA; cell mL}^{-1}] = 5.96 + 0.524 \times \log [\text{Chl } a; \text{ mg m}^{-3}]$) derived from Cole et al. (1988) 37

Figure 2-8 Temporal variations in ratio of mixo- and heterotrophic phytoplankton carbon biomass to autotrophic phytoplankton carbon biomass (H/A ratio) in (a) *Mawar*, (b) *Sinlaku*, (c) *Etau* and (d) *Malou* 38

Figure 2-9 Relationships between (a) Diatom proportion in total biomass and total biomass, (b) proportion of *Skeletonema* + *Chaetoceros* in diatom biomass and diatom biomass, (c) proportion of *Skeletonema* in total biomass and N/P ratio, and (d) proportion of *Chaetoceros* in total biomass and N/P ratio. The regression curves were (a) [Diatom proportion] = $0.31 + 0.084 * \ln [\text{Total biomass}]$ ($n = 33, r = 0.39, p < 0.05$), (b) [*Skeletonema* + *Chaetoceros* / diatom biomass] = $0.92 * [\text{diatom biomass}] / (15 + [\text{diatom biomass}]$ ($n = 17, r = 0.75, p < 0.001$), (c) $\log (\theta / (1 - \theta)) = 3.94 \times [\text{N/P}] / ([\text{N/P}] + 17.8) - 1.03$ ($n = 16, r = 0.65, p < 0.05; \theta = 1 - \text{dominance of } \textit{Skeletonema} \text{ spp.}$) and (d) $\log (\theta / (1 - \theta)) = 3.00 \times [\text{N/P}] / ([\text{N/P}] + 15.4) - 1.81$ ($n = 16, r = 0.60, p < 0.05; \theta = \text{dominance of } \textit{Chaetoceros} \text{ spp.}$). Date of (b) whose total dominance of *Skeletonema* spp. and *Chaetoceros* spp. in the diatom community exhibited more than 50% was used for analyses of (c) and (d) 39

Figure 3-1 Typhoon tracks and sampling area. Circles, triangles, squares and cross marks represents *Mawar*, *Sinlaku*, *Etau* and *Malou* passages, respectively, and each symbol shows the location at 3 am (Data obtained from the Japan Meteorological Agency). Solid lines and dashed lines show typhoons and extratropical cyclone, respectively 52

Figure 3-2 Temporal variations in diffuse attenuation coefficient at PAR (K_d) and euphotic depth. Closed and open circles represent K_d and euphotic depth, respectively 53

Figure 3-3 Temporal and vertical variations in (a) water temperature ($^{\circ}\text{C}$), (b) salinity, (c) density σ_t , (d) $\text{NO}_2 + \text{NO}_3$ (μM), (e) NH_4 (μM) (f) PO_4 (μM) and (g) $\text{Si}(\text{OH})_4$ (μM) at Sta. M. Solid lines with gray symbols indicate the euphotic depth (1%) 54

- Figure 3-4 Temporal and vertical variations in (a) bacterial abundance (BA, 10^6 cell mL^{-1}), (b) chl *a* concentration (mg m^{-3}), (c) pheopigment concentration (mg m^{-3}), (d) particulate organic carbon (POC, mg C m^{-3}), (e) ratio of POC to particulate organic nitrogen (C/N ratio, atomic ratio), (f) diatom (mg C m^{-3}), (g) *Chaetoceros* spp. (mg C m^{-3}), (h) *Cerataulina* spp. (mg C m^{-3}), (i) *Rhizosolenia* spp. (mg C m^{-3}), (j) dinoflagellate (mg C m^{-3}), (k) *Protoperdinium* spp. (mg C m^{-3}), (l) *Prorocentrum* spp. (mg C m^{-3}), (m) *Ceratium* spp. (mg C m^{-3}), (n) ratio of dinoflagellate to total phytoplankton (dinoflagellate dominance) and (o) ratio of phytoplankton carbon to POC (PC/POC ratio) at Sta. M. Solid lines with gray symbols indicate the euphotic depth (1%) 55
- Figure 3-5 Temporal variations in (a) bacterial production (BP; filled bar) and ratio of BP to bacterial abundance (BP/BA ratio; open circle), (b) primary production (PP; filled bar) and ratio of PP to chl *a* concentration (PP/Chl *a* ratio; open circle) and (c) ratio of BP to PP (BP/PP ratio) at the surface 57
- Figure 3-6 Relationships between salinity and nutrient concentrations of (a) $\text{NO}_2 + \text{NO}_3$, (b) NH_4 , (c) PO_4 and (d) $\text{Si}(\text{OH})_4$. Closed circle and open circle represent Sta. M and end-members, respectively 58
- Figure 3-7 Vertically integrated values of (a) bacterial abundance (BA) and (b) NH_4 concentration in the euphotic zone (open bar) and below the euphotic zone (filled bar) 59
- Figure 3-8 Relationships between (a) bacterial abundance (BA) and pheopigment concentration, (b) BA and chlorophyll *a* (chl *a*) concentration and (c) BA and NH_4 concentration below the euphotic zone during the study period at Sta. M. The relationships were significantly positive, and the regressions were (a) $[\text{BA}] = 1.3 \times [\text{pheopigment}] + 0.5$ ($n = 21$, $r = 0.77$, $p < 0.001$), (b) $[\text{BA}] = 0.47 \times [\text{Chl } a] + 0.78$ ($n = 21$, $r = 0.70$, $p < 0.001$) and (c) $[\text{BA}] = 0.89 \times [\text{NH}_4] + 0.66$ ($n = 21$, $r = 0.64$, $p < 0.01$) 60
- Figure 4-1 Relationship between ratio of bacterial production to bacterial abundance (BP/BA ratio) and NH_4 concentration ($[\text{BP/BA ratio}] = 12.7 \times e^{0.409 \times [\text{NH}_4]}$, r

= 0.83, $n = 12$, $p < 0.001$) 66

Figure 4-2 Relationship between ratio of primary production to chlorophyll *a* concentration (PP/Chl *a* ratio) and Si(OH)₄ concentration ([PP/Chl *a* ratio] = $149 \times [\text{Si(OH)}_4] / ([\text{Si(OH)}_4] + 10.2)$, $r = 0.68$, $n = 19$, $p < 0.01$) 67

Figure 4-3 Distribution of chlorophyll *a* concentration during *Mawar*, *Sinlaku*, *Etau* and *Malou*. These data were derived from remote sensing platform (MODIS) 68

Figure 4-4 Potential negative feedback with global warming. The paths show mechanisms for increased diatom production leading to increased carbon export and consequent enhanced CO₂ draw down, promoting cooling. This figure was modified from Kemp & Villareal (2013) 70

Chapter I

General introduction

Phytoplankton and bacteria are major aquatic organisms of lower trophic levels and at the base of aquatic food web. Their abundance and growth, as well as biogeochemistry, can be influenced by regular seasonal variations of biotic and abiotic factors, and irregularly and strongly influenced by climatic and anthropogenic perturbations in coastal and estuarine waters (Paerl et al. 2006). However, biogeochemical and food web changes induced by these perturbations are complex, and our knowledge of how coastal and estuarine waters are influenced by different types of perturbations remains rudimentary.

Phytoplankton and bacterial biomass and production fluctuate seasonally in temperate regions. In spring, as energy of the solar radiation becomes higher, mixed layer depth becomes shallower than critical depth, and phytoplankton blooms occur using ample nutrients that are accumulated in winter. Since the water column is strongly stratified and nutrients are depleted, phytoplankton biomass and production exhibit relatively low during summer and early autumn. Thus, although plenty light is available for phytoplankton photosynthesis during the season, nutrient is a major limiting factor for primary production. In autumn, decrease in water temperature of the upper layer causes deepened mixed layer depth, and induces phytoplankton bloom again. In winter, the mixed layer depth becomes deeper than the critical depth, and primary production in water column declines. Bacterial biomass generally demonstrates a positive relationship with chlorophyll (Bird & Kalff 1984, Cole et al. 1988, Ducklow & Carlson 1992, Gasol & Duarte 2000). Bacterial production consist averaged 10-30% of planktonic primary production in the euphotic zone (Cole et al. 1988, Ducklow 1999), which indicates that bacterial biomass and production are controlled by the availability of phytoplankton-derived resources. During the summer and early autumn, since phytoplankton growth is limited by depletion of nutrients, bacterial production also can be limited by resources derived from primary production. Biological communities of lower trophic levels in coastal ecosystems in productive seasons are regulated by strong bottom-up effects such as photosynthetic available radiation (PAR), water temperature, nutrients, organic matters and water stability (Baek et al. 2009; Baki et al. 2009).

Typhoons, including hurricanes and tropical cyclones, can enhance summer and autumn

primary and bacterial productivities by typhoon-induced physical disturbances. The physical disturbances, including terrestrial runoff, upwelling and sediment resuspension, loads nutrients and dissolved organic matter into the euphotic zone. This, in turn, may lead to large phytoplankton blooms, shifts in the composition of the phytoplankton community, and increase in the bacterial abundance and production (*e.g.* Fogel et al. 1999, Shiah et al. 2000, Chen et al. 2009, Chung et al. 2012; Tables 1-1, 1-2). In fact, chlorophyll *a* (chl *a*) concentration increased up to 32-fold in open waters and 12-fold in coastal waters after the passage of typhoon compared with the conditions prior to the typhoon passage (Table 1-1). For instance, typhoon *Morakot* in 2009 induced upwelling and terrestrial runoff, and led sizeable phytoplankton blooms and composition shift from *Trichodesmium* spp. to chain-forming centric diatoms in the southern East China Sea, northeast of Taiwan (Chung et al. 2012). Hurricane Gordon in 1994 induced sediment resuspension, which caused nutrients from sedimentary pore waters to be transferred to surface waters, and resulted in increased heterotrophic bacterial production in the water column (Fogel et al. 1999, Table 1-2).

Although remote-sensing observations offer high data resolution and the frequency of remote-sensing observations showing typhoon passages influencing chl *a* concentrations has increased (*e.g.* Zheng & Tang 2007, Sun et al. 2010), the observational platform is restricted to clear-sky conditions, one optical depth (the reciprocal of the attenuation coefficient; k , m^{-1}) and limited biogeochemical parameters (Smith 1981, Chang and Gould 2006, Milutinovic 2011, Chung et al. 2012). In addition, chl *a* values derived from remote-sensing observations may be misleading due to the change in phytoplankton composition or the presence of suspended particles and chromophoric dissolved organic matter (Hoge & Lyon 2002, Shang et al. 2008, Tang et al. 2008, Hung et al. 2010). *In situ* observations can acquire robust information, from physical-chemical parameters, such as salinity and nutrient concentrations, and biological parameters, such as phytoplankton composition, primary production and bacterial production, at higher vertical resolutions. However, *in situ* observations are limited in horizontal spatial resolution and sometimes rough ocean conditions prevent safe samplings. Only a few *in situ* samplings with high temporal resolution, such as daily, just after the passage of typhoon have been conducted owing to danger of *in situ* sampling and difficulty in predicting typhoon track. Thus, little is known about the variations of physical-chemical environments and production dynamics of phytoplankton and bacteria just after the passage of typhoon.

Since the 1950s, many of the observed changes are unprecedented over decades to millennia, and warming of the climate system is unequivocal (Fifth assessment report of Intergovernmental Panel on Climate Change 2013). As the reality of climate change and global warming has become more apparent, the intensity of typhoons, tropical cyclones, and hurricanes has increased (Emanuel 2005, Webster et al. 2005, Elsner et al. 2008, Yamada et al. 2010). The destructiveness of typhoons has increased over the past 30 years, showing high correlation with rising sea surface temperatures (Emanuel 2005). There were upward trends in the wind speeds of the strongest typhoons in all basins for the highest quantile considered (99th percentile; Elsner et al. 2008). A simulation using a global cloud-system-resolving model (GCRM) predicted the increase in the frequency of more intense typhoons with global warming (Yamada et al. 2010). Based on these studies, it is conceivable that intensification of typhoons will cause stronger physical disturbances in aquatic ecosystems, and impacts of typhoons on oceanic biogeochemistry will also be augmented (Hoegh-Guldberg & Bruno 2010).

Biological responses to typhoons are possibly different among typhoons with different atmospheric characteristics such as translation speed, size in vortex diameter, rainfall and winds (Wetz & Paerl 2008, Lin 2012). Their variable characteristics influence subsequent physical disturbances, which determine nutrient sources, such as river water, deep sea water and sedimentary pore water, during the passage of typhoons. Significant alterations to marine ecosystem functions have been documented after the passage of large and strong typhoons (*e.g.* Paerl et al. 1998, Paerl et al. 2001, Zheng & Tang 2007). However, little effort has been put forth to understand the temporal evolution of dynamics of lower trophic levels following typhoons of different types and magnitudes. The knowledge can be fundamental and important in order to estimate the effects of typhoon on temperate coastal ecosystems in the future. In Chapter 2, I examined the variations of physical-chemical environments and responses of lower trophic levels to the passages of different types of typhoons in order to clarify the consistent and different biological responses.

The effects of physical disturbances accompanied by the passage of typhoon on ocean environments could be different among areas with different topographic and geographic features. Storm-associated winds have the potential of completely mixing shallow continental shelf waters (20-50 m) down to the sediment surface (Ridderinkhof 1992, Fogel et al. 1999). Thus, shallow inshore area may be influenced strongly by sediment resuspension in addition to terrestrial runoff

and upwelling, while the effects of terrestrial runoff and upwelling can be dominant in deep offshore area (>100 m depth). Bacterial production can be enhanced by sediment resuspension because the resuspension results in nutrient and organic matter load to the water column (Chróst and Riemann 1994). Therefore, it is predicted that biological responses to the passage of typhoon are different between inshore and offshore areas.

Passages of typhoon can affect not only physical-chemical environments and biological productions in the euphotic zone but also chemical and biological processes below the euphotic zone. Typhoon Herb in 1996 induced increases in particulate organic carbon (POC) and bacterial biomass in the whole water column in the continental shelf of the Taiwan Strait (Shiah et al. 2000). The POC sinking flux after the passage of typhoon Fengwong and Sinlaku in 2008 was enhanced up to 1.7-fold compared with that of no typhoon period in the southern East China Sea (Hung et al. 2010). However, limited number of vertical observations with high temporal resolution (*e.g.* daily) after the passage of typhoon has been conducted (Chung et al. 2012). In Chapter 3, I examined how the passage of typhoon affects ocean environments vertically.

Effects of episodic typhoon events on the dynamics of phytoplankton and bacteria should be examined by conducting samplings in the area where the comparable background data have been accumulated. Japan is located in the western North Pacific Ocean in temperate zone, and average typhoons of 5.5 ± 2.0 Japan annually. From 1951 to 2012, there is no significant long-term trend of the number of typhoons approaching Japan, indicating that several typhoons consistently approach Japan every year. More than half of the numbers of typhoons approach Japan in August and September (Fig. 1-1). Sagami Bay, located on the southern coast of central Honshu, or referred to as Japanese mainland, is also subject to the passage of typhoon, in other words, the annual average of 3.1 typhoons approach Sagami Bay. Sagami Bay is one of the representative temperate waters, and many researchers have investigated physical, chemical and biological environments intensively over a long period in the bay (*e.g.* Ogura 1975, Hogetsu & Taga 1977, Horikoshi 1977, Nakata 1985, Kitazato et al. 2000, Kuwahara et al. 2000a, b, Kanda et al. 2003, Fujiki et al. 2004, Hashimoto et al. 2005, Miyaguchi et al. 2008, Ara & Hiromi 2009, Ara et al. 2011). Sagami Bay is also well-known for the richness of its marine organisms, with great biodiversity (Tanaka 1953, Nakata 1985). For example, 25 orders, 220 families and 946 species of fishes have been recorded in Sagami Bay (Nakata 1985). In addition to the high biodiversity, the primary production in Sagami Bay is

considered to be relatively high and can be comparable to those in the Oyashio region, which is one of the highest primary production areas adjacent to the seas of Japan (Nakata 1985). From the 1960s to the present, the total annual fishery capture in Sagami Bay has been maintained at ca. 30,000 tons wet weight year⁻¹; therefore, this bay can be regarded as the most stable ground for fishery production in Japan (Kobata 2003). The high biological productivity can be maintained owing to the high nutrient loadings from twenty rivers including two large rivers (Sakawa River and Sagami River) flowing into the bay (Hirano 1969). Those rivers may provide a large amount of nutrients to stratified surface water after the passage of typhoon. River discharge causes higher amounts of nitrogen and silicic acid loadings compared to phosphate, which results in high nitrogen to phosphate ratio (N/P ratio) and phosphorus limitations during the spring and summer season (Fujiki et al. 2004).

Seasonal variations in biomass and production of lower trophic levels have been also well studied in Sagami Bay (*e.g.* Ara & Hiromi 2009, Baki et al. 2009). In the spring season, the water column is gradually stratified with ample nutrients, and spring phytoplankton blooms are dominated by diatoms (*e.g.* Aono 2001). In the summer season, the water column is highly stratified and nutrient is relatively depleted, which results in the dominance of dinoflagellates such as *Ceratium furca* and *Ceratium fusus* (Satoh et al. 2000, Baek et al. 2008). However, variations in physical-chemical environments and responses of lower trophic levels to episodic events such as the passage of typhoon are still only fragmentally understood.

The overall goal of the present study was to examine the short-term temporal responses of lower trophic levels to the passage of typhoons in the temperate coastal ecosystem. To achieve this goal, detailed time series measurements of biological and physical-chemical variables were carried out at an inshore (5 m depth) station and an offshore station (120 m depth). We examined biological responses to the passage of four typhoons with different characteristics at the inshore station in Chapter 2, and biological responses in euphotic and disphotic zones to the passage of typhoon at the offshore station in Chapter 3. Finally, in Chapter 4, I discussed the effects of typhoon on the temperate coastal ecosystem, combining the results of Chapter 2 and Chapter 3. The knowledge of short-term temporal variations and relationships between physical-chemical parameters and biological responses after the passage of typhoon can be the basic and important information to predict how intensification of typhoons accompanied by global warming and climate change affects

the biological production in the coastal regions.

Table 1-1. Summary of chlorophyll *a* (Chl *a*) concentration and primary production before and after typhoon passages.

Study site	Region	Name of typhoon*	Chl <i>a</i> (mg m ⁻³)			Primary production			Reference
			Before (B)	After (A)	A/B	Before (B)	After (A)	A/B	
<hr/>									
mg C m ⁻² d ⁻¹									
Oceanic									
South China Sea	Tropical	<i>Kai-Tak</i>	0.10	3.2	32	3.0×10 ²	2.8×10 ³	9.3	Lin et al. 2003
South China Sea	Tropical	<i>Ling-Ling</i>	0.14	0.45	3.2	2.7×10 ²	2.6×10 ³	9.6	Zhao et al. 2008
South China Sea	Tropical	<i>Kai-Tak</i>	0.15	0.56	3.7	3.1×10 ²	4.1×10 ³	13	Zhao et al. 2008
South China Sea	Tropical	<i>Hagibis</i>	0.14	0.74	5.3				Sun et al. 2010
<hr/>									
mg C m ⁻³ d ⁻¹									
North Carolina	Temperate	<i>Gordon</i>	0.56	1.1	2.0				Fogel et al. 1999
Gulf of Mexico**	Temperate	<i>Ivan</i>	0.24-0.36	0.81-0.99	2.3-4.1				Walker et al. 2005
South China Sea	Tropical	<i>Damrey</i>	0.15	0.72	4.8				Zheng & Tang 2007
Philippine Sea**	Tropical	<i>Pabuk,</i> <i>Wutip,</i> <i>Sepat</i>	0.06-0.11	0.22-0.56	2.0-5.6	7.6-8.0	12-76	1.5-10	Chen et al. 2009
Estuarine and coastal									
South Carolina**	Temperate	<i>Dennis</i>	1.0-11	2.5-6.0	0.56-2.58	0.13-2.1 ×10 ³	0.83-2.5 ×10 ³	1.2-6.3	Zeeman 1985
the Reef of Tiafura	Tropical	<i>Wasa</i>	0.12	0.21	1.8	9.1	14	1.5	Delesalle et al. 1993
Northern Taiwan	Tropical	<i>Tim</i>	0.40-1.8	4.2	2.3-11				Chang et al. 1996
Northern Taiwan	Tropical	<i>Caitlin,</i> <i>Doug</i>	0.30	3.5	12				Chang et al. 1996
Northern Taiwan	Tropical	<i>Fred</i>	0.60	2.0	3.3				Chang et al. 1996
North Carolina**	Temperate	<i>Gordon</i>	0.56	0.56-3.4	1.0-6.0	18	53	2.9	Fogel et al. 1999
Taiwan Strait**	Tropical	<i>Herb</i>	0.28-0.48	0.42-0.91	0.89-2.1	2.2-2.6	10-50	3.9-19	Shiah et al. 2000
Pamlico Sound	Temperate	<i>Dennis, Floyd,</i> <i>Irene</i>	4.8	5.6-20.7	1.2-4.3				Paerl 2001
Neuse River Estuary	Temperate	<i>Helene</i>	20.6	24.5	1.2				Wetz & Paerl 2008
Neuse River Estuary	Temperate	<i>Isabel</i>	27.1	31.1	1.1				Wetz & Paerl 2008
Neuse River Estuary	Temperate	<i>Alex, Bonnie,</i> <i>Charley</i>	8	17.3	2.2				Wetz & Paerl 2008
Northeast of Taiwan	Tropical	<i>Morakot</i>	0.3-0.4	3.7	9.3-12				Chung et al. 2012

*Typhoon in the table includes tropical cyclones and hurricanes

**Ranges of data are based on individual calculations from multiple sampling stations

Table 1-2. Summary of bacterial abundance and bacterial production before and after typhoon passages.

Study site	Name of typhoon*	Bacterial abundance (10^6 cell mL^{-1})			Bacteria production			Reference
		Before (B)	After (A)	A/B	Before (B)	After (A)	A/B	
North Carolina***	<i>Gordon</i>				$\text{mg m}^{-2} \text{d}^{-1}$ **			Fogel et al. 1999
					40.5-76.0	98.5-103	1.3-2.5	
Taiwan Strait***	<i>Herb</i>	0.29-0.41	0.63-1.26	1.9-4.3	$\text{mg C m}^{-3} \text{d}^{-1}$			Shiah et al. 2000
					0.77-1.13	2.74-5.06	3.1-6.4	

*Typhoon in the table includes tropical cyclones and hurricanes

**Bacterial production was expressed by protein synthesis rate

***Ranges of data are based on individual calculations from multiple sampling stations

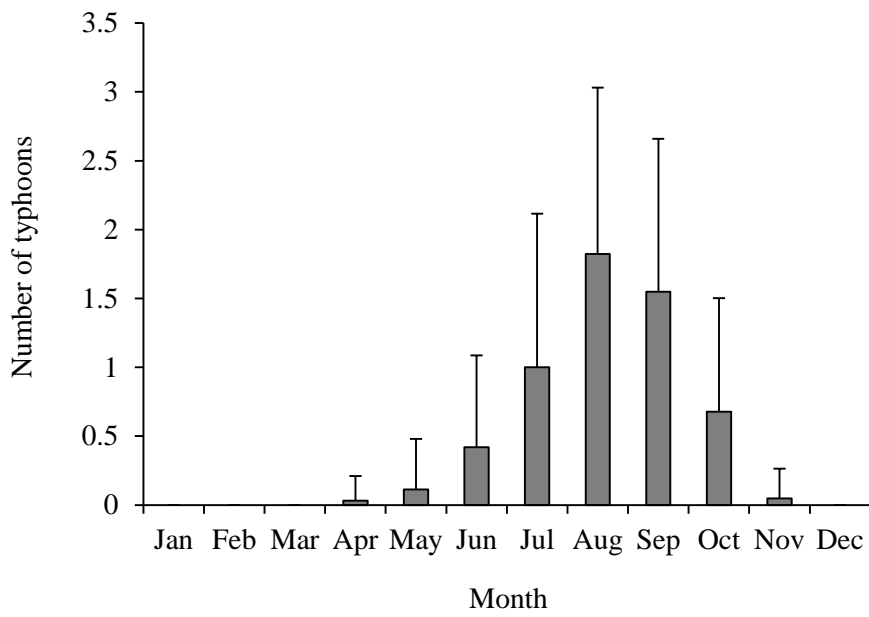


Fig. 1-1 Number of typhoons approaching Japan excluding Okinawa Islands

Chapter II

Responses of phytoplankton and bacteria to the passage of typhoons at inshore waters in Sagami Bay, Japan

2.1. Introduction

A passage of typhoons causes physical disturbances such as upwelling and vertical mixing, (Price 1981, Lin et al. 2003, Zheng & Tang 2007), terrestrial runoff (Zheng & Tang 2007, Chen et al. 2009) and sediment resuspension (Fogel et al. 1999), which supply nutrients to the euphotic zone (Chang et al. 1996, Chen et al. 2009, Chung et al. 2012). In open water, nutrients are loaded by upwelling after a passage of typhoons (*e.g.* Sun et al. 2010), whereas in coastal waters nutrients are loaded by terrestrial runoff, sediment resuspension and/or upwelling (*e.g.* Shiah et al. 2000). The nutrient loadings enhance primary production and bacterial production up to 19 and 6.4 times, respectively, compared to those of before the passage of typhoon or normal conditions (*e.g.* Fogel et al. 1999; Shiah et al. 2000, Chen et al. 2009).

The roles of marine bacteria in biogeochemical cycles and foodweb energetics depend on bacterial utilization of organic matter produced by phytoplankton (Azam et al. 1983, Azam 1998, Williams 1998). Typhoon-induced perturbations load nutrients and organic substrate, which can enhance bacterial productivity. Fogel et al. (1999) reported that bacterial production was enhanced by sediment resuspension accompanied by typhoon passage in North Carolina. Sediment resuspension caused by simulated storms led to a dramatic short-term (one day) increase in bacterial production in coastal waters during a mesocosm experiment (Chróst & Riemann 1994). Although it is foreseeable that bacterial production and abundance might exhibit a short-term variation before and after the passage of typhoon based on those previous studies, little is known about the short-term evolution of bacterial production and abundance during the passage of typhoon. Contrarily, phytoplankton bloom is known to occur in 3 to 6 days after the passage of typhoons (Subrahmanyam et al. 2002, Lin et al. 2003, Walker et al. 2005, Hoover et al. 2006, Zheng & Tang 2007, Tsuchiya et al. 2013a, Tsuchiya et al. 2013b). Therefore, it is predicted that relationships between bacteria and phytoplankton (such as the ratio of bacterial abundance to chlorophyll *a* concentration [BA/Chl *a* ratio] and the ratio of bacterial production to primary production [BP/PP ratio]; Bird & Kalff 1984, Cho et al. 2001) is temporally fluctuated with typhoon passage. The

elucidation of short temporal changes of the relationship between phytoplankton and bacteria is central to understanding and predicting the major energy pathways in the oceans during the passage of typhoon.

Contribution of the increased primary production to annual primary production has been estimated chiefly in tropical and subtropical regions. In the oligotrophic South China Sea, Lin et al. (2003) observed chlorophyll *a* (chl *a*) concentrations before and after the passage of typhoon *Kai-Tak* using three remote sensing observational platforms (SeaWiFS, TRMM and Quick-SCAT), estimated primary production using a vertical generalized production model algorithm (VGPM; Behrenfeld & Falkowski 1997), and reported that the estimated primary production resulting from the typhoon alone contributed at least 2-4% to the annual new production, which is supported by nutrient inputs from outside the euphotic zone such as nitrate. Given an annual average of fourteen typhoons passing over the South China Sea, the contribution of typhoons to the South China Sea's annual new production may be as much as 20-30% (Lin et al. 2003). Although typhoons are episodic events, the effect of a typhoon on primary production is significant, and should be considered to estimate annual primary production. However, quantitative estimates of its contributions to the annual primary production during typhoons are still limited.

Recent studies have revealed some noticeable effects of typhoon disturbances on phytoplankton communities. After typhoon passages, diatoms, such as *Skeletonema* spp., *Chaetoceros* spp. and *Nitzschia* spp., often dominated in various regions (Glynn et al. 1964, Zeeman 1985, Furnas 1989, Chang et al. 1996, Chen et al. 2009, Chung et al. 2012; Table 2-1). In the Philippine Sea, typhoon passages induced a shift in the phytoplankton community from *Trichodesmium* spp. to diatoms, which subsequently could have caused sinking enhancement of biogenic carbon (Chen et al. 2009) because *Trichodesmium* spp. are positively buoyant (Walsby 1992), and turbulence from typhoons is a stress that increases sinking of diatoms (Ruiz et al. 2004). Phytoplankton successions are known to be linked to and regulated by variability of nutrients (Escaravage et al. 1996, Rees et al. 1999, Estrada et al. 2003, Lagus et al. 2004). The nutrient environment after the passage of typhoons may vary depending on the relative contribution of nutrient sources, *i.e.* terrestrial runoff, sediment resuspension and upwelling, each of which has inherent unique nutrient ratios (Howarth 1988). For example, terrestrial water contains rich nitrogen relative to phosphorus, which leads to higher nitrogen to phosphorus ratio (Hecky & Kilham 1988),

whereas the nitrogen to phosphorus ratios of deep sea water were relatively low (*e.g.* Tsunogai & Noriki 1983). Nutrient concentrations and stoichiometry are possibly variable depending on characteristic of typhoons (*e.g.* typhoon track, moving velocity, wind speed and rainfall). For instance, high wind speed and slow moving velocity of typhoon can cause stronger wind stress on the sea surface, and then induce significant upwelling, supplying nutrient-rich deep water to the surface. Upwelling is not induced by weak and/or fast moving typhoons. In addition, strength of rainfall might affect the nutrient amount, which can influence bloom formation of phytoplankton. Deep sea water and river water exhibit their own nutrient concentrations and stoichiometry (*e.g.* Hecky & Kilham 1988). Therefore nutrient sources loaded by typhoon passage could control phytoplankton succession.

In this chapter, I examined the influences of typhoon disturbances on physical-chemical environments, phytoplankton and bacteria at inshore waters of Sagami Bay by conducting *in situ* time-series observations of typhoon *Mawar* (T0511), *Sinlaku* (T0813), *Etau* (T0909) and *Malou* (T1009) which occurred in 2005, 2008, 2009 and 2010, respectively. The specific objectives of the study were 1) to elucidate short temporal variations of relationship between phytoplankton and bacteria during the passage of typhoons, 2) to quantify the contribution of enhanced primary production to annual primary production and 3) to clarify the relationship between phytoplankton assemblage and nutrient stoichiometry after the passage of typhoons.

2.2. Materials and methods

2.2.1. Typhoons investigated in the present study

Four typhoons were investigated; *Mawar* (T0511), *Sinlaku* (T0813), *Etau* (T0909) and *Malou* (T1009) (Fig. 1). *Mawar* occurred near Ogasawara Islands in southern Japan as a tropical depression on 20 August 2005. The lowest sea-level *pressure* of *Mawar* was 930 hPa and the maximum wind speed recorded approximately 50 m s^{-1} . *Mawar* then moved northwestward and its track changed northward with an average speed of 16.3 km h^{-1} . At 0:00 in 26 August 2005, *Mawar* passed through Sagami Bay. *Mawar* with the largest diameter of storm wind of approximately 260 km coincided with heavy precipitation around the central Japan region. After *Mawar* passed through Sagami Bay, it was downgraded to an extra-tropical cyclone on 28 August 2005 off the east coast of Japan Islands.

Sinlaku occurred in the Philippine Sea at 9:00 on 8 September 2008. The lowest sea-level pressure of *Sinlaku* was 935 hPa and the maximum wind speed was approximately 50 m s^{-1} . *Sinlaku* then moved northward and its track changed northeastward with an average speed of 16.0 km h^{-1} . At 0:00 on 20 September 2008, *Sinlaku* approached Sagami Bay. After *Sinlaku* passed Sagami Bay, it was downgraded to a tropical depression on 21 September 2008 around the Kuroshio extension region.

Etau occurred in southern Japan as a tropical depression at 9:00 on 8 August 2009. The lowest sea-level pressure of *Etau* was 992 hPa and the maximum wind speed was approximately 20 m s^{-1} . *Etau* then moved northwestward and its track changed eastward with an average speed of 25.2 km h^{-1} . At 9:00 on 11 August 2009, *Etau* approached Sagami Bay. After *Etau* passed Sagami Bay, it was downgraded to a tropical depression on 13 August 2009 around the Kuroshio extension region.

Malou occurred in the East of the Philippine Sea as a tropical depression on 3 September 2010. The lowest sea-level pressure of *Malou* was 992 hPa and the maximum wind speed was approximately 25 m s^{-1} . *Malou* passed over the East China Sea, Tsushima Straits and Japan Sea, and then it made landfall from Japan Sea on 8 September 2010. After *Malou* made landfall, it was downgraded to a tropical depression at 12:00 on 8 September 2010.

2.2.2. Study site, sampling procedures and analytical methods

The present study was conducted in Sagami Bay, located in the central part of Japan (Fig. 2-1), opening towards the Pacific Ocean to the south. Sampling was conducted at Sta. A located at the mouth of Manazuru Port ($35^{\circ} 09' 49'' \text{ N}$, $139^{\circ} 10' 33'' \text{ E}$, maximum depth 5 m; Fig. 2-1) in Sagami Bay during four typhoon passages. The sampling periods were from 25 August 2005 to 2 September 2005 during *Mawar*, from 21 September 2008 to 27 September 2008 during *Sinlaku*, from 10 August 2009 to 18 August 2009 during *Etau*, and from 8 September 2010 to 15 September 2010 during *Malou*. Samplings were conducted every 12 h at 0:00 and 12:00 during *Mawar*, and every 24 h at 12:00 during *Sinlaku*, *Etau* and *Malou*. The sampling at 0:00 on 26 August 2005 during *Mawar* could not be conducted due to safety issues. In this study, we defined the day each typhoon passed Sta. A as Day 0.

Surface seawater samples were collected for analyzing salinity, nutrients, chlorophyll *a*

(chl *a*), particulate organic carbon (POC), phytoplankton assemblage, primary production, bacterial abundance and bacterial production. Surface temperature was measured with a mercury thermometer. Collected water samples were prescreened through 180 µm nylon mesh to remove large zooplankton and debris at the site, and were carried immediately to the field laboratory (Manazuru Marine Center for Environmental Research and Education, Yokohama National University) less than 2 km away from Sta. A.

Salinity was obtained using a light-refraction salinometer (model S-10, SHIBUYA) during *Mawar*, while an inductive salinometer (Inductively coupled salinometer model 601 Mk1V, Watanabe Keiki MFG. Co., Ltd.) was used during the other three typhoons. Triplicate subsamples for nutrient analysis were filtered through a 0.45 µm pore size membrane filter (Millex SLHA, Millipore), placed into 10 ml plastic tubes and stored at -20°C until analysis. The concentrations of nitrate (NO₃), nitrite (NO₂), phosphate (PO₄) and silicic acid (Si(OH)₄) were measured as described by Parsons et al. (1984) using a nutrient auto-analyzer (AACS-II, Bran + Luebbe during *Mawar*, *Sinlaku* and *Etau*, and SWAAT, BL TEC during *Malou*). During *Malou*, ammonium (NH₄) concentration was measured as described by Hansen & Koroleff (1999) using a nutrient auto-analyzer (SWAAT, BL TEC). Size-fractionated chl *a* analysis during *Mawar* was conducted as described by Tsuchiya et al. (Tsuchiya et al. 2013a), and total chl *a* concentration was estimated by integrating the size fractions. During *Sinlaku*, *Etau* and *Malou*, subsamples for chl *a* analysis were filtered onto a GF/F filter (Whatman), immersed in *N,N*-dimethylformamide (DMF) and stored at 4°C for 24 h (Suzuki & Ishimaru 1990). Chl *a* concentration was determined fluorometrically (Model 10-AU, Turner Design) according to Holm-Hansen et al. (1965). In the present study, there was no significant difference between the integrated total chl *a* concentrations and GF/F chl *a* concentrations (Student t-test, $p > 0.94$; data not shown). For POC measurement, duplicate subsamples of 300 to 500 mL were filtered onto pre-combusted (450°C, 4 h) glass fiber filters (GF/F, Whatman). The filters were treated with HCl fumes for 2 h to remove inorganic carbon, dried at 60°C for 12 h in a dry oven and stored in a desiccator until analysis. POC concentrations were determined using an elemental analyzer (Instruments NA-1500 CNS, Fisions during *Mawar*, and Flash EA-1112, Thermo Finningan during *Sinlaku*, *Etau* and *Malou*). Samples for phytoplankton taxonomic identification (500 mL) were fixed by 2% glutaraldehyde solution. Five to twenty mL of the phytoplankton sample was poured into a settling chamber (HYDRO-BIOS), and settled for 24 h

(Hasle, 1978). Identification and enumeration of microphytoplankton species, especially diatom and dinoflagellate, were conducted using an inverted microscope (Axiovert 25, Carl Zeiss) according to Fukuyo et al. (1990) and Chihara et al. (1997) for dinoflagellates, and Hasle & Syvertsen (1997) for diatoms. Cell volume of each phytoplankton species was calculated according to Hillebrand et al. (1999). Carbon content of diatom and dinoflagellate was also estimated using a regression equation between the cell volume and the carbon content of the cell according to Strathmann (1967).

Primary production was measured using the stable isotope ^{13}C (Hama et al. 1983). During *Mawar*, subsamples collected from the surface water at 9:00 were dispensed into acid washed 4 L polycarbonate bottles (two light bottles and one dark bottle). During *Malou*, subsamples collected from the surface water were dispensed into acid washed 1 L polycarbonate bottles (three light bottles and one dark bottle). They were incubated *in situ* for 24 h after the addition of ^{13}C -sodium bicarbonate (final ^{13}C atom% of total dissolved inorganic carbon was ~10% of that in the ambient water, Hama et al. 1983). After incubation, particulate matter was filtered onto pre-combusted (450°C, 4 h) GF/F filters (Whatman) to determine the bulk carbon fixation rate. The filters were treated with HCl fumes for 2 h to remove inorganic carbon, dried at 60°C for 12 h in a dry oven, and stored in a desiccator until analysis. The concentration of POC and the isotopic ratios of ^{13}C and ^{12}C were determined by a mass spectrometer (TracerMat, Finnigan MAT) combined with an elemental analyzer (Instruments NA-1500 CNS, Fisions) during *Mawar*, and by a mass spectrometer (ANCA-MS, Europe Scientific) during *Malou*. Primary production of phytoplankton was calculated according to Hama et al. (1983). In the present study, dissolved inorganic carbon (DIC) was not measured, and primary production was calculated assuming DIC = 2.2 mM (Gao & McKinley 1994). The primary production was corrected for the rate obtained from the dark bottle. During *Mawar*, in order to calculate the amount of carbon fixed per unit of chl *a* per day, chl *a* concentration was measured at the start of incubation.

Samples for bacterial abundance were fixed with pre-filtered (< 2 μm) buffered formaldehyde (1% final concentration). For enumeration of bacterial abundance, 1.6-2.0 mL of a formaldehyde-fixed sample was filtered on a 0.2 μm black membrane filter (Isopore, Millipore) and stained with SYBR-Gold (Molecular Probes) following Shibata et al. (2006). Bacteria were counted with an epifluorescence microscope (Axioskop 2 plus, Carl Zeiss).

The sea water samples collected from the surface were dispensed into dark bottles, and

were incubated with 20 nM final concentration of bromodeoxyuridine (BrdU; Sigma-Aldrich) at *in situ* temperature for 3 h. BrdU incorporation was halted by adding excess thymidine (100 μ M final) at the end of incubation time. The BrdU incorporation rate was measured by antigen-antibody reaction (Steward & Azam 1999), with a few modifications to the procedure (Hamasaki 2006). BrdU incorporation rates ($\text{pmol L}^{-1} \text{h}^{-1}$) were converted to thymidine (TdR) incorporation rates ($\text{pmol L}^{-1} \text{h}^{-1}$) using the conversion equation ($[\text{BrdU}] = 0.80 \times [\text{TdR}] - 0.016$; Hamasaki 2006), and TdR incorporation rates were converted to bacterial cell production using a theoretical conversion factor of $2 \times 10^{18} \text{ cell mol}^{-1}$ (Ducklow & Carlson 1992). For calculating the bacterial carbon production, we used 20 fg C per bacterium as a cell-to-carbon conversion factor (Lee & Fuhrman 1987).

Wind speed and wind direction were obtained from the Japan Meteorological Agency (2011) at the Ajiro Office ($35^{\circ}02.7' \text{ N}$, $139^{\circ}05.5' \text{ E}$), and precipitation data were obtained at the Odawara Office ($35^{\circ}16.6' \text{ N}$, $139^{\circ}09.3' \text{ E}$). Both observatories are located less than 15 km away from our sampling site. Wind speed and wind direction are mean values per hour. Precipitation is shown as daily integrated values.

2.2.3. Statistical analysis

The background environmental conditions (data from non-typhoon periods) for Sta. A was obtained from the monthly sampling of surface water for the months from July to September (during typhoon seasons) from 2008 to 2010. The average background data for water temperature, salinity, NO_2+NO_3 , PO_4 , $\text{Si}(\text{OH})_4$ and chl *a* were $25.7 \pm 1.7^{\circ}\text{C}$, 32.5 ± 1.8 , $4.2 \pm 2.1 \mu\text{M}$, $0.12 \pm 0.18 \mu\text{M}$, $20 \pm 13 \mu\text{M}$ and $2.5 \pm 1.0 \text{ mg m}^{-3}$, respectively ($n = 9$). Statistical comparisons of inorganic macronutrient concentrations and chl *a* concentrations between typhoon and non-typhoon periods were conducted using a Student's t-test.

2.3. Results

2.3.1. Meteorological and physical parameters, and nutrient stoichiometry

Mawar

Before *Mawar* passage, relatively high wind speed was observed, and reached a maximum of 14.6 m s^{-1} with gusts to 31.7 m s^{-1} on Day 0 (Fig. 2-2a). During *Mawar* passage, the wind direction was

west-southwest. A maximum precipitation of 92 mm d^{-1} was observed on Day -1 (Fig. 2-2b). Water temperature rose from 25.5 (Day -0.5) to 27.0°C (Day 0.5) with *Mawar* passage (Fig. 2-2c). Water temperature gradually declined to 24.0°C until Day 6. Salinity declined significantly from 35 to 25 on Day 0.5 during *Mawar* passage (Fig. 2-2d), deviating from the background data. Salinity stabilized at around 30.5 ± 0.7 on average from Day 4 to Day 9. After *Mawar* passed (Day 0.5 to Day 2.5), the concentration of NO_2+NO_3 tripled to $13.4 \pm 3.2 \mu\text{M}$, which was 3.2 times higher than the background data ($p < 0.001$; Fig. 2-2e), and declined abruptly to $1.4 \pm 0.3 \mu\text{M}$ on Day 4.5. PO_4 concentrations increased during *Mawar* passage, and relatively high concentrations lasted until Day 4.5 ($1.08 \pm 0.24 \mu\text{M}$), which was 8.9 times higher than the background data ($p < 0.001$; Fig. 2-2f). It decreased to $0.21 \pm 0.02 \mu\text{M}$ on Day 6.5. Si(OH)_4 concentration also increased after *Mawar* passage, and relatively high concentrations ($59.0 \pm 11.8 \mu\text{M}$) lasted until Day 7, which was 2.9 times higher than the background data ($p < 0.001$; Fig. 2-2g). From Day 8 to Day 9, Si(OH)_4 decreased to $19.8 \pm 4.3 \mu\text{M}$. N/P ratio showed an average of 7.2 before *Mawar* passage (Fig. 2-2h). After *Mawar* passage, the N/P ratio was stabilized around 15.9 ± 8.9 except for an anomaly of 1.0 on Day 4.5.

Sinlaku

A maximum north-northeast wind of 17 m s^{-1} with gusts to 24.2 m s^{-1} was observed on Day 0 during *Sinlaku* passage (Fig. 2-2i). Precipitation lasted until Day 2, and integrated precipitation was 89.0 mm (Fig. 2-2j). Water temperature did not fluctuate drastically, and showed the mean value of $24.9 \pm 0.6^\circ\text{C}$ during the sampling period (Fig. 2-2k). Salinity showed a minimum of 27.5 on Day 1, and recovered to background levels on Day 5 (Fig. 2-2l). NO_2+NO_3 concentration showed a maximum of $16.9 \pm 0.1 \mu\text{M}$ on Day 1, which was 4.0 times higher than the background data ($p < 0.001$; Fig. 2-2m). Afterward the concentration decreased gradually to $3.9 \pm 0.1 \mu\text{M}$ until Day 5. The concentration of PO_4 also showed a maximum of $0.54 \pm 0.02 \mu\text{M}$ on Day 1, which was 4.5 times higher than the background data ($p < 0.001$; Fig. 2-2n). Thereafter it declined, and the concentrations from Day 2 to Day 7 showed no significant difference to the background data ($p > 0.05$). Si(OH)_4 concentration reached a maximum of $44.8 \pm 0.3 \mu\text{M}$ on Day 3, and was 2.2 times higher than the background data ($p < 0.001$; Fig. 2-2o). The N/P ratio was 31.3 on Day 1, thereafter increased gradually to 103.1 on Day 5 (Fig. 2-2p).

Etau

A maximum north-northeast wind speed of 9.4 m s^{-1} with gusts to 14.7 m s^{-1} was observed on Day 0 (Fig. 2-2q). Integrated precipitation between Day -1 and Day 0 was 42.2 mm (Fig. 2-2r). Water temperature was relatively higher than the background levels and showed a maximum of 27.8°C on Day 6 (Fig. 2-2s). Salinity decreased during *Etau* passage and showed a minimum of 26.1 on Day 0 (Fig. 2-2t), which was 6.4 lower than the background level. Salinity recovered to 32.3 ± 0.1 between Day 2 and Day 4, slightly decreasing to 30.3 on Day 5. Prior to the passage of *Etau*, NO_2+NO_3 concentration was $10.2 \pm 0.1 \mu\text{M}$, which was 2.4 times higher than the background data ($p < 0.001$; Fig. 2-2u), decreasing to a minimum of $2.4 \pm 0.1 \mu\text{M}$ on Day 2. PO_4 concentration showed a maximum of $0.70 \pm 0.02 \mu\text{M}$ on Day -1, which was 5.7 times higher than the background data ($p < 0.001$; Fig. 2-2v), decreasing to an average of 0.15 ± 0.03 from Day 4 to Day 7 (Fig. 2-2v). $\text{Si}(\text{OH})_4$ concentration showed a maximum of $58.7 \pm 0.2 \mu\text{M}$ on Day -1, which was 2.9 times higher compared to the background data ($p < 0.001$; Fig. 2-2w). It showed another peak of $50.5 \pm 1.2 \mu\text{M}$ on Day 5. The N/P ratio showed relatively low value (7.6) on Day 1 (Fig. 2-2x). The N/P ratio increased from Day 3 and reached a maximum of 39.3 on Day 6.

Malou

During *Malou* approach, a west-southwest wind of 8.3 m s^{-1} with gusts to 18.2 m s^{-1} was observed (Fig. 2-2y). A maximum precipitation of 238.5 mm d^{-1} was observed on Day 0 (Fig. 2-2z). During *Malou* passage, water temperature showed a minimum of 23.7°C on Day 0, and then increased gradually to 28.1°C on Day 4 (Fig. 2-2aa). Salinity also showed a minimum of 22.1 on Day 0, which was 10.4 lower than the background level (Fig. 2-2ab). Salinity recovered to an average of 32.4 ± 0.5 from Day 3 to Day 7. NO_2+NO_3 concentration on Day 1 was 4.3 times higher than the background data ($p < 0.001$; Fig. 2-2ac), showing a maximum of $18.1 \pm 0.2 \mu\text{M}$, and decreased to $5.2 \pm 0.0 \mu\text{M}$ on Day 6. NH_4 concentration showed a maximum of $8.4 \pm 0.1 \mu\text{M}$ on Day 0, and decreased to $1.3 \pm 0.0 \mu\text{M}$ on Day 6. PO_4 concentrations showed a maximum of $1.05 \pm 0.01 \mu\text{M}$ on Day 0, which was 8.6 times higher than the background data ($p < 0.001$; Fig. 2-2ad), and decreased to $0.04 \pm 0.01 \mu\text{M}$ on Day 6. $\text{Si}(\text{OH})_4$ concentrations showed a maximum of $61.2 \pm 0.9 \mu\text{M}$ on Day 1, which was 3.1 times higher than the background data ($p < 0.001$; Fig. 2-2ae), showing a

decreasing trend until Day 6. N/P ratio showed a minimum of 11.7 on Day 0, and a peak of 55 on Day 1 (Fig. 2-2af). From Day 2 to Day 5, the ratio was stabilized around 24.8 ± 3.1 , and increased abruptly to 127.3 on Day 6.

2.3.2. Primary production and bacterial production

Mawar

Sea surface primary production was $81.3 \text{ mg C m}^{-3} \text{ d}^{-1}$ on Day 1, just after the passage of *Mawar* (Fig. 2-3a). The highest value of $349 \text{ mg C m}^{-3} \text{ d}^{-1}$ was reached on Day 3. After that, primary production was relatively high until Day 9. The ratio of primary production to chl *a* concentration (PP/Chl *a* ratio) showed relatively high values from Day 1, and lasted to Day 9 ($131 \pm 29 \text{ mg C [mg Chl } a]^{-1} \text{ d}^{-1}$; Fig. 2-3b).

Malou

Primary production at the surface was relatively low values of $131 \pm 64 \text{ mg C m}^{-3} \text{ d}^{-1}$ from Day 1 to Day 3 (Fig. 2-4a). From Day 4, primary production increased, and then reached a maximum of $554 \pm 32 \text{ mg C m}^{-3} \text{ d}^{-1}$ on Day 5. PP/Chl *a* ratio showed a maximum ($134 \text{ mg C [mg Chl } a]^{-1} \text{ d}^{-1}$) and averaged $134 \text{ mg C [mg Chl } a]^{-1} \text{ d}^{-1}$ during the sampling period (Fig. 2-4b).

Bacterial production at the surface was relatively high values of $114 \pm 21 \text{ mg C m}^{-3} \text{ d}^{-1}$ and $132 \pm 14 \text{ mg C m}^{-3} \text{ d}^{-1}$ on Day 1 and Day 2, respectively (Fig. 2-4c). From Day 3, bacterial production was $77 \pm 23 \text{ mg C m}^{-3} \text{ d}^{-1}$ from Day 3 to Day 7. The ratio of bacterial production to bacterial abundance (BP/BA ratio) showed relatively high value on Day 1 ($85 \text{ fg C cell}^{-1} \text{ d}^{-1}$), and reached a maximum of $133 \text{ fg C cell}^{-1} \text{ d}^{-1}$ on Day 2 (Fig. 2-4d). From Day 3, the BP/BA ratio decreased and stabilized at $37 \pm 12 \text{ fg C cell}^{-1} \text{ d}^{-1}$. The ratio of bacterial production to primary production (BP/PP ratio) showed a maximum of 1.5 on Day 1 (Fig. 2-4e). And then the ratio decreased and showed a minimum of 0.10 on Day 5 when the primary production was a maximum.

2.3.3. Chl *a* concentration, ratio of POC to chl *a* concentration, bacterial abundance and ratio of bacterial abundance to chl *a* concentration

Mawar

Before *Mawar* passage, chl *a* concentration was 2.2 mg m^{-3} (Fig. 2-5a). Just after *Mawar* passage,

chl *a* concentrations decreased to 0.51 mg m^{-3} on Day 0.5, and then abruptly increased showing the highest value of 7.84 mg m^{-3} on Day 5. The chl *a* concentration from Day 4 to Day 5 ($5.8 \pm 1.8 \text{ mg m}^{-3}$) were significantly higher than the background concentration ($p < 0.001$). Ratio of particulate organic carbon to chl *a* (POC/Chl *a* ratio) showed a maximum of 523 on Day 1 and then decreased to a minimum of 60.8 on Day 5 when chl *a* concentration reached a maximum (Fig. 2-5b). Bacterial abundance showed a minimum value of $0.48 \times 10^6 \text{ cell mL}^{-1}$ on Day 0.5 (Fig. 2-5c). And then, bacterial abundance slightly increased on Day 1, and showed relatively high value, $1.7 \pm 0.0 \times 10^6 \text{ cell mL}^{-1}$ on from Day 1 to Day 2. Bacterial abundance reached a maximum of $4.9 \pm 0.3 \times 10^6 \text{ cell mL}^{-1}$ on Day 7, decreasing to $1.0 \pm 0.1 \times 10^6 \text{ cell mL}^{-1}$ on Day 8. Ratio of bacterial abundance to chl *a* (BA/Chl *a* ratio) was $0.59 \times 10^{12} \text{ cell mg}^{-1}$ on Day -1 and then shot up to $5.3 \times 10^{12} \text{ cell mg}^{-1}$ on Day 1.5 (Fig. 2-5d). The ratio decreased to a minimum of $0.34 \times 10^{12} \text{ cell mg}^{-1}$ on Day 5.

Sinlaku

Relatively low chl *a* concentrations were observed from Day 1 to Day 2 after typhoon passages ($2.5\text{-}4.5 \text{ mg m}^{-3}$; Fig. 2-5e), and then increased to abnormally high values from Day 3 to Day 5 ($15.7 \pm 1.3 \text{ mg m}^{-3}$), which was significantly higher than the background concentration ($p < 0.001$). POC/Chl *a* ratio showed a maximum of 314 on Day 1 and then decreased to a minimum of 34.5 on Day 3 (Fig. 2-5f). Bacterial abundance was relatively high on Day 1 and then decreased to $2.4 \pm 0.5 \times 10^6 \text{ cell mL}^{-1}$ on Day 2 (Fig. 2-5g). Bacterial abundance increased and reached a maximum of $4.6 \pm 0.2 \times 10^6 \text{ cell mL}^{-1}$ on Day 4. BA/Chl *a* ratio showed a maximum of $1.1 \times 10^{12} \text{ cell mg}^{-1}$ on Day 1 and then decreased to a minimum of $0.19 \times 10^{12} \text{ cell mg}^{-1}$ on Day 3 (Fig. 2-5h).

Etau

Chl *a* concentrations showed low values from Day -1 to Day 3 ($2.7 \pm 1.4 \text{ mg m}^{-3}$; Fig. 2-5i), and relatively high values from Day 4 to Day 6 ($7.0 \pm 1.9 \text{ mg m}^{-3}$), which was significantly higher than the background concentration ($p < 0.001$). POC/Chl *a* ratio showed a maximum of 299 on Day -1 and then decreased to a minimum of 61.8 on Day 4 (Fig. 2-5j). Bacterial abundance showed the highest value of $3.1 \pm 0.4 \times 10^6 \text{ cell mL}^{-1}$ on Day -1 (Fig. 2-5k). Thereafter, bacterial abundance decreased, and showed a minimum of $1.4 \pm 0.1 \times 10^6 \text{ cell mL}^{-1}$ on Day 4. BA/Chl *a* ratio showed a maximum of $2.5 \times 10^{12} \text{ cell mg}^{-1}$ on Day -1 and then decreased to $0.17 \times 10^{12} \text{ cell mg}^{-1}$ on Day 4

(Fig. 2-5l).

Malou

Chl *a* concentrations showed relatively low values of $1.1 \pm 0.4 \text{ mg m}^{-3}$ from Day 0 to Day 3, and then reached a maximum of 7.7 mg m^{-3} on Day 6 (Fig. 2-5m). The chl *a* concentration from Day 5 to Day 7 ($4.8 \pm 2.5 \text{ mg m}^{-3}$) were significantly higher than the background concentration ($p < 0.05$). POC/Chl *a* ratio showed a maximum of 659 on Day 0 and then decreased to a minimum of 53.9 on Day 6 (Fig. 2-5n). Bacterial abundance showed relatively low values of $1.1 \pm 0.2 \times 10^6 \text{ cell mL}^{-1}$ from Day 0 to Day 3, and then reached a maximum of $2.8 \pm 0.1 \times 10^6 \text{ cell mL}^{-1}$ on Day 6 (Fig. 2-5o). BA/Chl *a* ratio showed relatively high values of $1.9 \times 10^{12} \text{ cell mg}^{-1}$ and $2.0 \times 10^{12} \text{ cell mg}^{-1}$ on Day 1 and Day 3, respectively, and then showed a minimum of $0.35 \times 10^{12} \text{ cell mg}^{-1}$ on Day 6 (Fig. 2-5p).

2.3.4. Phytoplankton assemblage

Mawar

On Day -1, the carbon biomass of diatom *Skeletonema* spp. was most dominant (119 mg C m^{-3} ; Fig. 2-6a), and dinoflagellate *Dinophysis* spp. were the second dominant group with a carbon biomass of 66.9 mg C m^{-3} (included in other dinoflagellates; Fig. 2-6a). Carbon biomass showed relatively low levels after *Mawar* passage until Day 3. Carbon biomass increased abruptly from Day 4, and reached a maximum of 530 mg C m^{-3} on Day 5. At the peak, *Skeletonema* spp. were most dominant at 453 mg C m^{-3} , accounting for 85 % of the total phytoplankton carbon biomass (Fig. 2-6b). Following the first peak, the most dominant taxon changed to *Chaetoceros* spp., which were dominant at $51 \pm 4\%$ from Day 7 to Day 9 (Fig. 2-6a, b). The proportion of dinoflagellates was highest at 85 %, dominated by *Protoperdinium* spp. on Day 2, and decreased with increase in phytoplankton biomass thereafter (Fig. 2-6c).

Sinlaku

Phytoplankton carbon biomass reached a maximum of 1002 mg C m^{-3} on Day 4 (Fig. 2-6d) composed of *Chaetoceros* spp., and accounted for 90% of the total phytoplankton carbon biomass (Fig. 2-6d, e). Phytoplankton carbon biomass decreased on Day 6. Relatively high contribution of

dinoflagellates to the phytoplankton biomass was observed on Day 1 and Day 3, accounting for 44% and 57%, respectively. On Day 1, dinoflagellate *Gymnodinium* spp. and *Dinophysis* spp. were dominant with carbon biomasses of 28.5 mg C m⁻³ and 18.2 mg C m⁻³, respectively, and on Day 3 *Protoperdinium* spp. and *Gymnodinium* spp. were dominant with carbon biomasses of 193 mg C m⁻³ and 120 mg C m⁻³, respectively. The proportions of dinoflagellates decreased and showed less than 10 % during the phytoplankton biomass peak from Day 4 to Day 5 (Fig. 2-6f).

Etau

Phytoplankton carbon biomass showed low values from Day -1 to Day 3 (60.1 ± 31.8 mg C m⁻³; Fig. 2-6g) and relatively high values from Day 4 to Day 6 (331.3 ± 90.2 mg C m⁻³). Dinoflagellates such as *Ceratium* spp. and *Protoperdinium* spp. dominated the phytoplankton communities on Day 0 and Day 1, accounting for 69% (45.1 mg C m⁻³ and 8.2 mg C m⁻³, respectively) and 83% (25.0 mg C m⁻³ and 14.2 mg C m⁻³, respectively), respectively (Fig. 2-6g, h). As phytoplankton carbon biomass increased, diatoms dominated the community (84 ± 8%) from Day 2 to Day 7 (Fig. 2-6i), where *Chaetoceros* spp. were most dominant with a maximum carbon biomass of 315 mg C m⁻³ on Day 6.

Malou

Phytoplankton carbon biomass showed relatively low values (41.6 ± 30.3 mg C m⁻³) from Day 1 to Day 4 (Fig. 2-6j), when dinoflagellates such as *Ceratium* spp., *Protoperdinium* spp. *Prorocentrum* spp. and *Dinophysis* spp. dominated the phytoplankton community (64 ± 17%; Fig. 2-6k, l). Diatoms dominated the community (96 ± 3%) from Day 5 to Day 7, and phytoplankton carbon biomass showed a maximum of 315 mg C m⁻³ on Day 6 (Fig. 3j). During the carbon biomass peak, *Chaetoceros* spp. and *Cerataulina* spp. dominated the community at 53% and 33%, respectively.

2.4. Discussion

When concentrations of dissolved inorganic nitrogen, phosphate and silicate are <1.0, 0.2 and 2.0 μM, respectively, they are considered limiting for phytoplankton growth (Dortch & Whitley 1992, Justic et al. 1995). During summer months (background concentration) at Sta. A, NO₂+NO₃ and Si(OH)₄ concentrations (4.2 ± 2.1 and 20 ± 13 μM, respectively) are generally much higher than the

limiting concentrations, while PO_4 concentrations ($0.12 \pm 0.18 \mu\text{M}$) are lower than the limiting concentrations, suggesting phytoplankton growth limitation by PO_4 during this season. Fujiki et al. (2004) reported that primary productivity was phosphorus limited in spring and summer in Sagami Bay. However, during episodic typhoon events all inorganic macronutrient concentrations especially PO_4 significantly increased (Fig. 2). After the passage of *Mawar*, relatively high PO_4 concentrations lasted until Day 4 (Fig. 2-2f). On the other hand, after the passages of *Sinlaku*, *Etau* and *Malou*, PO_4 concentrations reached their maximums during the passages of typhoons (Day -1 to Day 1), and then decreased rapidly. Incidentally, the PO_4 concentrations during *Sinlaku*, *Etau* and *Malou* were significantly lower than during *Mawar* (Tukey-Kramer, $p < 0.01$), which led to relatively higher N/P ratios. Remote sensing SST data derived from NOAA remote sensing data revealed a cold water mass prevailed around Sagami Bay along the typhoon track after the passage of *Mawar* (Kanagawa Prefectural Fisheries Technology Center, 2012; <http://www.agri-kanagawa.jp/suisoken/noaa2/noaa2.asp>). Thus, a large proportion of nutrients during *Mawar* may have originated from upwelled nutrient-rich deeper water. On the other hand, after the passages of *Sinlaku*, *Etau* and *Malou*, a cold water track similar to *Mawar* was not observed based on remote sensing SST data (Kanagawa Prefectural Fisheries Technology Center 2012). Nutrient concentrations during these typhoons showed relatively high values with low salinity, suggesting a large proportion of macronutrients might be attributable to terrestrial runoff rather than upwelling. Higher N/P ratios during *Sinlaku*, *Etau* and *Malou* than that during *Mawar* can be another evidence for the high contribution of river discharge because riverine waters generally has higher N/P ratios than oceanic waters (Fujiki et al. 2004).

Relatively high BA/Chl *a* ratio before and after the passages of typhoons suggested that the ecosystem might have been relatively heterotrophic system (Fig. 2-5). The residuals of observed BA/Chl *a* ratio and estimated BA/Chl *a* ratio according to the regression equation ($\log [\text{BA}; \text{cell mL}^{-1}] = 5.96 + 0.524 \times \log [\text{Chl } a; \text{mg m}^{-3}]$; Cole et al. 1988) showed relatively large positive values before and after the passage of typhoons (Fig. 2-7), which suggested that bacteria might have depended not only upon phytoplankton-derived substrates but also upon other carbon sources. Typhoon-induced physical perturbations such as terrestrial runoff and sediment resuspension loaded allochthonous organic and inorganic substrates. The high BP/PP ratio, 1.5, on Day 1 during *Malou* evidenced that bacterial growth might have been supported by allochthonous substrates rather than

autochthonous substrates derived from phytoplankton (Fig. 2-6e). In the photic zone of the ocean, bacterial production is significantly correlated with primary production, and averages 10-30% of planktonic primary production (Cole et al. 1988, Ducklow 1999). Assuming a bacterial growth efficiency of 0.5 (Coveney & Wetzel 1995), BP/PP ratios of >0.5 indicate that daily bacterial carbon demand exceeded daily primary production (bacterial carbon demand = bacterial production / growth efficiency; Nagata et al. 1996). The POC/Chl *a* ratios showed relatively high values just before and after the passages of typhoons (Fig. 2-5b, f, j, n). High POC/Chl *a* ratios are caused by high carbon biomass of heterotrophic organisms such as bacteria, and detritus relative to phytoplankton carbon biomass, which indicates that the system is heterotrophic (Gasol et al. 1997, Vargas et al. 2007).

Accompanied by phytoplankton blooms, the BA/Chl *a* ratios decreased and the residuals of observed BA/Chl *a* ratio and estimated BA/Chl *a* ratio showed around zero (Fig. 2-7), which indicated that the environments might have been changed to autotrophic systems. During *Malou*, BP/PP ratio of around 0.2 evidenced the autotrophic environments when phytoplankton bloom occurred. In addition, POC/Chl *a* ratio decreased during phytoplankton blooms. The dynamics agreed with the previous studies (*e.g.* Vargas et al. 2007). Therefore, accompanied by typhoon passages, the ocean environments changed from heterotrophic to autotrophic systems within several days.

The PP/Chl *a* ratios during *Mawar* and *Malou* were significantly higher than the mean PP/Chl *a* ratio, $40 \text{ mg C} [\text{mg Chl } a]^{-1} \text{ d}^{-1}$, observed in August and September in Sagami Bay (Student's t-test, $p < 0.01$) reported by Sugawara et al. (2003). Previous studies utilizing remote sensing measurements reported time lags of three to six days between phytoplankton blooms and their preceding typhoons (Subrahmanyam et al. 2002, Lin et al. 2003, Walker et al. 2005, Hoover et al. 2006, Zheng & Tang 2007). In the present study, phytoplankton exhibited high photosynthetic activity just after the passage of typhoons, due to the high nutrient concentrations following the passage of *Mawar* and *Malou*. The results suggest that the passage of typhoon significantly enhanced primary productivity for nine days during *Mawar* and seven days during *Malou*.

The integrated primary productions for the duration of nine days after the passage of *Mawar* and for the duration of seven days after the passage of *Malou* were $2.10 \times 10^3 \text{ mg C m}^{-3}$ and $2.07 \times 10^3 \text{ mg C m}^{-3}$, which accounts for 7.1–9.1% of the annual primary production in the

upper waters of Sagami Bay [annual primary production values were derived from Satoh et al. 2000 (2.92×10^4 mg C m⁻³ yr⁻¹), Sugawara et al. 2003 (2.30×10^4 mg C m⁻³ yr⁻¹) and Ara & Hiromi 2009 (2.82×10^4 mg C m⁻³ yr⁻¹)]. Approximately 3 typhoons on average approach Sagami Bay annually (Japan Meteorological Agency), which implies that primary production in the upper waters of Sagami Bay may be enhanced in the range of 21.3–27.3% of the annual primary production. The present study verified that episodic events such as typhoons can make large contributions to annual primary production in temperate coastal regions. In the oceanic region of the South China Sea, integrated primary production at the bloom center after typhoon passages have been calculated, and accounted for 9.9–23% of the annual primary production derived from Liu et al. (2002) (Lin et al. 2003, Zhao et al. 2008).

Relatively high proportions of dinoflagellates just after the passage of typhoons in the present study agreed with prior studies conducted after the episodic events in Chesapeake Bay (Loftus & Seliger 1976), South Carolina (Zeeman 1985), Hellshire coast of Jamaica (Webber et al. 1992), and Kaneohe Bay of Hawaii (Hoover et al. 2006). Typhoon-driven runoff may contribute to the formation of a shallow, low salinity, and nutrient-rich fresh water layer at the surface, as suggested by Satoh et al. (2000). It is known that the swimming behavior of dinoflagellates could serve to concentrate cells into the nutrient-rich fresh water layer at the surface (Donaghay & Osborn 1997). Hoover et al. (2006) suggested that the early appearance of dinoflagellates after episodic events is consistent with observations (Sellner et al. 2001) that they were better adapted to utilize high-nutrient concentrations under low-turbulence conditions than other phytoplankton groups. Further, dinoflagellates have been known to utilize organic substrates for nutrition (Zeeman 1985), and the typhoon could have enriched the waters with organic compounds through runoff. Thus, these physical and physiological features may have allowed relative success of dinoflagellates just after the passage of typhoons in the present study.

The dominance of dinoflagellate genera, *Protoperidinium* spp., *Dinophysis* spp., *Prorocentrum* spp., *Gymnodinium* spp. and *Ceratium* spp., in the present study after the passage of typhoons were consistent with those of previous studies conducted after the episodic events such as *Protoperidinium* spp. (Webber et al. 1992), *Protoperidinium* spp. (Hoover et al. 2006), and *Ceratium trichoceros*, *Gymnodinium* sp., and *Dinophysis caudata* (Zeeman 1985). These genera and species are considered as heterotrophic or mixotrophic dinoflagellates (Lessard & Swift 1985,

Hansen 1991, Strom & Morello 1998, Jacobson 1999, Jeong 1999, Morton 2000, Ismael 2003, Nishitani et al. 2003, Sherr & Sherr 2007), which suggested that typhoon passage, including episodic storm events, might lead phytoplankton communities to relatively heterotrophic ones. The ratios of mixo- and heterotrophic phytoplankton carbon biomass to autotrophic phytoplankton carbon biomass increased just after the passage of typhoons, and then generally decreased (Fig. 2-8). The results imply that after the passage of typhoon phytoplankton communities initially shifted to heterotrophic ones, and subsequently changed to autotrophic ones accompanied by a phytoplankton bloom mainly of diatoms.

After relatively high proportions of dinoflagellates, phytoplankton biomass increased dramatically, dominated by diatoms. A significantly positive relationship between total phytoplankton biomass and proportions of diatom biomass was observed ($p < 0.05$, Fig. 2-9a). Prior studies in subtropical regions reported successions of phytoplankters after episodic events (*e.g.* Chung et al. 2012). In Kaneohe Bay of Hawaii, dinoflagellate *Protooperidinium* sp. dominated the community just after a storm; thereafter diatoms increased and dominated (Hoover et al. 2006). In the southern East China Sea, the diatom population was dominated by chain-forming centric diatoms (*Chaetoceros* spp.) instead of the *Trichodesmium* and *Gymnodinium* spp. that prevailed before the typhoon (Chung et al. 2012). In the present study, $\text{Si}(\text{OH})_4$ concentrations were not less than $12.1 \mu\text{M}$, Si/N ratios were not less than 1 (data not shown) except for Day 0 during *Malou* (0.997) and Si/P ratio were not less than 10 (data not shown), which suggested that silica was not a limiting nutrient for diatom growth (Harrison et al. 1976, Harrison et al. 1977, Levasseur & Therriault 1987, Dortch & Whitedge 1992, Justic et al. 1995). Diatoms are superior competitors for light and nutrients when silicate is available (Riegman et al. 1998). Therefore, the silica-rich nutrient environment after typhoon passage derived from terrestrial and upwelling influences may allow diatoms to dominate after a brief increase of other phytoplankton groups such as dinoflagellates.

When the diatom proportion to total phytoplankton biomass was higher than the median of 77.9% (Fig. 2-9a), the proportion of *Skeletonema* spp. and *Chaetoceros* spp. biomasses in the diatom community showed a significant hyperbolic curve with increases in diatom biomass ($p < 0.05$; Fig. 2-9b). This relationship suggests that either *Skeletonema* spp. or *Chaetoceros* spp. selectively increased and dominated the diatom communities after the passage of respective

typhoons, possibly due to their capacity for high growth rates (*e.g.* Finenko & Krupatkina-Akinina 1974, Han & Furuya 2000), euryhaline capabilities (Brand 1984, Sigaud & Aidar 1993, Balzano et al. 2011) and/or short time lags between nutrient uptake and growth (*e.g.* Collos 1986).

There are significant relationships between *Skeletonema* spp. and *Chaetoceros* spp. dominances within the phytoplankton communities, and their respective N/P ratios ($p < 0.05$; Fig. 2-9c, d), suggesting that *Skeletonema* spp. dominated under the condition of lower N/P ratio and *Chaetoceros* spp. dominated under the condition of higher N/P ratio. The N/P ratios after typhoon passages were 9.9 in South Carolina (Zeeman 1985) and 11.5 in northern Taiwan (Chang et al. 1996), which are similar to the value (12.4) found after the passage of *Mawar* when *Skeletonema* spp. were dominant. Roden and O'Mahony (1984) conducted an outdoor experiment in an enclosure and reported that *Skeletonema* spp. favor low N/P ratios and were dominant when the N/P ratio was less than 30. On the other hand, *Chaetoceros* spp. were not phosphorus limited when the N/P ratio was more than 30. Alkaline phosphatase activity of *Chaetoceros affinis* was higher than that of *Skeletonema costatum*, especially under high N/P ratio (Møller et al. 1975). The previous studies support the notion that *Chaetoceros* spp. could dominate under higher N/P ratios, or lower PO₄ concentrations. These relationships support the classic interpretation where the N/P ratio determines the dominant phytoplankton bloom (*e.g.* Tilman et al. 1986, Escaravage et al. 1996, Rees et al. 1999, Estrada et al. 2003, Lagus et al. 2004). Temporal coupling between *Chaetoceros* blooms and increases in the N/P ratio during *Sinlaku*, *Etau* and *Malou* suggested drawdown of PO₄ (Figs. 2-2, 2-6). It is important to emphasize, however, that PO₄ levels during these three typhoons were relatively low near background levels which may have contributed to the high N/P ratios. These results suggest that low PO₄ concentrations and coupled high N/P ratios facilitated *Chaetoceros* spp. blooms, while high PO₄ concentrations and associated low N/P ratios were more favorable conditions for *Skeletonema* spp. bloom formation.

In the present study, contribution of nutrient sources was different between *Mawar* and the other three typhoons; upwelling and terrestrial runoff were likely the dominant nutrient sources in *Mawar*, and terrestrial runoff was the dominant nutrient source in *Sinlaku*, *Etau* and *Malou*. Terrestrial waters supply a large amount of nitrogen to coastal regions (Edmond et al. 1985, Turner et al. 1990, Fujiki et al. 2004), which results in higher N/P ratios compared to that of deep water in Sagami Bay (Kamatani et al. 2000). The results of the present study and the experiment suggest that

the proportional contribution of nutrient sources, which determines nutrient stoichiometry after the passage of typhoons, is an important factor in controlling phytoplankton community succession.

In the present chapter, the responses of phytoplankton and bacteria to physical-chemical variations induced by the passage of typhoons at the surface of inshore waters were examined. Major biological production changed from bacterial production to primary production in a few days after the passage of typhoon, in other words, changed from heterotrophic system to autotrophic system. The temporally integrated primary production enhanced by the passage of typhoon accounted for 7.1–9.1% of the annual primary production in the upper waters of Sagami Bay. Phytoplankton succession from dinoflagellates to diatoms occurred. The diatom succession might be controlled by nutrient stoichiometry which was determined by nutrient sources after the passage of typhoons.

Table 2-1. Major phytoplankton species in the pre- and post- typhoon passage (B: Before typhoon, A: After typhoon).

Location	Typhoon	Phytoplankton species		Reference
		B	A	
Puerto Rico		-	<i>Skeletonema</i> spp.	Glynn et al. (1964)
South Carolina	Dennis	<i>Skeletonema</i> spp. <i>Rhizosolenia alata</i> <i>Thalassiothrix</i> sp. <i>Ondontella autita</i>	<i>Skeletonema</i> spp. <i>Rhizosolenia alata</i> <i>Pleurosigma</i> sp. <i>Coscinodiscus</i> sp. <i>Ceratium tirhoceros</i> <i>Gymnodinium</i> sp. <i>Dinophysis caudata</i>	Zeeman (1985)
the Great Barrie Reef		-	<i>Chaetoceros curvisetum</i> <i>Nitzschia</i> sp. small pennate diatoms	Furnas (1989)
the Reef of Tiafura	Wasa	-	<i>Nitzschia closterium</i> <i>Nitzschia bicapitata</i> pennate diatoms	Delessalle et al. (1993)
Northern Taiwan	Tim, Caitlin, Doug and Fred	-	<i>Skeletonema</i> spp. <i>Chaetoceros</i> sp. <i>Nitzschia</i> sp.	Chang et al. (1996)
Kuroshio	Pabuk, Wutip, and Sepat	<i>Tricodesmium</i> sp. (Unicellular cyanobacteria)	<i>Hemiaulus</i> spp. <i>Guinardia</i> sp. <i>Chaetoceros</i> spp.	Chen et al. (2009)
Neuse River Estuary	Helene	Dinoflagellates	<i>Dinoflagellates</i> , <i>cryptophytes</i>	Wetz & Paerl 2008
	Isabel Alex, Bonnie, and Charley	Dinoflagellates Cyanobacteria	<i>Diatoms</i> <i>Cyanobacteria</i> , <i>dinoflagellates</i>	Valdes-Weaver et al. 2006 Wetz & Paerl 2008
Northeast of Taiwan	Morakot	Trichodesmium	<i>Chaetoceros</i> spp.	Chung et al. 2012

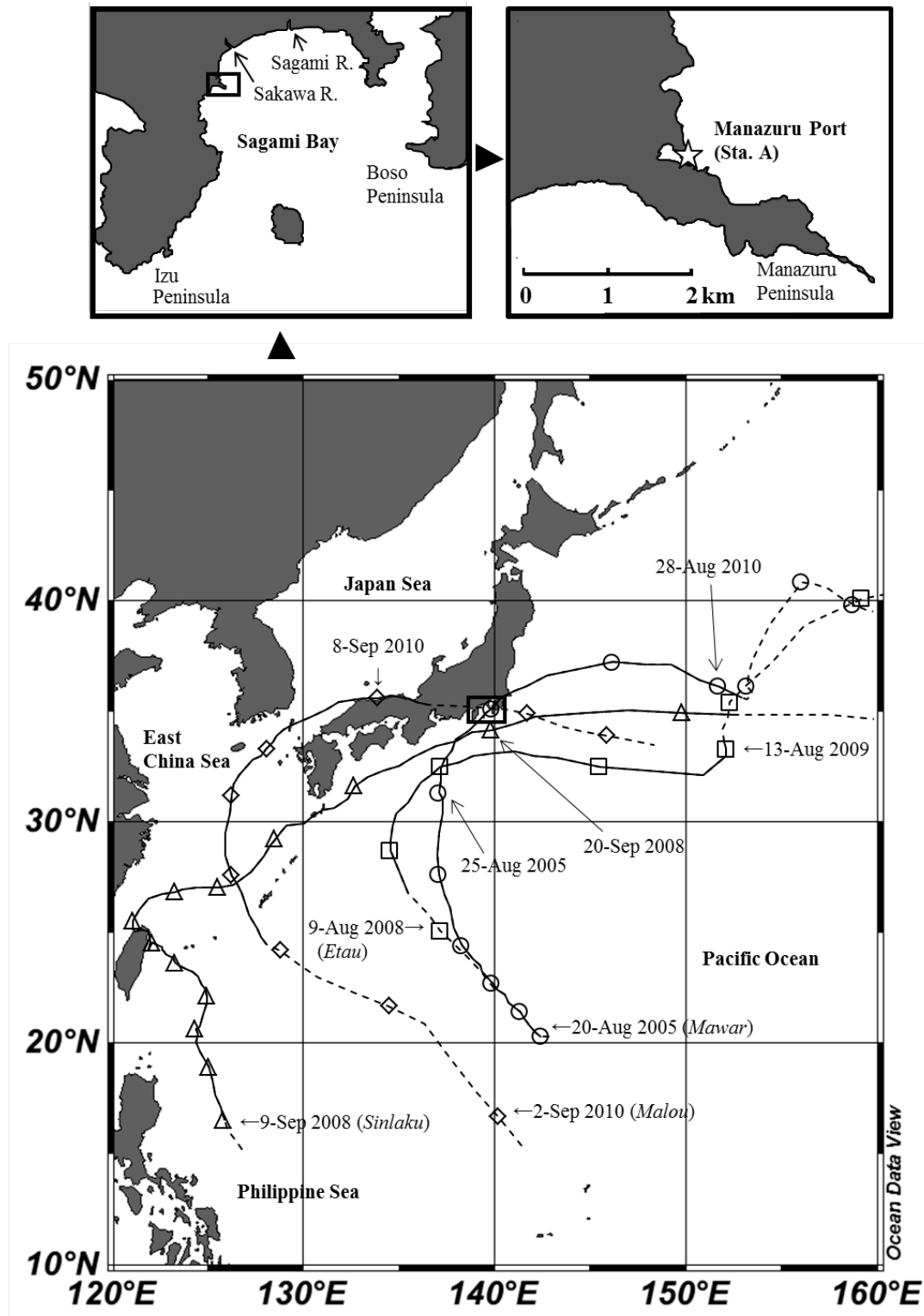


Fig. 2-1 Typhoon tracks and sampling area. Circles, triangles, squares and diamond shapes represents *Mawar*, *Sinlaku*, *Etau* and *Malou* passages, respectively, and each symbol shows the location at 3 am (Data obtained from the Japan Meteorological Agency). Solid lines and dashed lines show typhoons and tropical depression (including extratropical cyclone), respectively

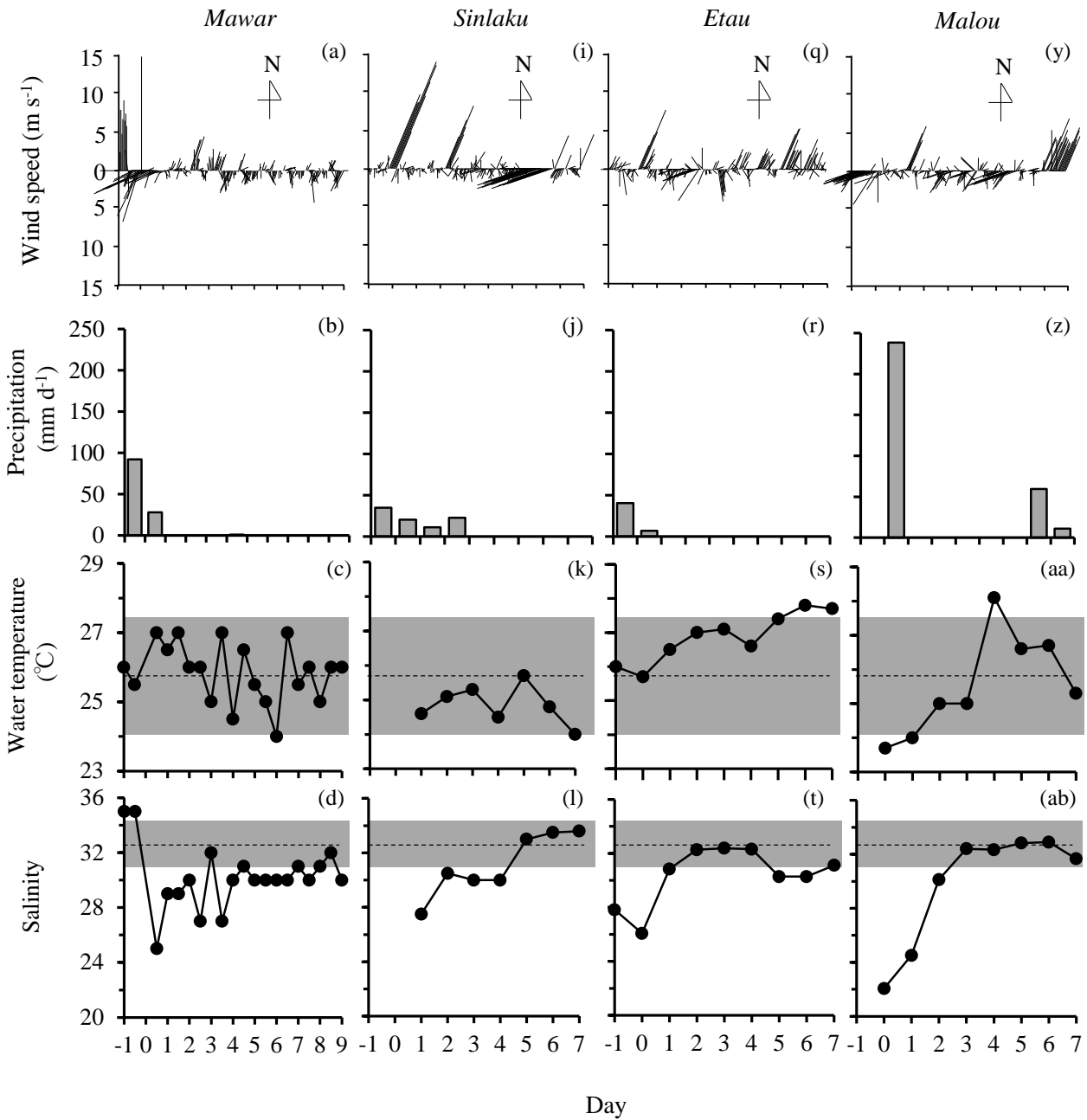


Fig. 2-2 Temporal variations in wind speed, precipitation, water temperature, salinity, NO_2+NO_3 , PO_4 , $\text{Si}(\text{OH})_4$ and N/P ratio in (a-h) *Mawar*, (i-p) *Sinlaku*, (q-x) *Etau* and (y-af) *Malou*. Dashed lines and gray shadows indicate the background data (non-typhoon) and the standard deviations, respectively

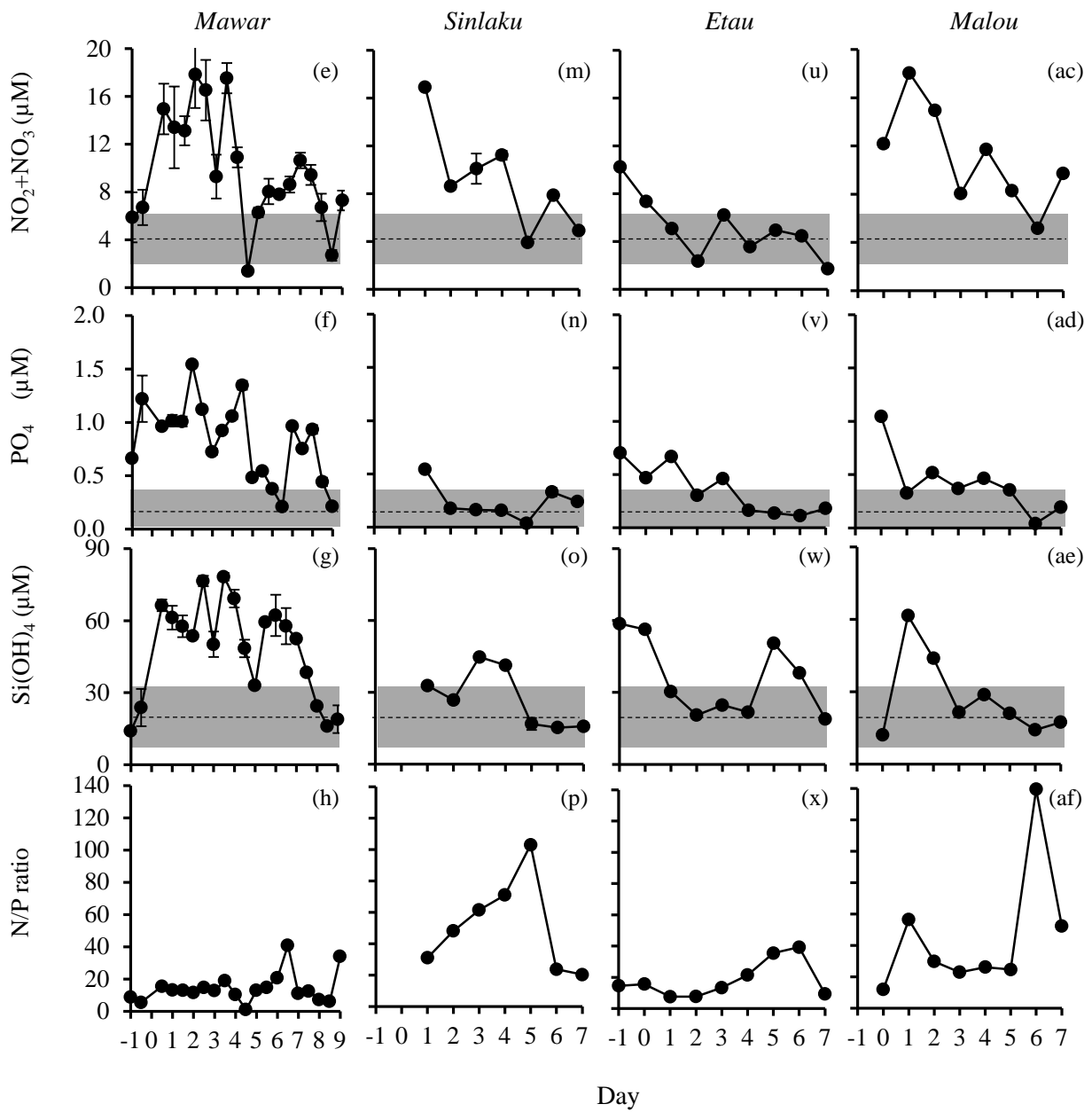


Fig. 2-2 (Continued)

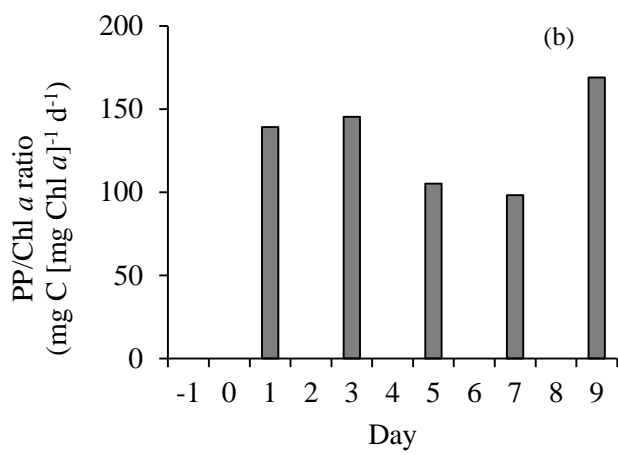
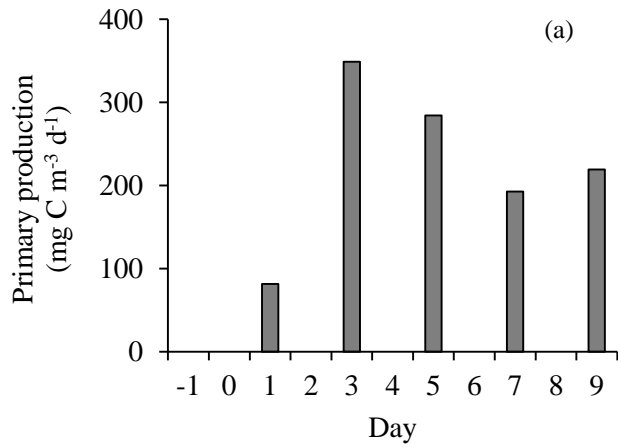


Fig. 2-3 Temporal variations in (a) primary production and (b) ratio of primary production to chlorophyll *a* concentration (PP/Chl *a* ratio) during *Mawar*

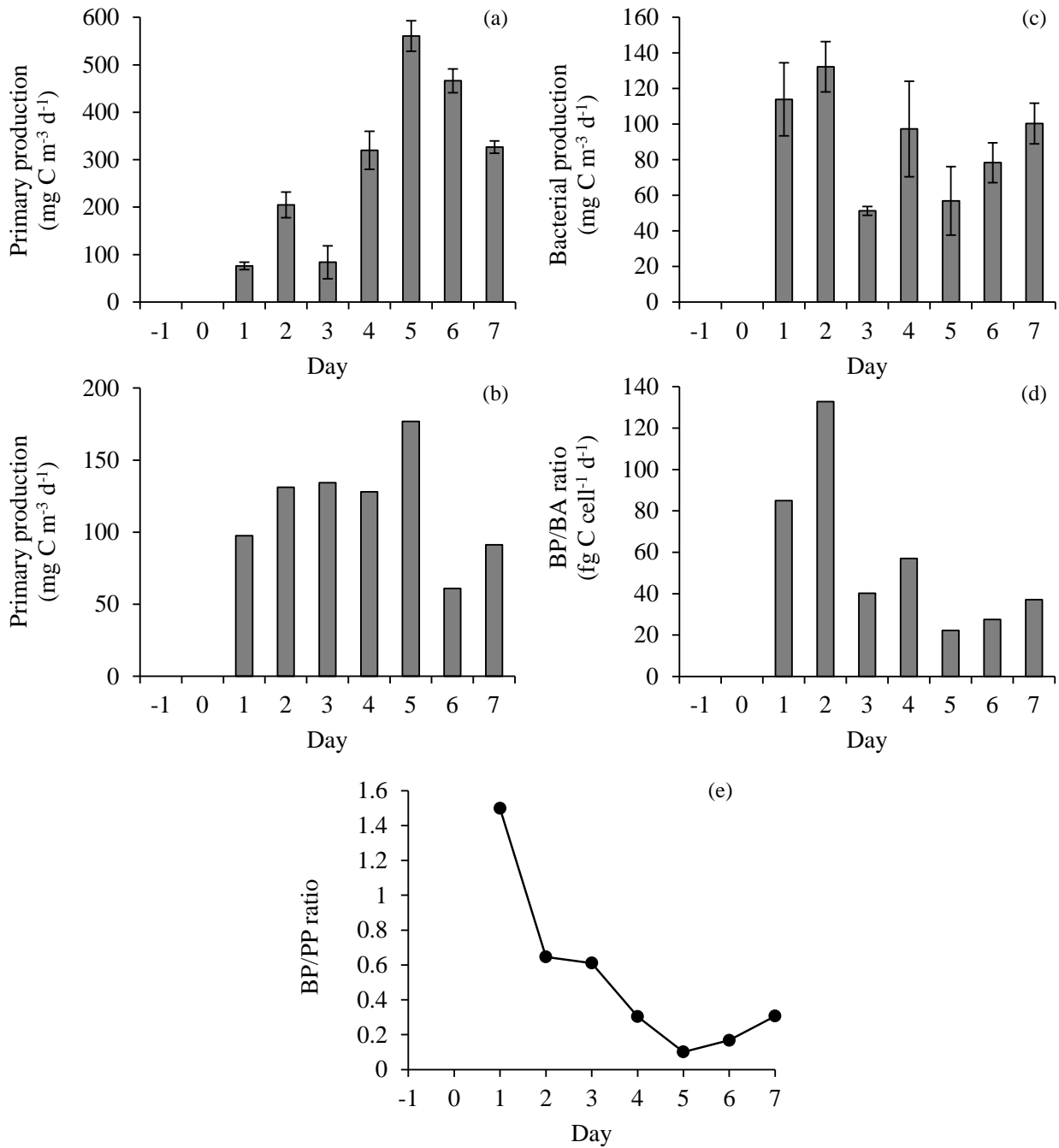


Fig. 2-4 Temporal variations in (a) primary production, (b) ratio of primary production to chlorophyll *a* (PP/Chl *a* ratio), (c) bacterial production, (d) ratio of bacterial production to bacterial abundance (BP/BA ratio) and (e) ratio of bacterial production to primary production (BP/PP ratio) during *Malou*

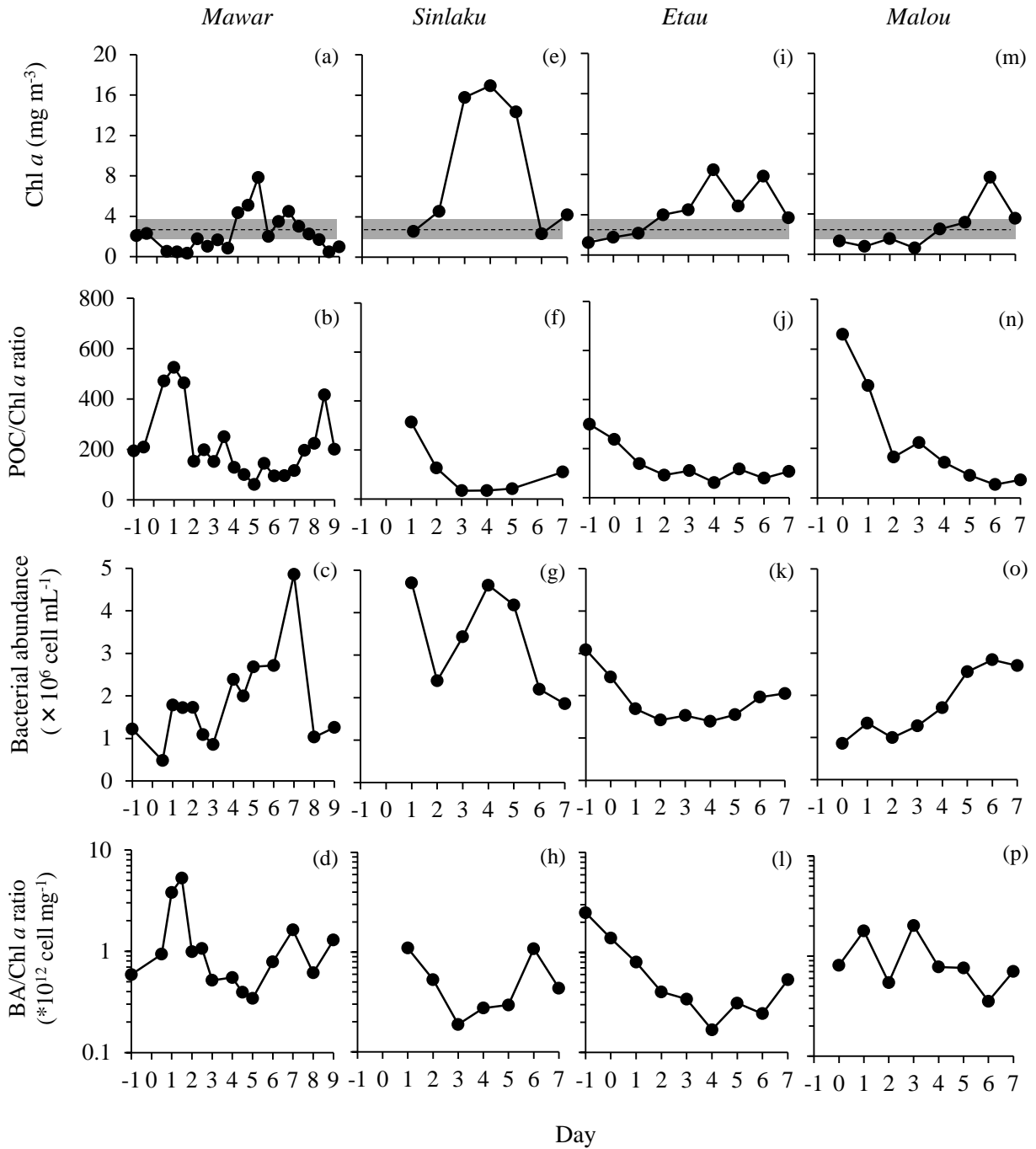


Fig. 2-5 Temporal variations in chlorophyll *a* concentration (Chl *a*), ratio of particulate organic carbon to chl *a* (POC/Chl *a* ratio), bacterial abundance and ratio of bacterial abundance to chl *a* (BA/Chl *a* ratio) in (a-d) *Mawar*, (e-h) *Sinlaku*, (i-l) *Etau* and (m-p) *Malou*. Dashed lines and gray shadows indicate the background data (non-typhoon) and the standard deviations, respectively

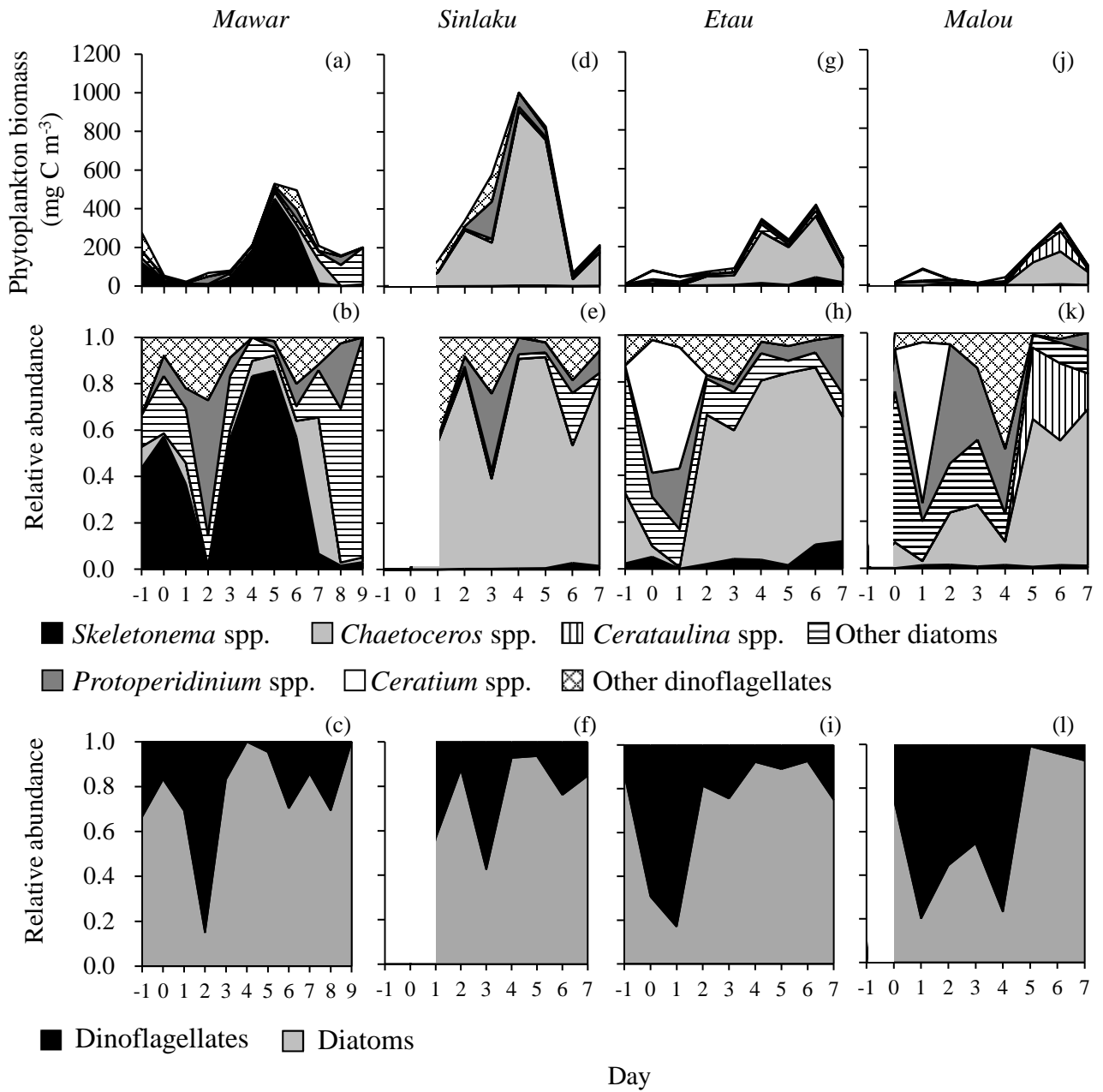


Fig. 2-6 Temporal variations in phytoplankton biomass, relative abundance, and relative diatom and dinoflagellate abundance in (a-c) *Mawar*, (d-f) *Sinlaku*, (g-i) *Etau* and (j-l) *Malou*

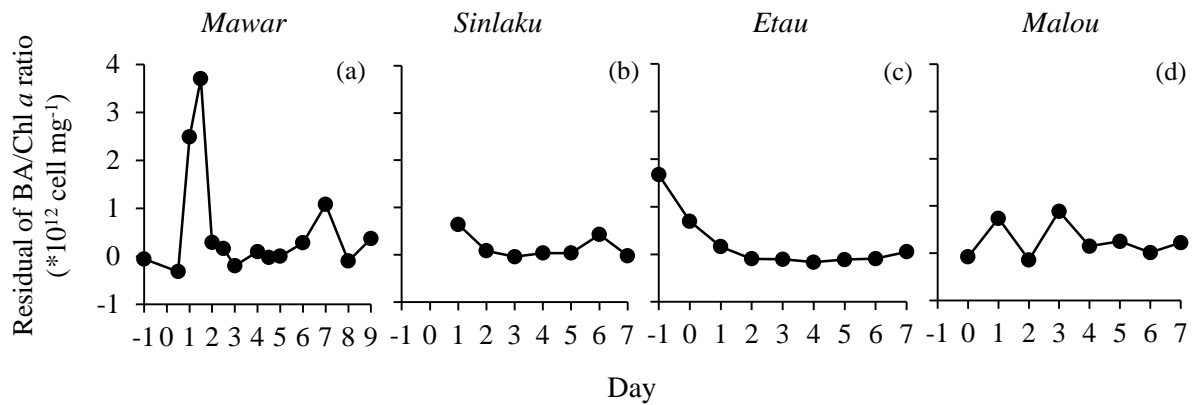


Fig. 2-7 Temporal variations in residual of ratio of bacterial abundance to chlorophyll *a* concentration (BA/Chl *a* ratio) between observed and estimated BA/Chl *a* ratios in (a) *Mawar*, (b) *Sinlaku*, (c) *Etau* and (d) *Malou*. The estimated BA/Chl *a* ratio was calculated using the equation $(\log [\text{BA}; \text{cell mL}^{-1}] = 5.96 + 0.524 \times \log [\text{Chl } a; \text{mg m}^{-3}])$ derived from Cole et al. (1988)

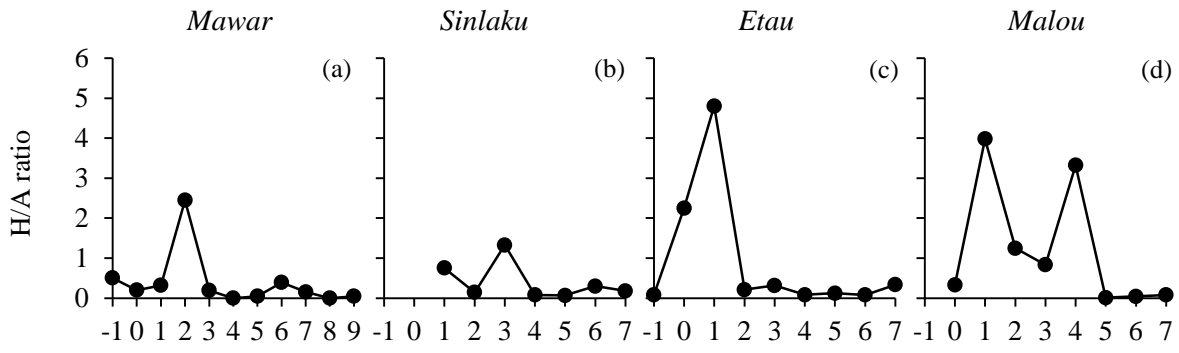


Fig. 2-8 Temporal variations in ratio of mixo- and heterotrophic phytoplankton carbon biomass to autotrophic phytoplankton carbon biomass (H/A ratio) in (a) *Mawar*, (b) *Sinlaku*, (c) *Etau* and (d) *Malou*

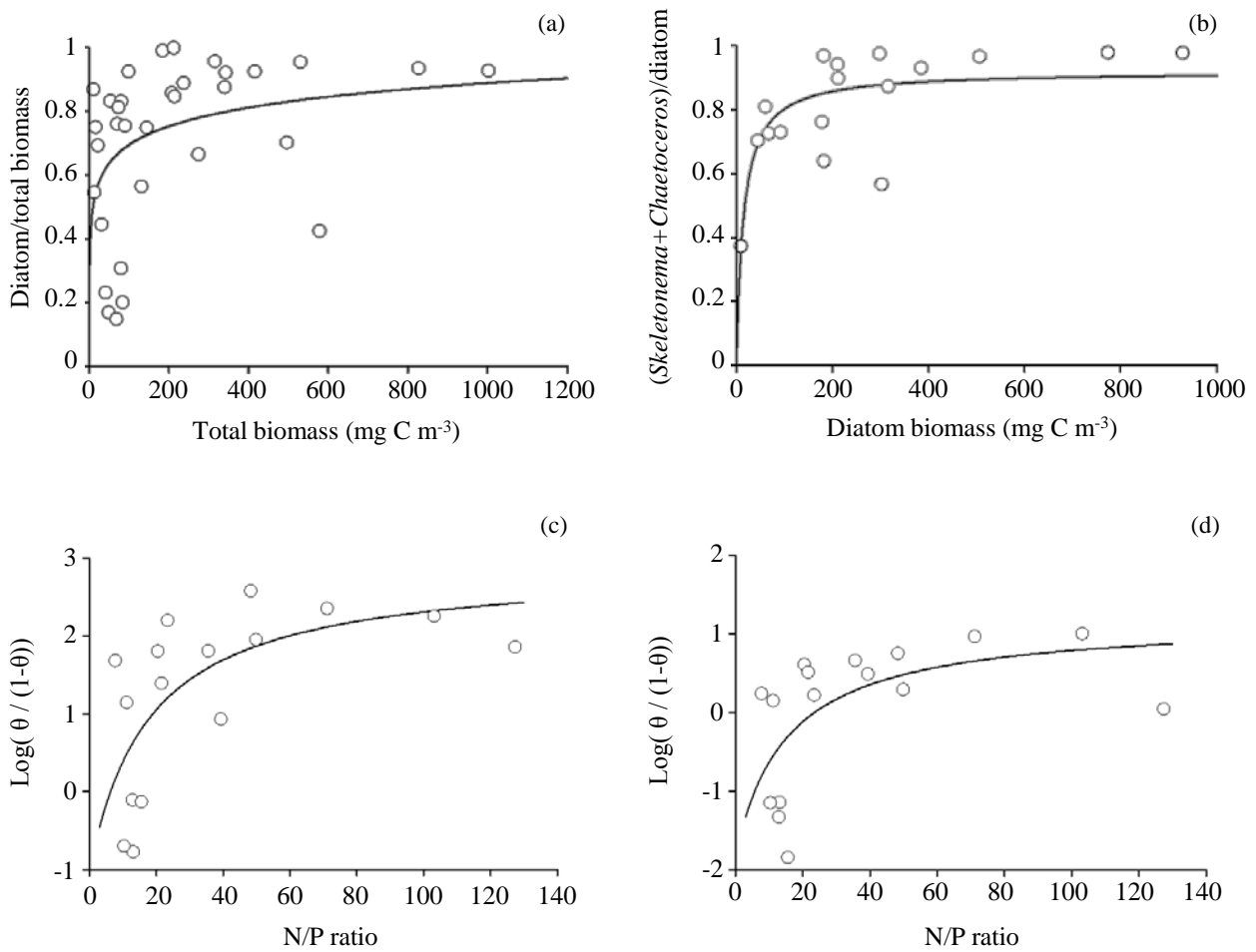


Fig. 2-9 Relationships between (a) Diatom proportion in total biomass and total biomass, (b) proportion of *Skeletonema* + *Chaetoceros* in diatom biomass and diatom biomass, (c) proportion of *Skeletonema* in total biomass and N/P ratio, and (d) proportion of *Chaetoceros* in total biomass and N/P ratio. The regression curves were (a) [Diatom proportion] = $0.31 + 0.084 * \ln$ [Total biomass] ($n = 33, r = 0.39, p < 0.05$), (b) [*Skeletonema* + *Chaetoceros* / diatom biomass] = $0.92 * [\text{diatom biomass}] / (15 + [\text{diatom biomass}])$ ($n = 17, r = 0.75, p < 0.001$), (c) $\log(\theta / (1 - \theta)) = 3.94 \times [\text{N/P}] / ([\text{N/P}] + 17.8) - 1.03$ ($n = 16, r = 0.65, p < 0.05$; $\theta = 1 - \text{dominance of } \textit{Skeletonema} \text{ spp.}$) and (d) $\log(\theta / (1 - \theta)) = 3.00 \times [\text{N/P}] / ([\text{N/P}] + 15.4) - 1.81$ ($n = 16, r = 0.60, p < 0.05$; $\theta = \text{dominance of } \textit{Chaetoceros} \text{ spp.}$). Date of (b) whose total dominance of *Skeletonema* spp. and *Chaetoceros* spp. in the diatom community exhibited more than 50% was used for analyses of (c) and (d)

Chapter III

Vertical and temporal variations of phytoplankton, and microbial processes below the euphotic zone after the passage of typhoon at offshore waters in Sagami Bay, Japan

3.1. Introduction

Some *in situ* studies after the episodic events reported that dinoflagellate dominated the phytoplankton community in coastal regions (Loftus et al. 1972, Zeeman 1985, Webber et al. 1992, Hoover et al. 2006, Tsuchiya et al. 2013b). In Chesapeake Bay, dinoflagellate biomass increased to over 300 mg Chl m⁻³ following a heavy rainfall, with the populations aggregating in the thin buoyant lens of fresher water immediately below the surface (Loftus et al. 1972). In Kaneohe Bay, Hawaii, dinoflagellate *Protoperdinium* spp. and *Ceratium* spp. were dominant after the storm runoff (Hoover et al. 2006). After the runoff, shallow pycnocline with rich nutrients at the surface, and then dinoflagellates might accumulate in the layer using their swimming ability (Donaghay & Osborn 1997). After the dominance of dinoflagellates, diatoms such as *Chaetoceros* spp and *Skeletonema* spp. become dominant (Zeeman et al. 1985, Hoover et al. 2006). Collectively, dinoflagellates use a “swim” strategy, diatoms use a “sink” strategy (Smayda 1997), and diatom and dinoflagellate blooms rarely coincide in coastal systems (Smayda & Trainer 2010), which implies their temporal and vertical habitat segregations. However, the vertical distribution and bloom formation process of diatoms and dinoflagellates after the passage of typhoon are still relatively unknown.

Fates of increased phytoplankton in the euphotic zone after the passage of typhoon have received increased attention in recent years. Some previous studies suggested that high grazing pressure by micro- and mesozooplankton on phytoplankton based on the results of increase of meso- and macrozooplankton biomass (Hoover et al. 2006), abrupt termination of the diatom bloom within 24 h and increase of fecal pellets (Chung et al. 2012), and significantly positive correlation between phytoplankton growth rate and microzooplankton grazing rate through dilution experiments (Zhou et al. 2011). Especially, increase in fecal pellets can accelerate sinking of phytoplankton from euphotic zone to deeper waters (Turner 2002). In an incubation experiment conducted in the East China Sea simulating the passage of typhoon, diatom and ciliate populations

increased, which suggested enhancing biogenic carbon export in the water column (Yasuki et al. 2013). Typhoon-induced diatom blooms are predicted to contribute to sinking POC flux due to their relatively high sinking velocity (Passow 1991, Chen et al. 2009). In the southern East China Sea, typhoon events caused phytoplankton bloom and enhanced POC flux up to 1.7-fold higher than that of the same season when no typhoons occurred (Hung et al. 2010). In addition, in a coastal region, river runoff transports large amount of terrigenous organic matter (e.g. Kao & Liu 1997). These phenomena such as grazing activity, and sinking of phytoplankton, biogenic carbon and detrital POC might influence chemical-biological processes below the euphotic zone. Among them, nutrient regeneration caused by grazing activity and microbial decomposition of organic matter might be progressed below the euphotic zone. However, difficulty of *in situ* sampling after the passage of typhoon have not let us shed a light on the short-temporal variations of chemical-biological processes below the euphotic zone.

In this study, I conducted *in situ* daily observations of physical-chemical environments, phytoplankton and bacteria at an offshore station in Sagami Bay after the passage of typhoon *Malou* in 2010. The aim of the present study was to elucidate bloom formation process and their fate after the passage of typhoon.

3.2. Materials and methods

3.2.1. Typhoon investigated in the present study

Malou occurred in the East of the Philippine Sea as a tropical depression on 3 September 2010. The lowest sea-level pressure of *Malou* was 992 hPa and the maximum wind speed was approximately 25 m s^{-1} . *Malou* passed over the East China Sea, Tsushima Straits and Japan Sea, and then it made landfall from Japan Sea on 8 September 2010. After *Malou* made landfall, it was downgraded to a tropical depression at 12:00 on 8 September 2010.

3.2.2. Study site, sampling procedures and analytical methods

Daily samplings were carried out after the passage of typhoon *Malou* in 2010, at the shelf station (Sta. M, 120 m depth, $35^{\circ} 09.0' \text{ N}$, $139^{\circ} 10.5' \text{ E}$) from 9 to 13 September in 2010 (Fig. 3-1). The sampling at Sta. M was conducted using the R.V. “*Tachibana*” of the Manazuru Marine Laboratory, Yokohama National University. Surface water was collected by means of a bucket while seawater

from 10, 20, 30, 40, 60 and 100 m depths by 5 L Niskin bottles. Collected water samples were pre-screened through 180 μm nylon mesh to remove large zooplankton and debris, and were immediately brought back to the field laboratory (Manazuru Marine Center for Environmental Research and Education, Yokohama National University). In the present study, we defined 8 September in 2010, on which typhoon *Malou* made closest approach to Sagami Bay, as Day 0.

Solar irradiance profiles (at 0.5 m per second) were conducted using the PUV-500 submersible radiometer (Biospherical Instruments, Inc.) in order to determine the attenuation of photosynthetically available radiance (PAR) at Sta. A and Sta. M. The diffuse attenuation coefficient for downwelling irradiance of PAR (K_d) was determined from the slope of the linear regression of natural logarithm of downwelling irradiance against depth assuming that solar irradiance reduces exponentially,

$$E_d(z) = E_d(-0) e^{-K_d z} \quad (1)$$

where $E_d(z)$ is the downwelling irradiance at depth z , and $E_d(-0)$ is the downwelling irradiance just below the surface. From the K_d value, 1% attenuation depth was estimated using Eq. (1). The calculated 1% depth was defined as the “euphotic depth”.

Water temperature, salinity, inorganic macronutrients (NO_2+NO_3 , NH_4 , PO_4 and $\text{Si}(\text{OH})_4$), particulate organic carbon (POC), particulate organic nitrogen (PON), chl *a* concentration, pheopigment concentration, phytoplankton assemblage, primary production, bacterial abundance and bacterial production were investigated for seawater samples. As to river water, water temperature and inorganic macronutrients were measured.

Salinity was obtained using an inductive salinometer (Inductively coupled salinometer model 601 Mk1V, Watanabe Keiki MFG. Co., Ltd.). Triplicate subsamples for inorganic macronutrient analyses were filtered through a 0.45 μm pore size membrane filter (Millex SLHA, Millipore), placed into 10 mL plastic tubes, and stored at -20°C until analysis. The concentrations of NO_2 , NO_3 , NH_4 , PO_4 and $\text{Si}(\text{OH})_4$ were measured as described by Parsons et al. (1984) and Hansen & Koroleff (1999) using a nutrient auto-analyzer (SWAAT, BL TEC). Duplicate subsamples of 300 to 500 mL for POC measurement were filtered onto pre-combusted (450°C , 4 h) glass fiber filters (GF/F, Whatman). The filters were treated with HCl fumes for 2 h to remove inorganic carbon, dried at 60°C for 12 h in a dry oven, and stored in a desiccator until analysis. POC and PON concentrations were determined using an elemental analyzer (Flash EA-1112, Thermo Finningan).

For chl *a* and pheopigment measurements, the seawater subsamples of >100 mL were filtered onto GF/F filters (Whatman) and the filters were immersed in *N,N*-dimethylformamide (DMF) and stored at 4°C for 24 h (Suzuki & Ishimaru 1990). Chl *a* and pheopigment concentrations were determined fluorometrically (Model 10-AU, Turner Design) according to Holm-Hansen et al. (1965).

Primary production was measured using the stable isotope ^{13}C (Hama et al. 1983). Subsamples collected from the surface water were dispensed into acid washed 1 L polycarbonate bottles (three light bottles and one dark bottle), and were incubated *in situ* for 24 h after the addition of ^{13}C -sodium bicarbonate (final ^{13}C atom% of total dissolved inorganic carbon was ~10% of that in the ambient water, Hama et al. 1983). After incubation, particulate matter was filtered onto pre-combusted (450°C, 4 h) GF/F filters (Whatman) to determine the bulk carbon fixation rate. The filters were treated using the same procedure as for the POC measurements described above. The concentration of POC and the isotopic ratios of ^{13}C and ^{12}C were determined by a mass spectrometer (ANCA-MS, Europe Scientific). The primary production was corrected for the rate obtained from the dark bottle.

Samples for phytoplankton taxonomic identification were fixed in a 2% glutaraldehyde solution. Twenty to fifty mL of the phytoplankton sample was poured into a settling chamber (HYDRO-BIOS), and settled for 24 h (Hasle 1978). Identification and enumeration of microphytoplankton species, especially diatoms and dinoflagellates, was conducted using an inverted microscope (Axiovert 25, Carl Zeiss) according to Fukuyo et al. (1990) and Chihara et al. (1997) for dinoflagellates, and Hasle & Syvertsen (1997) for diatoms. Cell volume of each phytoplankton species was calculated according to Hillebrand et al. (1999). Carbon content of diatom and dinoflagellate was also estimated using a regression equation between the cell volume and the carbon content of the cell according to Strathmann (1967). Other phytoplankton taxa were excluded from the analysis due to low abundance.

Samples for bacterial abundance were fixed with pre-filtered (<2 μm) buffered formaldehyde (1% final concentration). For enumeration of bacterial abundance, 1.6-2.0 mL of a formaldehyde-fixed sample was filtered on a 0.2 μm black membrane filter (Isopore, Millipore) and stained with SYBR-Gold (Molecular Probes) following Shibata et al. (2006). Bacteria were counted with an epifluorescence microscope (Axioskop 2 plus, Carl Zeiss).

The sea water samples collected from the surface were dispensed into dark bottles, and were incubated with 20 nM final concentration of bromodeoxyuridine (BrdU; Sigma-Aldrich) at *in situ* temperature for 3 h. BrdU incorporation was halted by adding excess thymidine (100 μ M final) at the end of incubation time. The BrdU incorporation rate was measured by antigen-antibody reaction (Steward & Azam 1999), with a few modifications to the procedure (Hamasaki 2006). BrdU incorporation rates ($\text{pmol L}^{-1} \text{ h}^{-1}$) were converted to thymidine (TdR) incorporation rates ($\text{pmol L}^{-1} \text{ h}^{-1}$) using the conversion equation ($[\text{BrdU}] = 0.80 \times [\text{TdR}] - 0.016$; Hamasaki 2006), and TdR incorporation rates were converted to bacterial cell production using a theoretical conversion factor of $2 \times 10^{18} \text{ cell mol}^{-1}$ (Ducklow & Carlson 1992). For calculating the bacterial carbon production, we used 20 fg C per bacterium as a cell-to-carbon conversion factor (Lee & Fuhrman 1987).

Wind speed and wind direction were obtained from the Japan Meteorological Agency (2011) at the Ajiro Office ($35^{\circ} 02.7' \text{ N}$, $139^{\circ} 05.5' \text{ E}$), and precipitation data were obtained at the Odawara Office ($35^{\circ} 16.6' \text{ N}$, $139^{\circ} 09.3' \text{ E}$). Both observatories are located less than 15 km away from our sampling site. Wind speed and wind direction are mean values per hour. Precipitation is shown as daily integrated values.

3.3. Results

3.3.1. Meteorological and optical parameters

When *Malou* approached Sagami Bay, a west-southwest wind of 8.3 m s^{-1} with gusts to 18.2 m s^{-1} was observed. A maximum precipitation of 238.5 mm d^{-1} was observed on Day 0. From Day 1 to Day 5, there was no precipitation. Before the passage of *Malou*, no rain was observed for 26 days (Japan Meteorological Agency 2011). K_d at Sta. M showed relatively low value, 0.20 m^{-1} , on Day 1, and then generally increased and showed a maximum of 0.29 m^{-1} on Day 4 (Fig. 3-2). The euphotic zone depths were 23 m on Day 1 and 16 m on Day 4.

3.3.2. Physical and chemical parameters

Water temperature at the surface showed 25.2°C on Day 1, and then increased to 28.0°C on Day 4 (Fig. 3-3a). Salinity decreased and reached a minimum of 23.7 on Day 2 at the surface (Fig. 3-3b). And then salinity recovered to 33.0 on Day 5. Based on the results of water temperature and salinity,

upwelling was not likely to occur. Density σ_t at the surface were fluctuated between 14.5 on Day 2 and 21.4 on Day 5, and σ_t at 10 m depth showed values ranging between 22.0 and 22.1 (Fig. 3-3c), which suggested that sharp pycnocline was formed between the surface and 10 m depth. NO_2+NO_3 concentration increased to $26.8 \pm 0.1 \mu\text{M}$ with decrease in salinity at the surface on Day 2 (Fig. 3-3d). The NO_2+NO_3 concentration decreased abruptly in the euphotic zone, and showed a minimum value of $0.26 \pm 0.0 \mu\text{M}$ at 10 m depth on Day 5. NH_4 concentration increased to $1.81 \pm 0.25 \mu\text{M}$ at the surface on Day 2 (Fig. 3-3e). As day passed after the passage of *Malou*, the NH_4 concentration increased below the euphotic zone. PO_4 concentration showed relatively high values of 0.25 ± 0.05 and $0.31 \pm 0.01 \mu\text{M}$ at the surface on Day 1 and Day 2, respectively (Fig. 3-3f). From Day 3, the PO_4 concentrations were generally less than $0.05 \mu\text{M}$ in the euphotic zone. Si(OH)_4 concentration showed a maximum of $56.2 \pm 4.7 \mu\text{M}$ at the surface on Day 2 (Fig. 3-3g). The Si(OH)_4 concentrations at 10 and 20 m depths were relatively low values, $1.0 \pm 0.8 \mu\text{M}$ during the sampling period.

3.3.3. Bacterial abundance and bacterial production

Bacterial abundance showed relatively high value mainly in the euphotic zone (Fig. 3-4a). From Day 4, the abundance increased and showed $1.43 \pm 0.60 \times 10^6 \text{ cell mL}^{-1}$ on average below the euphotic depth, which was significantly higher compared to the average value, $0.85 \pm 0.35 \times 10^6 \text{ cell mL}^{-1}$, from Day 1 to Day 3 below the euphotic depth (Student t-test, $p < 0.01$). Bacterial production at the surface showed a maximum of $48 \pm 10 \text{ mg C m}^{-3} \text{ d}^{-1}$ on Day 4 and a minimum of $21 \pm 7 \text{ mg C m}^{-3} \text{ d}^{-1}$ on Day 5 (Fig. 3-5a). BP/BA ratio also showed similar variations of BP, showing a maximum of $31.4 \text{ fg C cell}^{-1} \text{ d}^{-1}$ on Day 4 and a minimum of $10.7 \text{ fg C cell}^{-1} \text{ d}^{-1}$ on Day 5 (Fig. 3-5a).

3.3.4. Chl *a* concentration, pheopigment concentration, POC and primary production

Chl *a* concentration in the euphotic zone from Day 1 to Day 3 showed $1.5 \pm 0.6 \text{ mg m}^{-3}$ on average (Fig. 3-4b), and showed a maximum of 8.0 mg m^{-3} on Day 4. From Day 4 to Day 5, relatively high chl *a* concentrations were observed below the euphotic zone. Pheopigment concentration in the euphotic zone from Day 1 to Day 3 showed 0.50 mg m^{-3} on average (Fig. 3-4c), and showed a maximum of 1.3 mg m^{-3} at 30 m depth on Day 5. From Day 4, relatively high pheopigment

concentrations were observed below the euphotic zone.

POC concentration increased mainly in the euphotic zone, showing a maximum of 735 mg C m⁻³ at the surface on Day 4 (Fig. 3-4d). In addition, the concentration increased below the euphotic zone on Day 5, and showed 197 ± 28 mg C m⁻³ on average below 30 m depth, which was significantly higher compared to the average value, 100 ± 31 mg C m⁻³, from Day 1 to Day 4 below 30 m depth (Student t-test, $p < 0.001$). C/N ratio in the euphotic zone showed 8.2 ± 0.8 during the study period (Fig. 3-4e). The ratio below the euphotic zone from Day 4 (8.4 ± 1.1) was similar to that of the euphotic zone.

Primary production at the surface reached a maximum of 512 mg C m⁻³ d⁻¹ on Day 4, and showed a minimum of 99 mg C m⁻³ d⁻¹ on Day 5 (Fig. 3-5b). PP/Chl *a* ratio showed relatively high values on Day 1 and reached a maximum of 135 mg C [mg Chl *a*]⁻¹ d⁻¹ on Day 2 (Fig. 3-5b). PP/Chl *a* ratio gradually decreased from Day 3, and then showed a minimum of 18 mg C [mg Chl *a*]⁻¹ d⁻¹ on Day 5. Ratio of BP to PP (BP/PP ratio) at the surface showed 0.13 ± 0.05 during the study period (Fig. 3-5c).

3.3.5. Phytoplankton assemblage

Diatom biomass showed 32.6 ± 7.4 mg C m⁻³ on average at 10 and 20 m depths from Day 1 to Day 2 (Fig. 3-4f). Thereafter, the diatom biomass showed maximums of 432 mg C m⁻³ at 10 m on Day 4 and 531 mg C m⁻³ at the surface on Day 5. This diatom bloom from Day 4 was contributed to by *Chaetoceros* spp., *Cerataulina* spp. and *Rhizosolenia* spp. (Fig. 3-4g, h, i). The diatom community also prevailed below the euphotic zone on Day 4 and Day 5.

Dinoflagellate communities were distributed mainly at the surface (Fig. 3-4j). The biomass of dinoflagellate at the surface showed 13.1 mg C m⁻³ on Day 1, increased to a maximum of 177 mg C m⁻³ on Day 4. In the dinoflagellate community, *Protoperdinium* spp. were dominant from Day 1 to Day 3 (Fig. 3-4k), and then *Prorocentrum* spp. and *Ceratium* spp. became dominant and reached maximum at the surface on Day 4 (Fig. 3-4l, m). The dinoflagellate community dominated the phytoplankton assemblage at the surface from Day 1 to Day 3 (81 ± 19 %, Fig. 3-4n), while diatom highly dominated from Day 4 in the whole water column (90.1 ± 12.4, Fig. 3-4j). Integrated phytoplankton carbon biomass below the euphotic zone on Day 4 and 5 (3402 mg C m⁻² on average) was higher compared to those from Day 1 to Day 3 (473 ± 159 mg C m⁻² on average).

PC/POC ratios from Day 4 to Day 5 in the euphotic zone (0.77 ± 0.46) and below the euphotic zone (0.35 ± 0.34) were significantly higher compared to those from Day 1 to Day 3 in the euphotic zone (0.14 ± 0.11) and below the euphotic zone (0.07 ± 0.04), respectively (Student's t-test, both are $p < 0.01$; Fig. 3-4o).

3.4. Discussion

Typhoon *Malou* investigated in the present study was characterized by intense rainfall of 238.5 mm in one day. At Sta. M located 2 km off the coast, salinity minimum was observed at the surface on Day 2, suggesting that significant influxes of river runoff reached the offshore station in two days. The sharp pycnocline formed by terrestrial runoff and increase of water temperature caused by sunny days after the passage of *Malou* might increase vertical stratification at the surface at Sta. M. According to temporal and vertical variations of water temperature and salinity at Sta. M, upwelling did not occur after the passage of *Malou*. In addition, typhoon-induced wind could not induce sediment resuspension at Sta. M. In order to examine the possible nutrient source, nutrient-salinity relationships at the surface water were plotted (Fig. 3-6). Solid lines designated conservative mixing relationships for nutrients assuming river and ocean end-members. Nutrient concentrations at the mouth of Sakawa River just after the passage of *Malou* were used for the river end-member, and concentrations of zero nutrients at salinity 34.5 were assumed for the ocean end-member. Nutrients at the surface of Sta. M after the passage of *Malou* were well related to the lines, suggesting that the most important possible nutrient sources might be river water.

The BP/PP ratios at the surface of 0.13 ± 0.05 (Fig. 3-5c) were similar to the value reported by Cole et al. (1988) and Ducklow (1999). They suggested two possibilities that BP/PP ratio generally ranges from 0.1 to 0.3: either (1) that both bacteria and phytoplankton grow in response to common factors (nutrient load, temperature, etc.); or (2) that phytoplankton or material produced by phytoplankton are important substrates for bacterial growth (Larsson & Hagström 1979, Fallon & Brock 1980, Cole et al. 1984). After typhoon *Herb* in 1996 in Taiwan Strait, both primary production and bacterial production increased, however the BP/PP ratio showed relatively consistent value, 0.34 at no typhoon condition and 0.24 after typhoon (Shiah et al. 2000). They suggested that the increase in bacterial production was due to the consumption of (1) labile organic matter derived from algal cells and other fragile planktonic organisms severely damaged by

typhoon-induced strong turbulence, (2) dissolved organic matter (DOM) released from actively growing phytoplankton and other planktonic organisms and (3) DOM from terrestrial inputs and sediment resuspension (Shiah et al. 2000). In the present study, the BP/BA ratio at the surface was not correlated to salinity and terrestrial runoff could not occur due to the depth (120 m), which suggested that allochthonous substrates did not support the bacterial growth. The BP/BA ratio was significantly correlated to primary production at the surface ([BP/BA ratio] = $0.056 \times [PP] + 2.1$; $n = 5$, $r = 0.953$, $p < 0.05$), which evidenced the importance of autochthonous substrates derived from phytoplankton for bacterial growth rather than allochthonous substrates at the surface of Sta. M.

PP/Chl *a* ratio at the surface from Day 1 to Day 4 (118 ± 24 mg C [mg Chl *a*]⁻¹ d⁻¹, Fig. 3-5b) was higher than the mean assimilation number, 40 ± 28 mg C mg chl *a*⁻¹ d⁻¹, observed in August and September in Sagami Bay (Student's t-test, $p < 0.01$) reported by Sugawara et al. (2003). On the other hand, the PP/Chl *a* ratio on Day 5 decreased to 18 mg C [mg Chl *a*]⁻¹ d⁻¹ probably due to the nutrient depletion (Fig. 3-3). The results suggest that the primary productivity was enhanced by the passage of *Malou* from Day 1 to Day 4. When the primary production is integrated during the enhanced period, the integrated primary production reaches 1.31×10^3 mg C m⁻³ for 4 days, which accounts for 4.5-5.7% of the annual primary production upper waters of Sagami Bay [annual primary production values were derived from Satoh et al. 2000 (2.92×10^4 mg C m⁻³ yr⁻¹), Sugawara et al. 2003 (2.30×10^4 mg C m⁻³ yr⁻¹) and Ara & Hiromi 2009 (2.82×10^4 mg C m⁻³ yr⁻¹)]. Although the Sta. M is located 2 km off the coast, the contribution of increased primary production of Sta. M to annual primary production is significant as well as Sta. A (Tsuchiya et al. 2013a).

As to phytoplankton assemblage, noticeable surface maximum of dinoflagellate was observed at Sta. M (Fig. 3-4j). Typhoon-induced runoff contributed to formation of low salinity water layer, in other words, sharp pycnocline at the surface. In addition, the surface layer contained high nutrient concentrations. It is known that the swimming behavior of dinoflagellates could serve to concentrate cells into the surface layer (Donaghay & Osborn, 1997). In addition, Ryther (1955) reported that harmful algal blooms is frequently formed in the pycnocline of coastal systems after heavy rainfall, calm sunny weather, influxes of estuarine waters, or interactions between dissimilar water masses. Some previous studies also reported the dominance of dinoflagellates after runoff induced by episodic storm events (Loftus & Seliger 1976, Zeeman 1985, Webber et al. 1992,

Hoover et al. 2006). Therefore, the results of the present study suggest that dinoflagellates accumulated and increased into the surface layer, which resulted in their dominance in the phytoplankton community after the passage of typhoon.

Dinoflagellates increase their biomass through photosynthesis (autotrophic), feeding organic substrates (heterotrophic) and both (mixotrophic). *Protoberidinium* spp. are considered as heterotrophic dinoflagellate due to lack of chloroplasts (e.g. Jacobson & Anderson 1986). As to vertical distribution of the taxa, the heterotrophic dinoflagellates mainly increased in numbers with depth or were randomly distributed, whereas autotrophic dinoflagellates mainly decreased in numbers with depth or were aggregated in their distribution at Aarhus Bay, Denmark (Mouritsen & Richardson 2003). At Sta. M in Sagami Bay, *Protoberidinium* spp. formed subsurface maximum during the non-typhoon period (unpublished data). In the present study, however, *Protoberidinium* spp. were distributed at the surface as well as autotrophic or potentially mixotrophic dinoflagellates such as *Prorocentrum* spp., and *Ceratium* spp. after the passage of *Malou* (Fig. 3-4k, l, m). These phototrophic dinoflagellates were likely to accumulate into the surface layer in order to utilize the abundant nutrients and light, whereas *Protoberidinium* spp. were accumulated into the surface layer in order to efficiently feed on prey organisms produced at the surface and/or organic substrates loaded by runoff. Zeeman (1985) suggested that one of the explanations for dominance of dinoflagellates after the passage of typhoon was utilization of organic matter by dinoflagellates for nutrition. Therefore, physical (i.e. sharp pycnocline at the surface induced by runoff) and biological (i.e. their swimming or physiological characteristics) interactions might make the concentrated layer of dinoflagellates at the surface just after the passage of *Malou*.

The dominant taxa at the surface started to change from dinoflagellates to diatoms from Day 4 at Sta. M (Fig. 3-4n). The dominances of diatoms after the passage of typhoons have been reported in various regions (Glynn et al. 1964, Zeeman 1985, Furnas 1989, Chang et al. 1996, Chen et al. 2009, Chung et al. 2012). Some prior studies imply that increased diatoms tend to sink and contribute to POC flux after the passage of typhoon (e.g. Chen et al. 2009). As to vertical distribution of diatoms, relatively high biomass was observed in the euphotic zone from Day 1 to Day 3. However, from Day 4 they prevailed below the euphotic zone during the bloom in addition to in the euphotic zone, which suggests that increased diatoms in the euphotic zone might sink or be advected to deeper water. In addition, the PC/POC ratio below the euphotic zone to 40 m depth on

Day 4 and Day 5 showed $54.3 \pm 35.1\%$, which suggests that phytoplankton contributed to approximately half of the POC below the euphotic zone (Fig. 3-4o). These results might reflect swim strategy for dinoflagellates and sink strategy for diatoms, as suggested by Smayda (1997).

In terms of fate of phytoplankton after the passage of typhoon, Chung et al. (2012) observed termination of diatom bloom and concurrent increase in copepods and fecal pellets after the passage of typhoon *Morakot* in the subtropical Northwest Pacific, and suggested that intensive grazing pressure was the main cause of the termination of diatom bloom. After the passage of typhoon *Fengshen* in northeastern South China Sea, the dilution experiments showed that the microzooplankton grazing rate was significantly positively correlated to phytoplankton growth rate (Zhou et al. 2011). In southern Kaneohe Bay, Hawaii, a storm-runoff event caused phytoplankton bloom, and then copepods and appendicularians were increased (Hoover et al. 2006). Pheopigments are known to be direct products of zooplankton grazing, and serve as a tag for herbivorous grazing (Shuman & Lorenzen 1975, Welschmeyer et al. 1984, Welschmeyer & Lorenzen 1985). In the present study, pheopigment concentrations increased and showed a maximum on Day 5 at Sta. M accompanied by phytoplankton bloom (Fig. 3-4c), which suggests that zooplankton grazing pressure on phytoplankton might have intensified.

Integrated bacterial abundance in the euphotic zone and below the euphotic zone showed clear increasing trend at Sta. M, and reached maximum of 111×10^{12} cell m^{-2} below the euphotic zone on Day 4 and 150×10^{12} cell m^{-2} in the whole water column on Day 5 (Fig. 3-7a). Integrated NH_4 also increased and reached maximum of 50.6 mmol m^{-2} below the euphotic zone and 67.5 mmol m^{-2} in the whole water column on Day 5 (Fig. 3-7b). The results suggest that microbial process was activated and rapid regeneration of NH_4 was occurred below the euphotic zone. There are significant positive correlations between bacterial abundance and pheopigment concentration ($[BA] = 1.3 \times [pheopigment] + 0.5$, $n = 22$, $r = 0.78$, $p < 0.001$; Fig. 3-8a), between bacterial abundance and chl *a* concentration ($[BA] = 0.47 \times [Chl\ a] + 0.78$ ($n = 21$, $r = 0.70$, $p < 0.001$; Fig. 3-8b) and between bacterial abundance and NH_4 concentration ($[BA] = 0.88 \times [NH_4] + 0.67$, $n = 22$, $r = 0.64$, $p < 0.01$; Fig. 3-8c) below the euphotic zone, whereas there was no significant correlation between pheopigment concentration and NH_4 concentration below the euphotic zone. These relationships suggest that bacterial activity was associated with zooplankton grazing and sunk/advection phytoplankton decomposition, and bacteria was a main component to contribute to

regeneration of NH_4 . Below the euphotic zone, NH_4 regeneration by the $<1 \mu\text{m}$ size fraction was approximately 75% of that in the larger size fractions, and remineralization below the euphotic zone can be achieved principally by bacteria (Probyn 1987). The relationship between BA and NH_4 (Fig. 3-8c) can be interpreted as evidence for a direct role of bacteria in NH_4 recycling, or an indirect role through regeneration by bacterivorous protozoa (Newell et al. 1988). An average of 80% of the dissolved organic nitrogen used by bacteria was converted to NH_4 , showing simultaneous assimilation and regeneration of NH_4 by the natural microbial population (Tupas & Koike 1991). The results in the present study suggest that produced organic matter such as phytoplankton in the euphotic zone induced rapid microbial activity below the euphotic zone just after the passage of typhoon.

In conclusion, *Malou* passage caused nutrient loadings to the offshore station through terrestrial runoff. Primary production was significantly enhanced, and might contribute up to 5.7% of the annual primary production in the upper waters of Sagami Bay as well as the inshore station. Bacterial production at the surface might depend on autochthonous substrate derived from phytoplankton. As to phytoplankton community, dinoflagellates dominated at the surface just after the passage of typhoon, which suggested that dinoflagellates swam and accumulated into the nutrient-rich surface pycnocline layer formed by typhoon-induced runoff. From Day 4, diatoms dominated the phytoplankton community in whole water column, and a certain part of the produced diatoms in the euphotic zone contributed to increase of POC below the euphotic zone. Accompanied by phytoplankton bloom, increase in pheopigment concentration indicated intensification of zooplankton grazing pressure on phytoplankton. Below the euphotic zone, both of NH_4 concentration and bacterial abundance increased, and showed significant positive correlation between them, which suggested that bacterial NH_4 regeneration was progressed. The present study suggested that typhoon passage could profoundly affect biogeochemical cycles not only in the euphotic zone but also even below the euphotic zone in coastal waters.

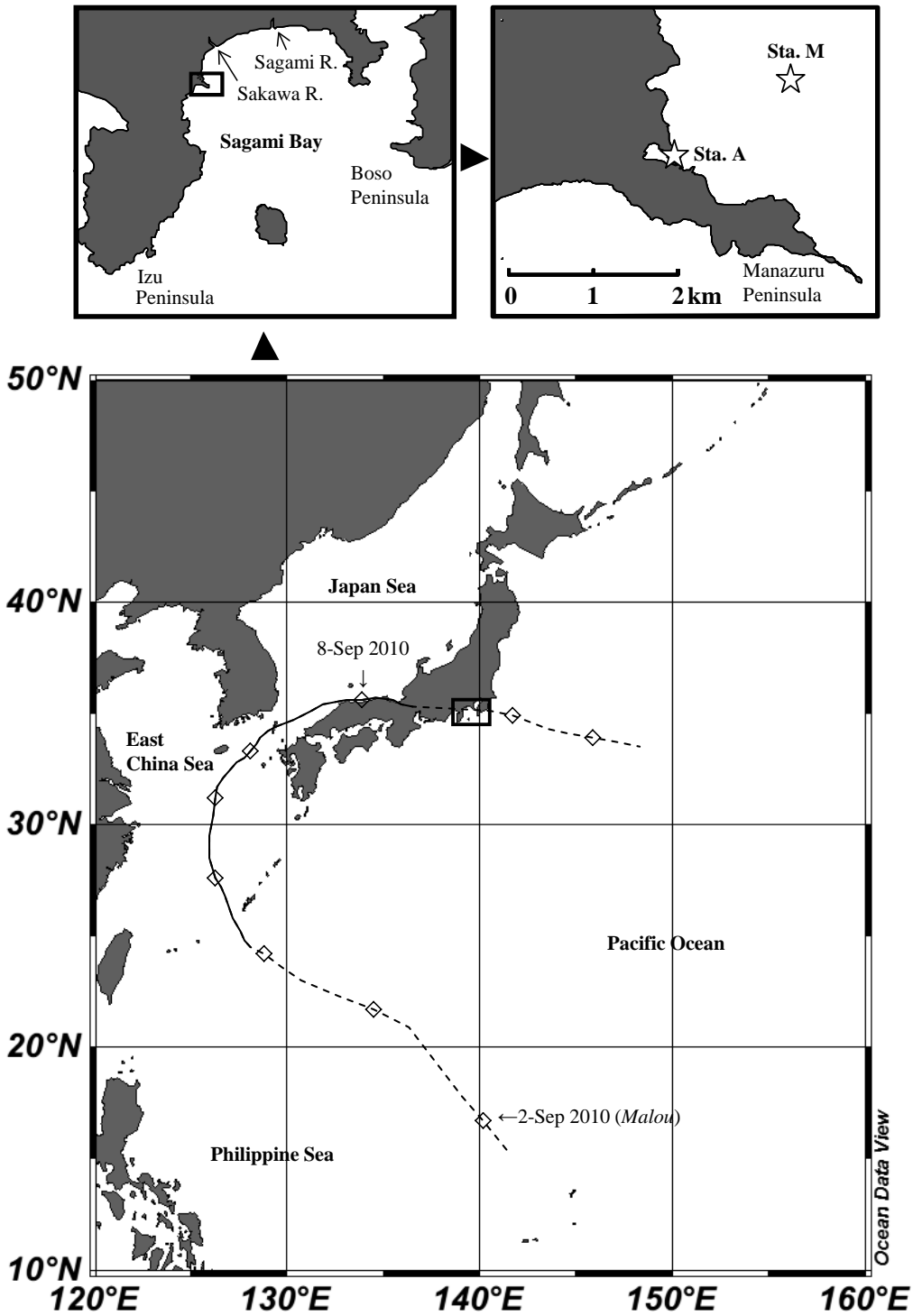


Fig. 3-1 Typhoon tracks and sampling area. Circles, triangles, squares and cross marks represents *Mawar*, *Sinlaku*, *Etau* and *Malou* passages, respectively, and each symbol shows the location at 3 am (Data obtained from the Japan Meteorological Agency). Solid lines and dashed lines show typhoons and extratropical cyclone, respectively

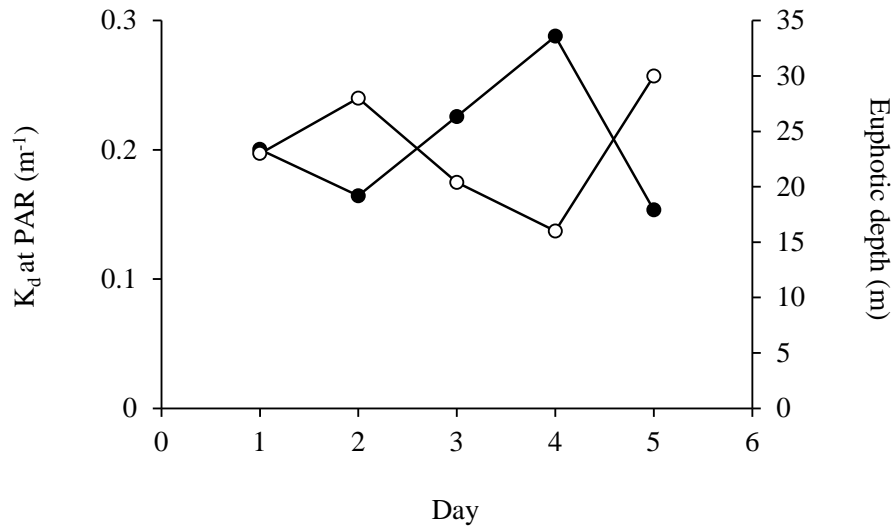


Fig. 3-2 Temporal variations in diffuse attenuation coefficient at PAR (K_d) and euphotic depth. Closed and open circles represent K_d and euphotic depth, respectively

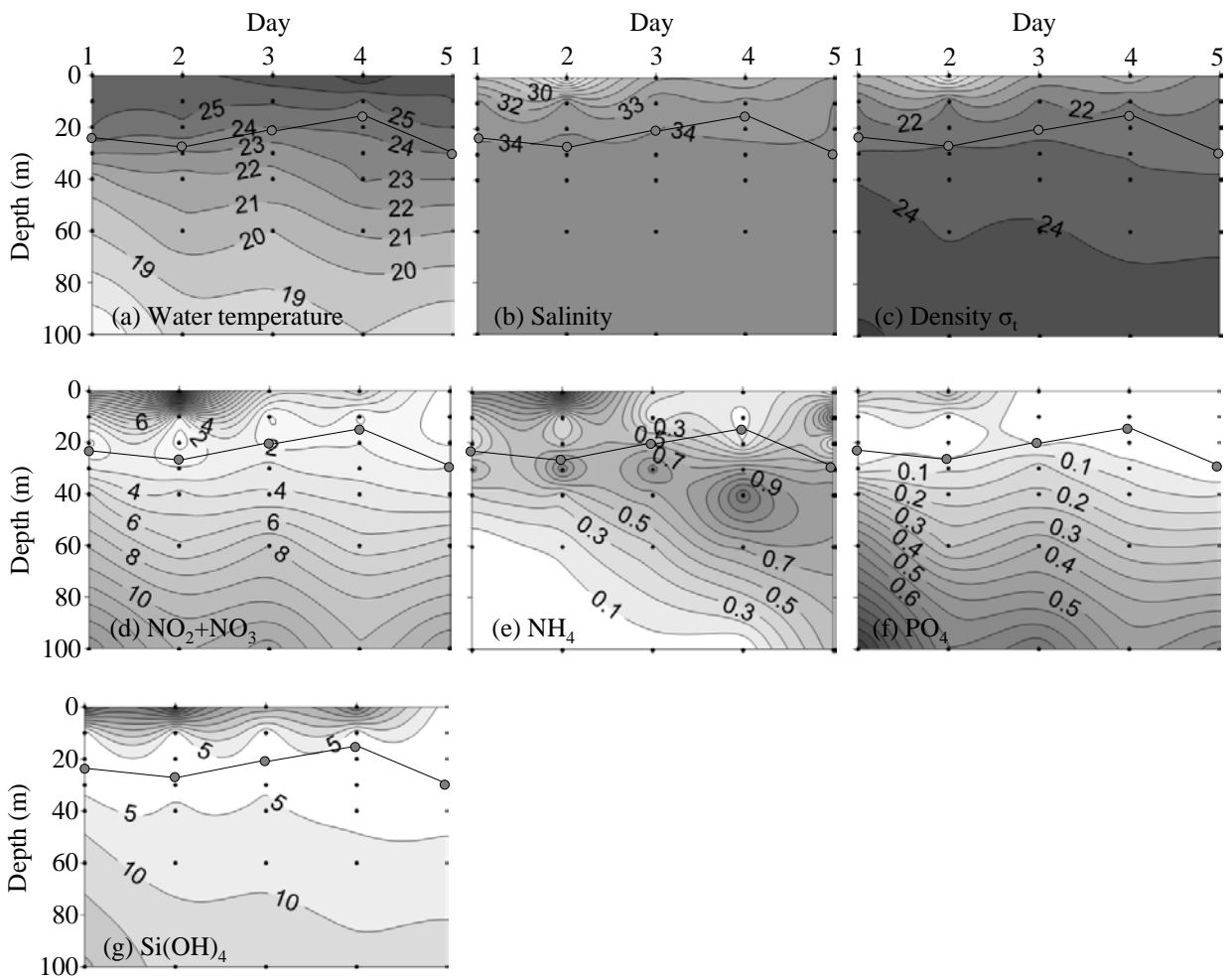


Fig. 3-3 Temporal and vertical variations in (a) water temperature ($^{\circ}\text{C}$), (b) salinity, (c) density σ_t , (d) $\text{NO}_2 + \text{NO}_3$ (μM), (e) NH_4 (μM) (f) PO_4 (μM) and (g) Si(OH)_4 (μM) at Sta. M. Solid lines with gray symbols indicate the euphotic depth (1%)

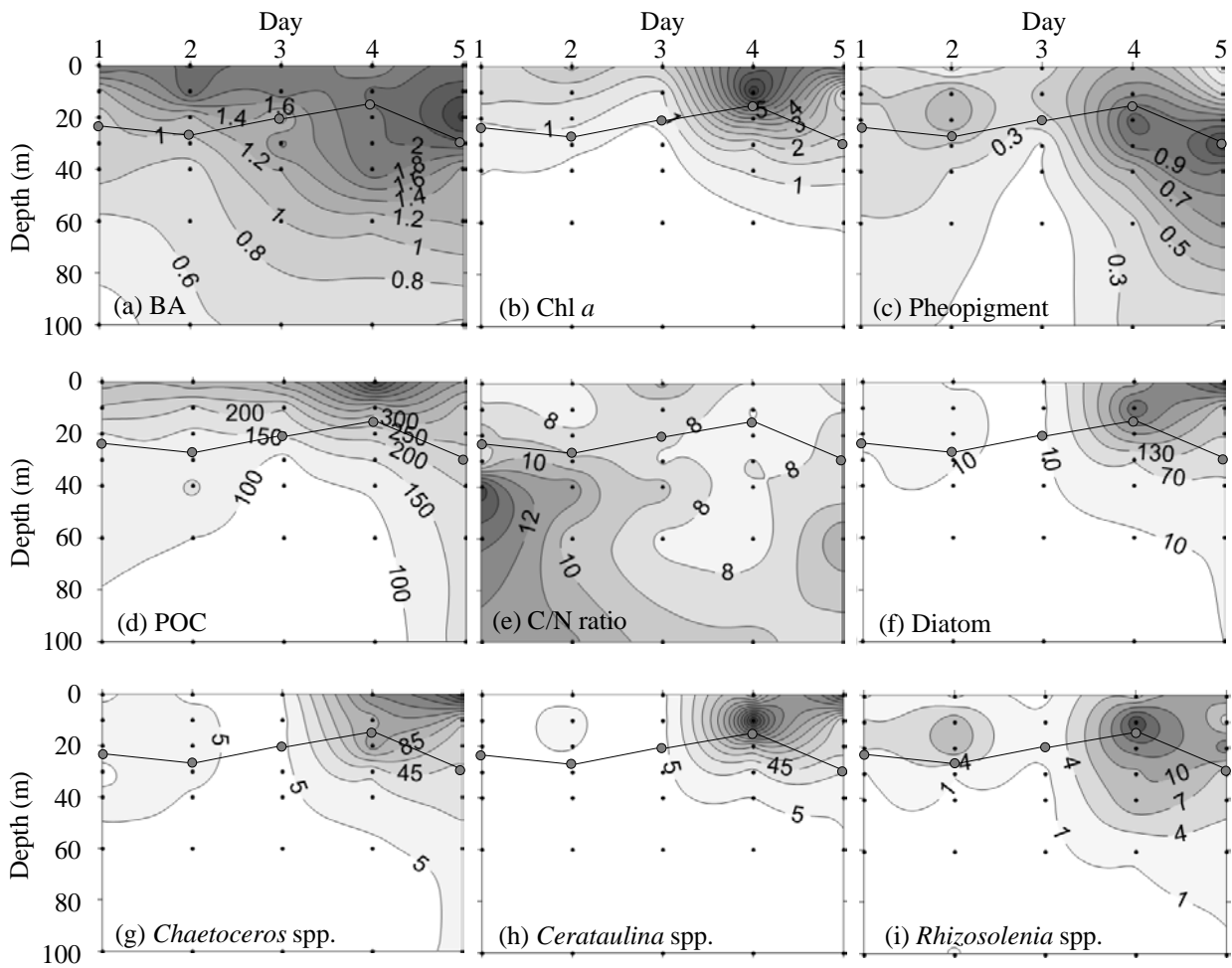


Fig. 3-4 Temporal and vertical variations in (a) bacterial abundance (BA, 10^6 cell mL^{-1}), (b) chl *a* concentration (mg m^{-3}), (c) pheopigment concentration (mg m^{-3}), (d) particulate organic carbon (POC, mg C m^{-3}), (e) ratio of POC to particulate organic nitrogen (C/N ratio, atomic ratio), (f) diatom (mg C m^{-3}), (g) *Chaetoceros* spp. (mg C m^{-3}), (h) *Cerataulina* spp. (mg C m^{-3}), (i) *Rhizosolenia* spp. (mg C m^{-3}), (j) dinoflagellate (mg C m^{-3}), (k) *Protoperidinium* spp. (mg C m^{-3}), (l) *Prorocentrum* spp. (mg C m^{-3}), (m) *Ceratium* spp. (mg C m^{-3}), (n) ratio of dinoflagellate to total phytoplankton (dinoflagellate dominance) and (o) ratio of phytoplankton carbon to POC (PC/POC ratio) at Sta. M. Solid lines with gray symbols indicate the euphotic depth (1%)

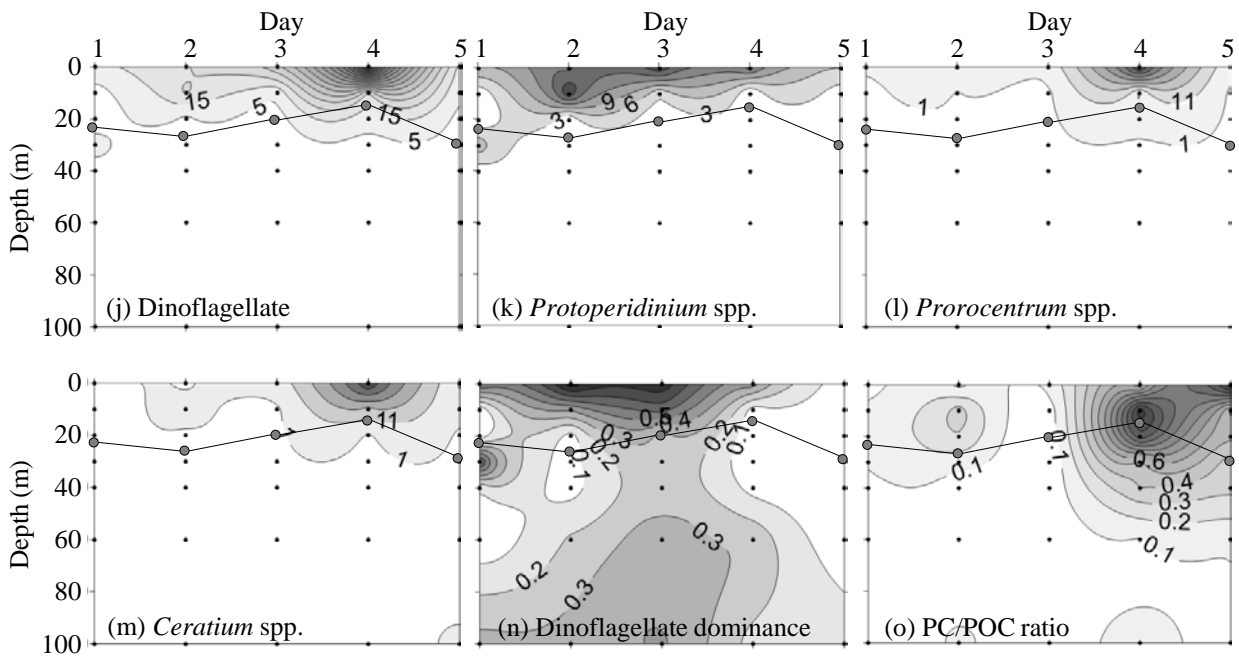


Fig. 3-4 (Continued)

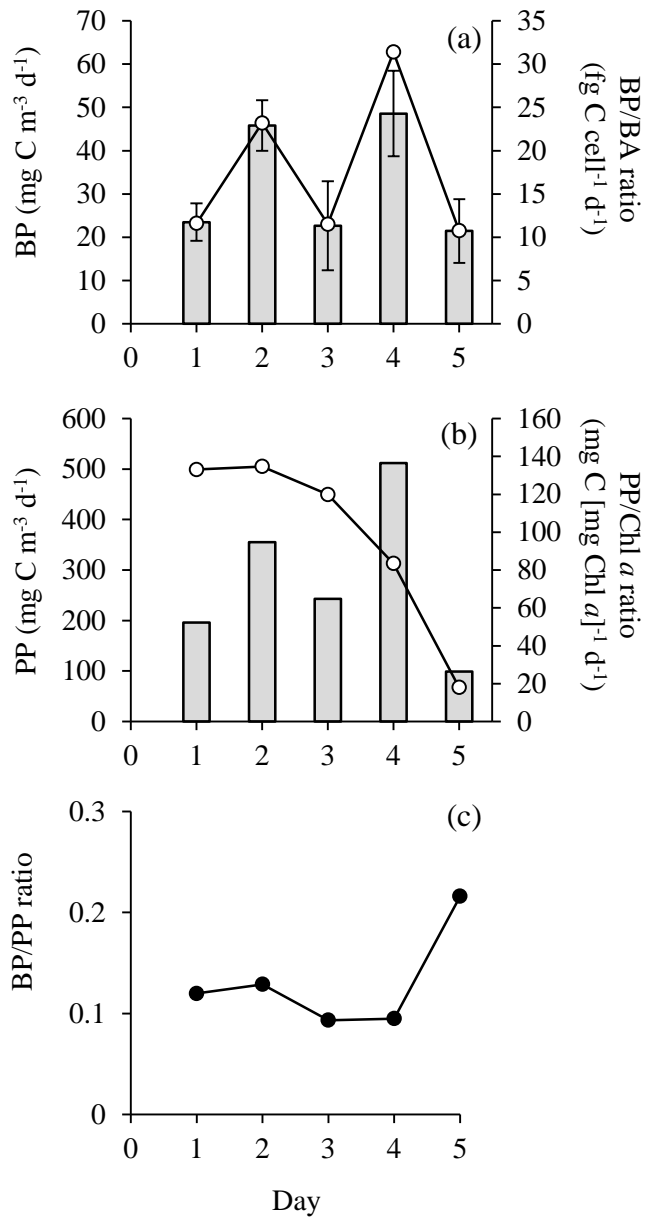


Fig. 3-5 Temporal variations in (a) bacterial production (BP; filled bar) and ratio of BP to bacterial abundance (BP/BA ratio; open circle), (b) primary production (PP; filled bar) and ratio of PP to chl *a* concentration (PP/Chl *a* ratio; open circle) and (c) ratio of BP to PP (BP/PP ratio) at the surface

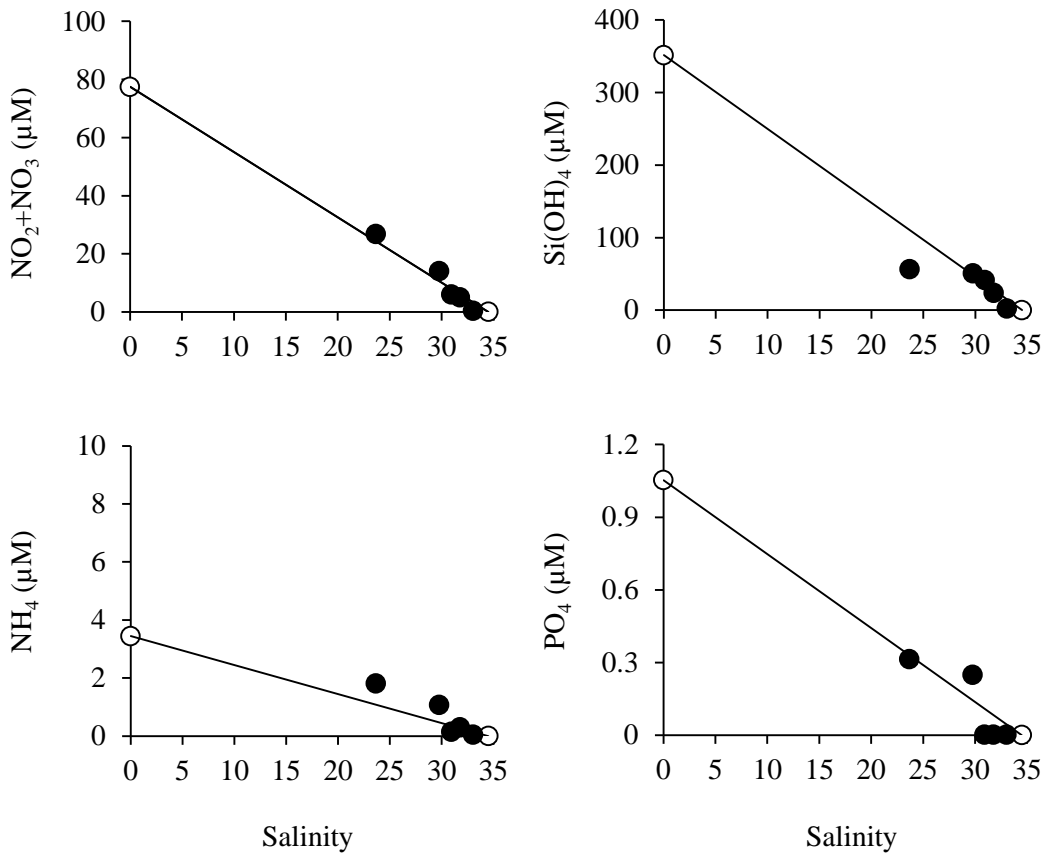


Fig. 3-6 Relationships between salinity and nutrient concentrations of (a) $\text{NO}_2 + \text{NO}_3$, (b) NH_4 , (c) PO_4 and (d) Si(OH)_4 . Closed circle and open circle represent Sta. M and end-members, respectively

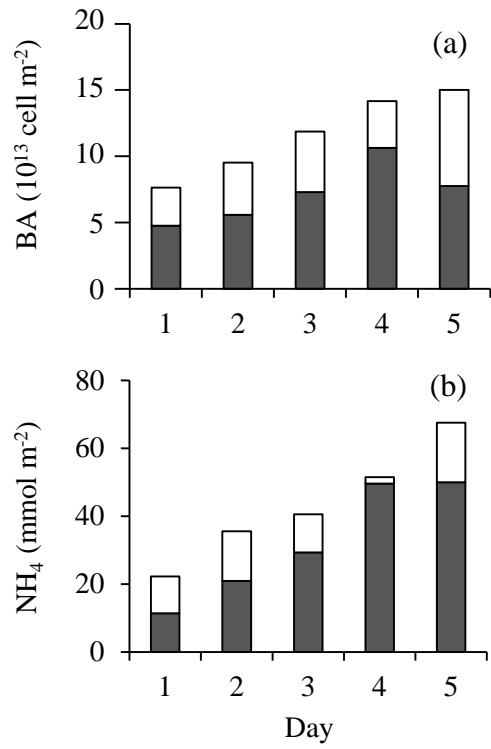


Fig. 3-7 Vertically integrated values of (a) bacterial abundance (BA) and (b) NH_4 concentration in the euphotic zone (open bar) and below the euphotic zone (filled bar)

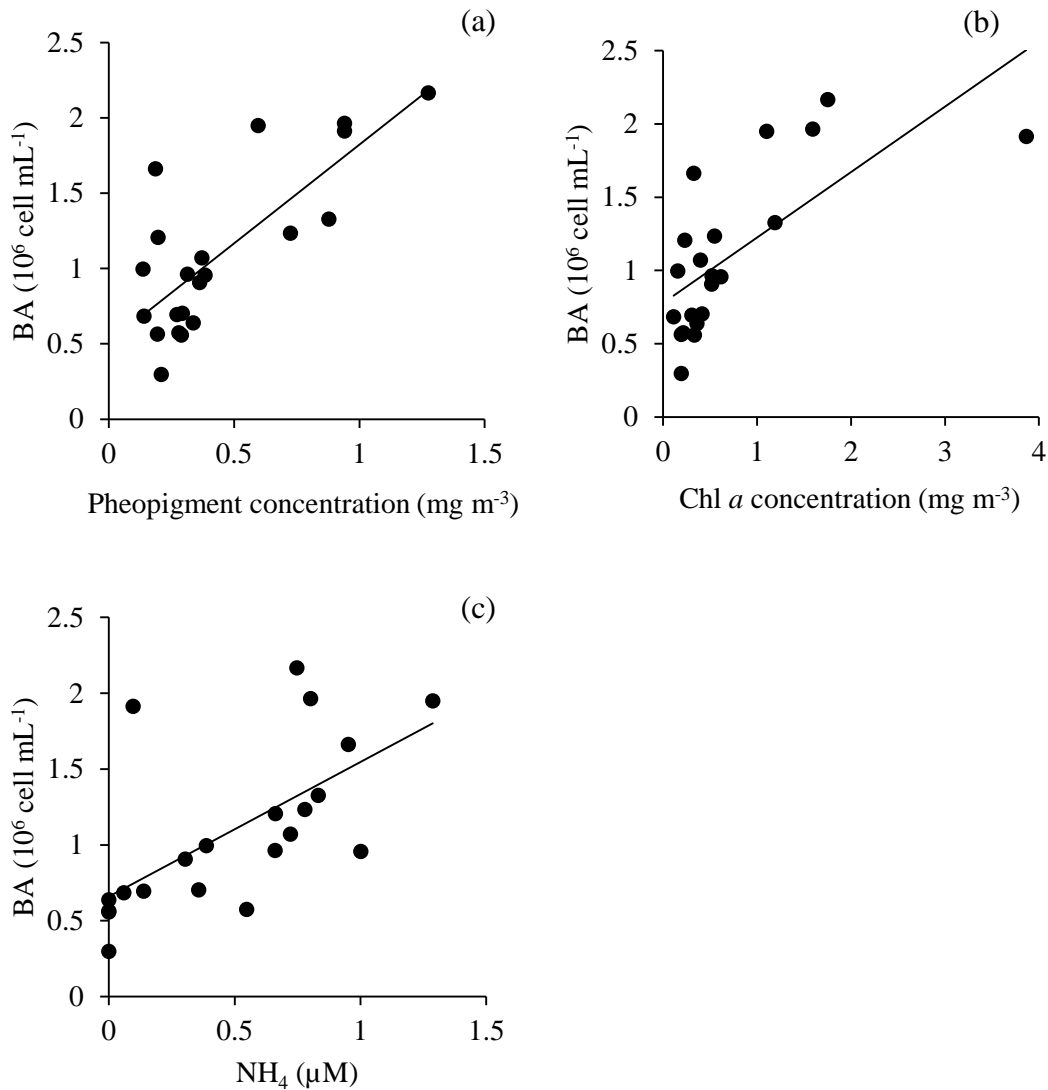


Fig. 3-8 Relationships between (a) bacterial abundance (BA) and pheopigment concentration, (b) BA and chlorophyll *a* (chl *a*) concentration and (c) BA and NH₄ concentration below the euphotic zone during the study period at Sta. M. The relationships were significantly positive, and the regressions were (a) $[BA] = 1.3 \times [\text{pheopigment}] + 0.5$ ($n = 21$, $r = 0.77$, $p < 0.001$), (b) $[BA] = 0.47 \times [\text{Chl } a] + 0.78$ ($n = 21$, $r = 0.70$, $p < 0.001$) and (c) $[BA] = 0.89 \times [\text{NH}_4] + 0.66$ ($n = 21$, $r = 0.64$, $p < 0.01$)

Chapter IV

General discussion

This study described responses of lower trophic levels to variations of physical and chemical environments induced by the passage of typhoons in the temperate coastal waters in Sagami Bay, conducting daily samplings. Previous studies have been conducted focusing on relatively large typhoons that resulted in significant, prolonged disruptions to ecosystem functioning (e.g. Fogel et al. 1999, Zheng & Tang 2007). Intensities of typhoons investigated in the present study ranged from strong (i.e. *Mawar* and *Sinlaku*) to relatively weak (i.e. *Etau* and *Malou*). Results from this study demonstrated that smaller but more frequent typhoons may also induce significant ecological changes as strong typhoons do, although the degree and the area of effect varied depending on the topographic features and the typhoon characteristics.

A clear difference in the bacterial response against nutrient enrichment was observed between inshore and offshore stations, which could be attributed to the difference in the types of physical disturbances. In Sta. A, bacterial production showed relatively high values of $114 \pm 21 \text{ mg C m}^{-3} \text{ d}^{-1}$ and $132 \pm 14 \text{ mg m}^{-3} \text{ d}^{-1}$ on Day 1 and Day 2, respectively, after the passage of *Malou*. The BP/PP ratio exhibited a maximum of 1.5 on Day 1. On the other hand, the BP/PP ratio at Sta. M was 0.13 ± 0.05 , which indicated that bacterial production did not exceed primary production. As to productivity, the BP/BA ratio of all data from Chapter 2 and Chapter 3 significantly correlated with nutrient concentration ($p < 0.001$, Fig. 4-1) and followed an exponential curve with the increase of NH_4 concentration, which indicated that higher nutrient loading could enhance BP more strongly. Storm-associated winds have the potential of completely mixing shallow continental shelf waters (20-50 m) down to the sediment surface (Ridderinkhof 1992), providing sedimentary pore water-related nutrients and organic matters, and particle-attached bacterial population to the water column (Fogel et al. 1999). In a mesocosm experiment, sediment resuspension enhanced bacterial production rapidly by entrainment of nutrients and organic matter (Chróst & Riemann 1994). In addition, since the condition several centimeters below the sediment surface is anaerobic, bacterial productivity is expected to be relatively low. Once sediment resuspension occurs, the bacteria in the sediment can be loaded to the water column where is the aerobic condition, which might lead to abrupt increase in bacterial production. Therefore, the fast response and the increase of bacterial

production at Sta. A might have been induced by sediment resuspension. On the other hand, sediment resuspension should not have occurred at Sta. M where the water depth is 120 m. The difference in topographical features between the two stations generated the difference in typhoon-related physical disturbances, and consequently the difference in bacterial responses.

Nutrient concentrations significantly increased in response to the passage of typhoons compared to the background data. The amount, duration and stoichiometry of nutrient loading were different among typhoons. During the passage of *Mawar*, upwelling occurred and loaded much amount of nutrients to the euphotic zone in addition to the contributions from terrestrial runoff and sediment resuspension. On the other hand, during *Sinlaku*, *Etau* and *Malou*, terrestrial runoff and sediment resuspension might have been the major nutrient source since upwelling was not observed in Sagami Bay. The difference in nutrient sources among typhoons determined nutrient stoichiometry at the inshore station, and consequently influenced the succession of phytoplankton assemblage after the passage of typhoons; i.e., *Skeletonema* spp. and *Chaetoceros* spp. dominated the phytoplankton communities under lower and higher N/P ratios, respectively.

Although phytoplankton assemblage responded differently to typhoons with different characteristics, chl *a* concentration, phytoplankton biomass and primary production significantly increased after the passage of each typhoon. The integrated primary productions for 9 days after the passage of *Mawar* and for 7 days after the passage of *Malou* accounted for 7.1–9.1% of the annual primary production in the upper waters of Sagami Bay. According to the data from Chapter 2 and Chapter 3, the PP/Chl *a* ratio significantly correlated with Si(OH)₄ concentration and followed a hyperbolic curve with the increase in Si(OH)₄ concentration (Fig. 4-2). River water and deep sea water can load much amount of Si(OH)₄ to the euphotic zone (e.g. Kamatani et al. 2000, Fujiki et al. 2004). Primary productivity would be saturated when Si(OH)₄ concentration was higher than 10.2 μM (Fig. 4-2). Therefore, during *Mawar* and *Malou*, although their nutrient sources were different, contributions of typhoon-induced increase in primary production to the annual primary production were equivalent and consistent. Similarly, Wetz and Paerl (2008) examined phytoplankton responses to hurricanes and tropical storms with different characteristics at Neuse R. Estuary in North Carolina, US, and concluded that relatively small tropical storms and hurricanes can lead to significant increase in phytoplankton biomass. However, in open ocean such as western North Pacific subtropical ocean, significant increases in chl *a* concentration were induced by only two of

eleven typhoons in 2003 (Lin 2012). In open waters, since possible nutrient source is limited to nutrient-rich deep water, upwelling is necessary to enhance phytoplankton growth in upper waters. There are four factors to be considered for inducing upwelling; (1) typhoon intensity, (2) typhoon translation speed, (3) typhoon size and (4) ocean precondition (Lin 2012). Therefore, relatively weak typhoons cannot induce phytoplankton blooms in open waters, while they can consistently do in coastal and estuarine ecosystems, which have various nutrient sources. In other words, terrestrial runoff and/or sediment resuspension considerably contribute to the enhancement of biological production in coastal ecosystem after the passage of typhoons that are not strong enough to induce upwelling.

After the passage of typhoon, diatom blooms consistently occurred in coastal areas of Pacific Ocean such as in the Great Barrie Reef (Furnas 1989), the Reef of Tiafura (Delesalle et al. 1993), Northern Taiwan (Chang et al. 1996), Philippine Sea (Chen et al. 2009), Northeast of Taiwan (Chung et al. 2012) and Sagami Bay (present study). In Atlantic Ocean, some studies reported diatom blooms after the passage of typhoon in Puerto Rico (Glynn et al. 1964), South Carolina (Zeeman 1985) and Neuse River Estuary (Valdes-Weaver et al. 2006). On the other hand, Wetz & Paerl (2008) reported dominances of dinoflagellates and cryptophytes after the passage of Helene and dominances of cyanobacteria and dinoflagellates after the passage of Alex, Bonnie and Charley in Neuse River Estuary. Diatom blooms require plenty of Si(OH)_4 because diatoms cannot accumulate Si(OH)_4 into their large central vacuoles (Tozzi et al. 2004), and it is known that diatoms are superior competitors for light and nutrients when Si(OH)_4 is available (Riegman et al. 1988). Helene, Alex, Bonnie and Charley were so small and weak that these typhoons could not cause enough silicate loading. Si/N ratio in North Pacific Ocean is approximately 2 (Kamatani et al. 2000), while that in North Atlantic Ocean is 0.93 (Millero 1996), suggesting that Pacific Ocean potentially serves as favorable environment for diatoms.

In order to discuss whether the passage of typhoons affected the entire area of Sagami Bay, chl *a* data around Sagami Bay derived from remote sensing (moderate resolution imaging spectroradiometer: MODIS) during *Mawar*, *Sinlaku*, *Etau* and *Malou* were shown in Fig. 4-3 (Japan Aerospace Exploration Agency 2014, http://kuroshio.eorc.jaxa.jp/ADEOS/mod_nrt_new/). High chl *a* concentrations were observed in the entire area of Sagami Bay after the passage of *Mawar*. This typhoon might have induced upwelling and nutrients could have been supplied entirely to the upper

area of Sagami Bay, which induced phytoplankton bloom in the whole area of Sagami Bay. During *Sinlaku*, relatively high chl *a* concentrations were distributed all over Sagami Bay on Day 3 and Day 4. These Days agreed to the timing of chl *a* peaks observed by *in situ* sampling in the present study. During *Etau*, although relatively high chl *a* concentrations were observed on Day 4 and Day 6, their distributions were limited in the nearshore area. After the passage of *Malou*, high chl *a* concentrations were observed in the entire area of Sagami Bay. Since major nutrient sources could have been terrestrial runoff during *Sinlaku*, *Etau* and *Malou*, the area affected by the passage of typhoon can be attributable to the amount of precipitation. Integrated precipitation during *Etau* was 42.2 mm, which was smallest of the all typhoons investigated in the present study. Therefore, the area affected by the passage of *Etau* might have been limited to nearshore regions. The results suggest that the threshold of whether a typhoon passage affects the entire area of Sagami Bay may be in the range of 42.2 mm and 89.0 mm in terms of integrated precipitation.

In Sagami Bay, one typhoon passage may enhance primary production, accounting up to 9.1% at the inshore station and up to 5.7% at the offshore station of the annual primary production in upper waters. Based on the annual average (three) of typhoon approaching Sagami Bay, the contribution to annual primary production is assumed to be up to 27.3%. The typhoon-induced high phytoplankton biomass is either consumed by herbivorous mesozooplankton (*e.g.* copepods) and efficiently transferred to higher trophic levels through a grazing food chain (Calbet and Landry 2004), or transported from the euphotic zone to deeper waters (Dugdale and Wilkerson, 1998). During the summer season, there are abundant tintinnids, heterotrophic dinoflagellates, copepod nauplii and copepod (CI-CVI) in Sagami Bay (Ara & Hiromi 2009), suggesting high predation pressure on phytoplankton. Moreover, zooplankton grazing becomes more active in a turbulent environment (Kiørboe 1993, Hwang et al. 1994). In the present study, increase in pheopigment concentrations over time was observed, which suggests possible grazing by zooplankton on phytoplankton. In addition, a large amount of fish larvae occurs in Sagami Bay and Tokyo Bay from summer to autumn, such as Japanese anchovy *Engraulis japonicas*, Japanese sardine *Sardinops melanostictus*, *Sardinella zunasi*, *Sillago japonica* and Perciformes species (Nakata & Mitani 1979, Kudo 1991, Nagaiwa et al. 2005, Sassa & Kawaguchi 2006). Most of the mortality occurs during the pelagic larval stage, and the rate of larval mortality is directly reflected in the population dynamics of fishes (*e.g.* May 1974). After the absorption of the yolk sac, fish-larvae must obtain

sufficient food to meet their metabolic requirements within 2-3 days or they will die (Smith and Lasker 1978). The survival of first-feeding larvae is affected by food concentrations (*e.g.* Houde 1977, Lasker & Smith 1977). Anchovy larvae were stimulated to feed when the phytoplankton concentration was more than $> 20\text{-}30$ cells mL^{-1} (Lasker 1975). The phytoplankton cell density after the passage of typhoons in the present study reached up to 1.5×10^4 cells mL^{-1} (Tsuchiya et al. 2013a), which might be a favorable condition for first-feeding fish larvae and enhance their survival rate. Therefore, the passage of typhoons might also contribute to the stabilization of high fishery production in Sagami Bay.

Recent analyses of past typhoons (including tropical cyclones and hurricanes) have suggested that global warming leads to increasing intensities of wind and rainfall of these episodic events (Emanuel 2005, Webster et al. 2005, Elsner et al. 2008, Knutson et al. 2010, Yamada et al. 2010). With the intensification of typhoons, diatom blooms and associated carbon export are expected to increase in magnitude since loading of nutrients and organic matter could be augmented. The higher production and more efficient carbon export to deeper water may result in CO_2 draw down from atmosphere, and the process is known as ocean storage of CO_2 through biological pump. The process can lead to a negative feedback of natural earth system on global warming (Fig. 4-4), in other words, leading to global cooling as a result of organic carbon-rich sedimentation.

In further study, fates of biological production induced by typhoon should be investigated in order to better understand the effects of typhoon on ocean biogeochemical cycles: (1) to measure primary production and POC export flux using a sediment trap before and after the passage of typhoon in order to assess how much typhoon-derived biogenic carbon is exported to deeper waters, (2) to examine grazing rates of nano-, micro- and mesozooplankton on primary producer and bacteria before and after the passage of typhoon in order to assess the functional changes of food web and (3) to determine the degradation rate of POM and regeneration rate of nutrients in order to predict the biogeochemical cycle in the water column after the passage of typhoon.

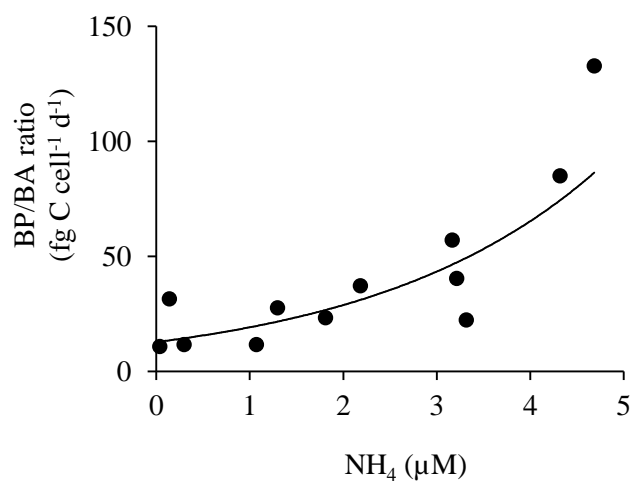


Fig. 4-1 Relationship between ratio of bacterial production to bacterial abundance (BP/BA ratio) and NH₄ concentration ($[\text{BP/BA ratio}] = 12.7 \times e^{0.409 \times [\text{NH}_4]}$, $r = 0.83$, $n = 12$, $p < 0.001$)

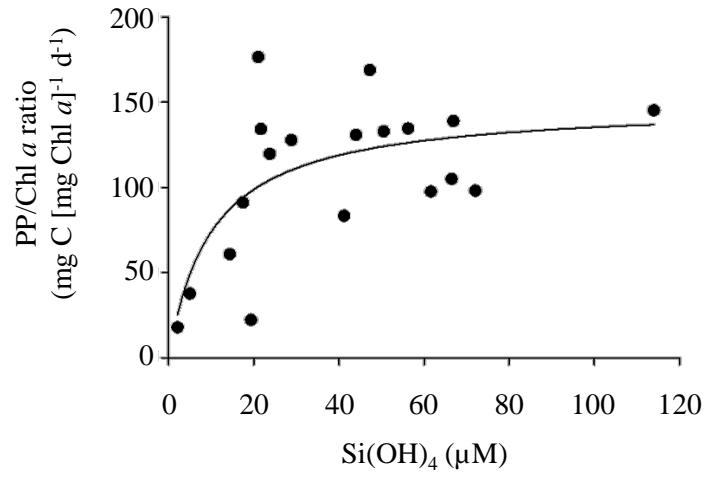


Fig. 4-2 Relationship between ratio of primary production to chlorophyll *a* concentration (PP/Chl *a* ratio) and Si(OH)₄ concentration ($[PP/Chl\ a\ ratio] = 149 \times [Si(OH)_4] / ([Si(OH)_4] + 10.2)$, $r = 0.68$, $n = 19$, $p < 0.01$).

Mawar

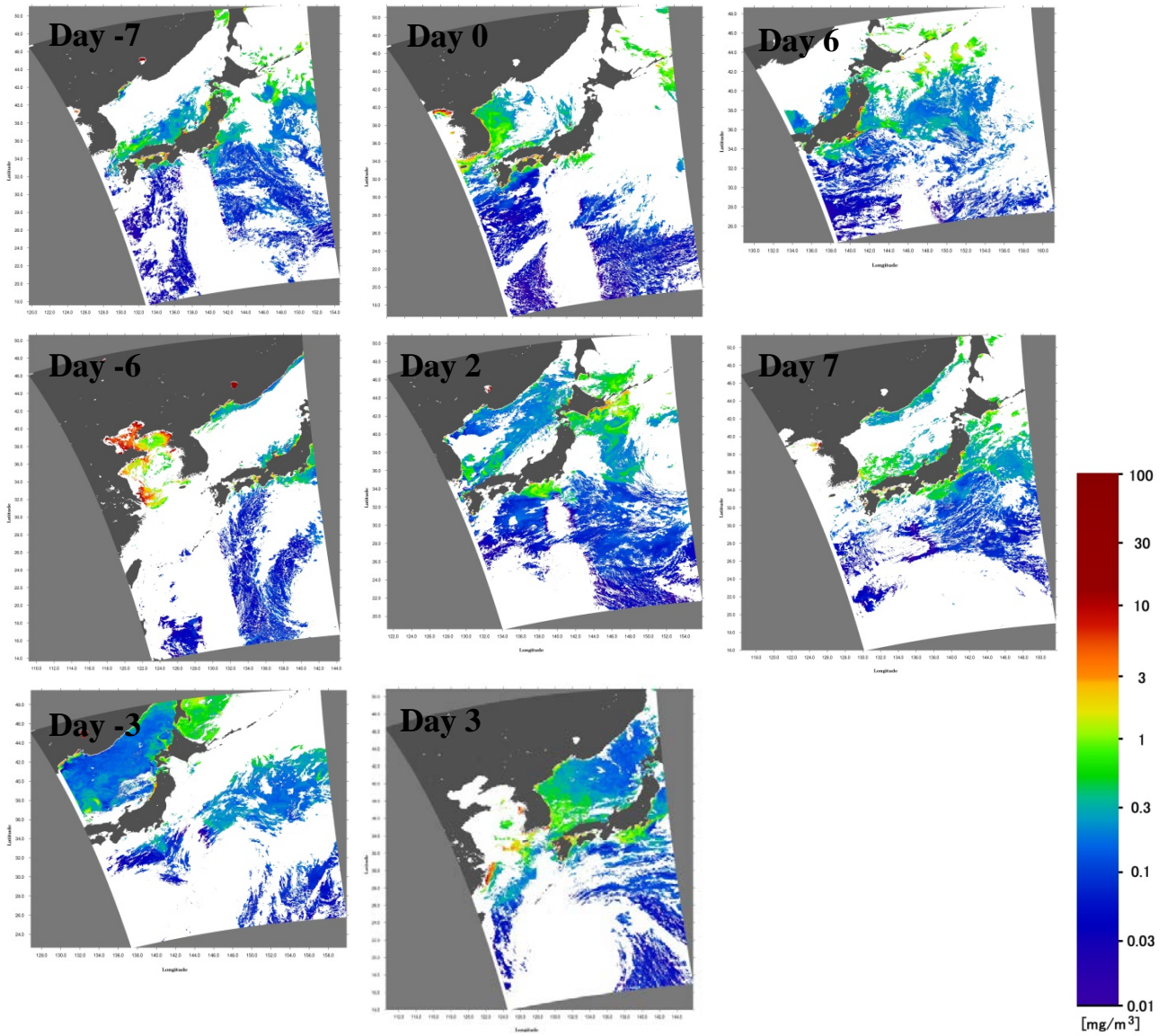


Fig. 4-3 Distribution of chlorophyll *a* concentration during *Mawar*, *Sinlaku*, *Etau* and *Malou*. These data were derived from remote sensing platform (MODIS)

Sinlaku

Etau

Malou

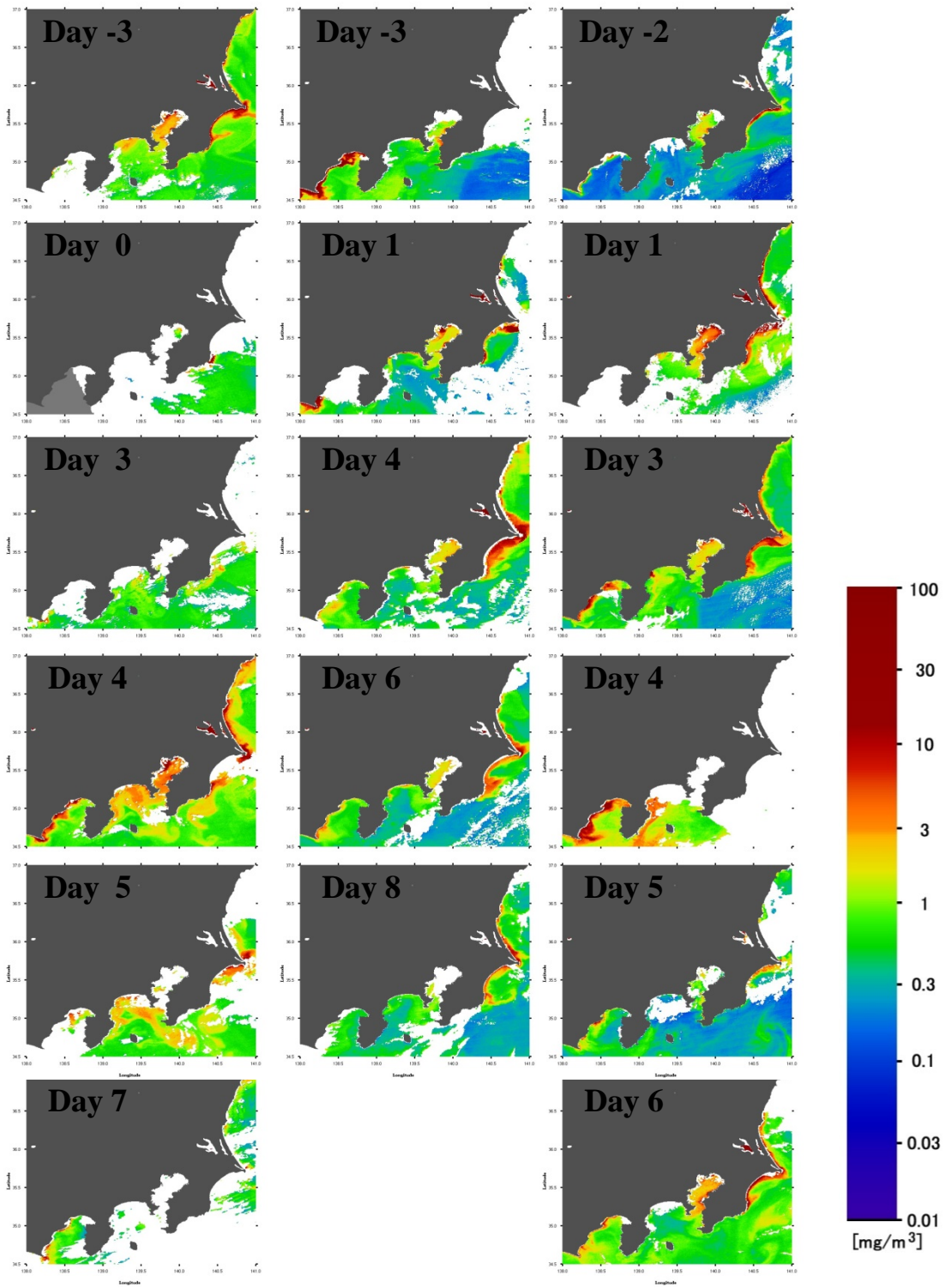


Fig. 4-3 (Continued)

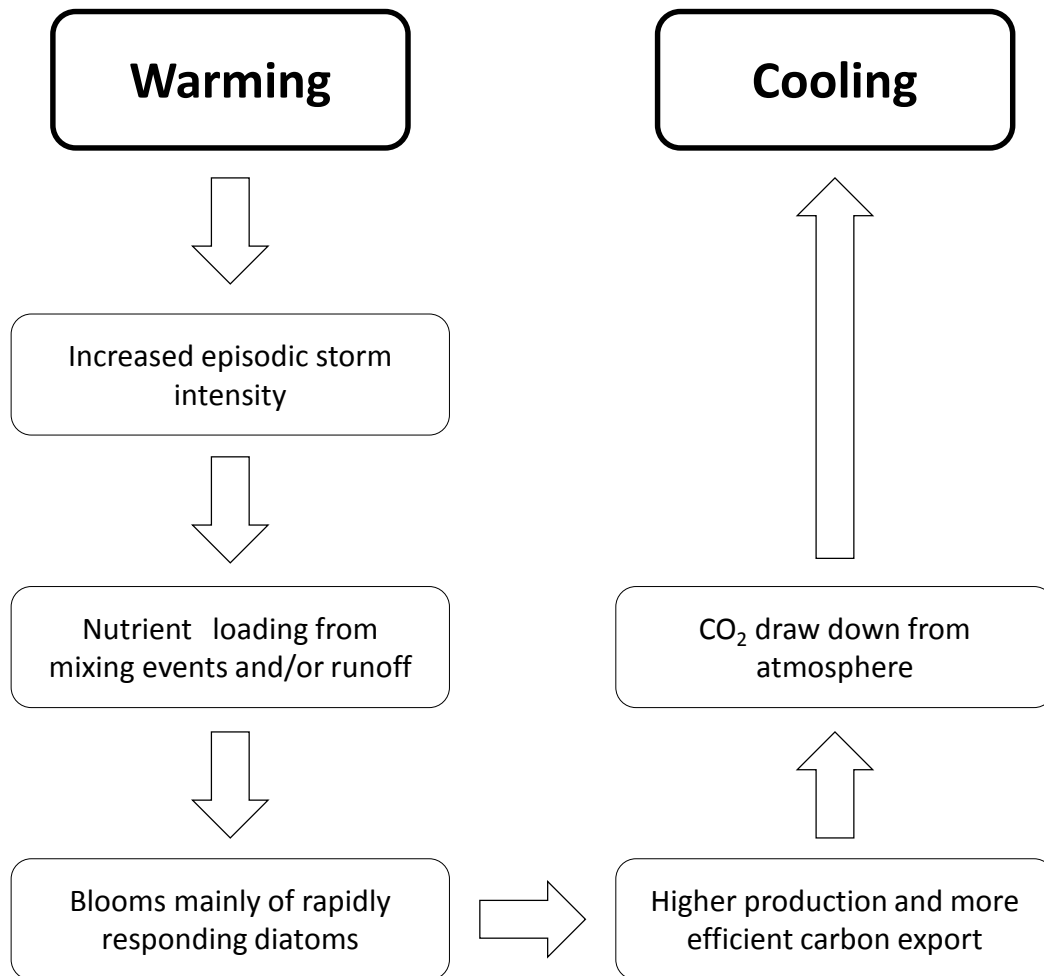


Fig. 4-4 Potential negative feedback with global warming. The paths show mechanisms for increased diatom production leading to increased carbon export and consequent enhanced CO₂ draw down, promoting cooling. This figure was modified from Kemp & Villareal (2013)

REFERENCES

- Aono H (2001) The changing process of phytoplankton communities during the spring bloom in Sagami Bay, central Japan. Master's thesis, Yokohama National University, Japan (in Japanese)
- Ara K, Hiromi J (2009) Seasonal variability in plankton food web structure and trophodynamics in the neritic area of Sagami Bay, Japan. *J Oceanogr* 65:757–779
- Ara K, Yamaki K, Wada K, Fukuyama S, Okutsu T, Nagasaka S, Shiimoto A, Hiromi J (2011) Temporal variability in physicochemical properties, phytoplankton standing crop and primary production for 7 years (2002–2008) in the neritic area of Sagami Bay, Japan. *J Oceanogr* 67: 87–111
- Azam F, Fenchel T, Field JG, Gray JS, Meyer-Reil LA, Thingstad F (1983) The ecological role of water-column microbes in the sea. *Mar Ecol Prog Ser* 10:257–263
- Azam F (1998) Microbial control of oceanic carbon flux: The plot thickens. *Science* 280:694–696
- Baek SH, Shimode S, Kikuchi T (2008) Growth of dinoflagellates, *Ceratium furca* and *Ceratium fusus* in Sagami Bay, Japan: The role of temperature, light intensity and photoperiod. *Harmful Algae* 7:193–173
- Baek SH, Shimode S, Kim HC, Han MS, Kikuchi T (2009) Strong bottom-up effects on phytoplankton community caused by a rainfall during spring and summer in Sagami Bay, Japan. *J Mar Syst* 75:253–264
- Baki MA, Motegi C, Shibata A, Fukuda H, Shimode S., Kikuchi T (2009) Temporal changes in chlorophyll *a* concentrations and bacterial, viral, and heterotrophic nanoflagellate abundances in the coastal zone of Sagami Bay, Japan: implications of top-down and bottom-up effects. *Coast Mar Sci* 32:1–10
- Balzano S, Sarno D, Kooistra WHCF (2011) Effects of salinity on the growth rate and morphology of ten *Skeletonema* strains. *J Plankton Res* 33:937–945
- Behrenfeld MJ, Falkowski PG (1997) Photosynthetic rates derived from satellite-based chlorophyll concentration. *Limnol Oceanogr* 42:1–20
- Bird DF, Kalff J (1984) Empirical relationships between bacterial abundance and chlorophyll concentration in fresh and marine waters. *Can J Fish Aquat Sci* 41:1015–1023
- Brand LE (1984) The salinity tolerance of forty-six marine phytoplankton isolates. *Estuar Coast Shelf Sci* 18:543–556
- Calbet A, Landry MR (2004): Phytoplankton growth, microzooplankton grazing, and carbon cycling in marine systems. *Limnol Oceanogr* 49:51–57
- Chang J, Chung C, Gong G (1996) Influences of cyclones on chlorophyll *a* concentration and

- Synechococcus abundance in a subtropical western Pacific coastal ecosystem. *Mar Ecol Prog Ser* 140:199–205
- Chang GC, Gould RW (2006) Comparisons of optical properties of the coastal ocean derived from satellite ocean color and *in situ* measurements. *Optics Express* 14:10149–10163
- Chen YL, Chen H, Jan S, Tuo S (2009) Phytoplankton productivity enhancement and assemblage change in the upstream Kuroshio after typhoons. *Mar Ecol Prog Ser* 385:111–126
- Chihara M, Fukuyo Y, Inoue H, Takayama H, Horiguchi T, Matsuoka K, Toriumi S, Kawachi M, Hara H, Takano H (1997) Division Dinophyta and Division Heterokontophyta. In: Chihara M., Murano M (eds) *An illustrated guide to marine plankton in Japan*. Tokai University Press, Tokyo, p 31–260 (in Japanese)
- Cho BC, Park MG, Shim JH, Choi DH (2001) Sea-surface temperature and f-ratio explain large variability in the ratio of bacterial production to primary production in the Yellow Sea. *Mar Ecol Prog Ser* 216:31–41
- Chróst RJ, Riemann B (1994) Storm-stimulated enzymatic decomposition of organic matter in benthic/pelagic coastal mesocosms. *Mar Ecol Prog Ser* 108:185–192
- Chung CC, Gong GC, Hung CC (2012) Effect of Typhoon Morakot on microphytoplankton population dynamics in the subtropical Northwest Pacific. *Mar Ecol Prog Ser* 448:39–49
- Cole JJ, Linkens GE, Hobbie JE (1984) Decomposition of planktonic algae in an oligotrophic lake. *Oikos* 42:257–266
- Cole JJ, Findlay S, Pace ML (1988) Bacterial production in fresh and saltwater ecosystems: a cross-system overview. *Mar Ecol Prog Ser* 43:1–10
- Collos Y (1986) Time-lag algal growth dynamics: biological constraints on primary production in aquatic environments. *Mar Ecol Prog Ser* 33:193–206
- Coveney MF, Wetzel RG (1995) Biomass, production, and specific growth rate of bacterioplankton and coupling to phytoplankton in an oligotrophic lake. *Limnol Oceanogr* 40:1187–1200
- Delesalle B, Pichon M, Frankignoulle M, Gattuso PJ (1993) Effects of a cyclone on coral reef phytoplankton biomass, primary production and composition (Moorea Island, French Polynesia). *J Plankton Res* 15: 1413–1423
- Donaghay PL, Osborn TR (1997) Toward a theory of biological-physical control of harmful algal bloom dynamics and impacts. *Limnol Oceanogr* 42:1283–1296
- Dortch Q, Whittedge TE (1992) Does nitrogen or silicon limit phytoplankton production in the Mississippi River plume and nearby regions? *Cont Shelf Res* 12:1293–1309
- Ducklow HW (1999) The bacterial component of the oceanic euphotic zone. *FEMS Microbiol Ecol* 30:1–10

- Ducklow HW, Carlson CA (1992) Oceanic bacterial production. *Adv Microb Ecol* 12:113–181
- Dugdale RC, Wilkerson EP (1998) Silicate regulation of new production in the equatorial Pacific upwelling. *Nature* 391:270–273
- Edmond JM, Spivack A, Grant BC, Hu MH, Chen X, Cheng S, Zeng X (1985) Chemical dynamics of the Changjiang Estuary. *Cont Shelf Res* 4: 17–36
- Elsner BJ, Kossin PJ, Jagger HT (2008) The increasing intensity of the strongest tropical cyclones. *Nature* 455:92–95
- Emanuel K (2005) Increasing destructiveness of tropical cyclones over the past 30 years. *Nature* 436:686–688
- Escaravage V, Prins TC, Smaal AC, Peethers JCH (1996) The response of phytoplankton communities to phosphorus input reduction in mesocosm experiments. *J Exp Mar Biol Ecol* 198:55–79
- Estrada M, Berdalet E, Vila M, Marrase C (2003) Effects of pulsed nutrient enrichment on enclosed phytoplankton: ecophysiological and successional responses. *Aquat Microb Ecol* 32:61–71
- Fallon RD, Brock TD (1980) Planktonic blue-green algae: production, sedimentation and decomposition in Lake Mendota, Wisconsin. *Limnol Oceanogr* 25:72–88
- Finenko ZZ, Krupatkina-Akinina DK (1974) Effect of inorganic phosphorus on the growth rate of diatoms. *Mar Biol* 26:193–201
- Fogel ML, Aguilar C, Cuhel R, Hollander DJ, Willey JD, Paerl HW (1999) Biological and isotopic changes in coastal waters induced by Hurricane Gordon. *Limnol Oceanogr* 44:1359–1369
- Fujiki T, Toda T, Kikuchi T, Aono H, Taguchi S (2004) Phosphorus limitation of primary productivity during the spring-summer blooms in Sagami Bay, Japan. *Mar Ecol Prog Ser* 283:29–38
- Fukuyo Y, Horiguchi T, Katsuhisa Y, Yoshimatsu S, Takayama H, Matsuoka K, Toriumi S, Ono C, Kuroda K, Inoue H, Pholpunthin P, Imamura K, Takano H (1990) III. Dinophyceae and IV. Bacillariophyceae. In: Fukuyo Y, Chihara M, Takano H, Matsuoka K (eds) *Red tide organisms in Japan: an illustrated taxonomic guide*. Uchida-Roukakuho, Tokyo, p 22–331 (in Japanese)
- Furnas MJ (1989) Cyclonic disturbance and a phytoplankton bloom in an tropical shelf ecosystem. In: Okaichi T, Anderson DM, Nemoto T (eds) *Red Tides: Biology, Environmental Science and Toxicology*. Elsevier, New York, p 273–276
- Gao K, McKinley KR (1994) Use of macroalgae for marine biomass production and CO₂ remediation: a review. *J Appl Phycol* 6: 45–60
- Gasol JM, del Giorgio PA, Duarte CM (1997) Biomass distribution in marine planktonic

- communities. *Limnol Oceanogr* 1997:1353–1363
- Gasol JM, Duarte CM (2000) Comparative analyses in aquatic microbial ecology: How far do they go? *FEMS microbiol Ecol* 31:99–106
- Glynn PW, Almodovar LR, Gonzalez JG (1964) Effects of hurricane Edith on marine life in La Parguera, Puerto Rico. *Caribb J Sci* 4:335–345
- Hama T, Miyazaki Y, Ogawa Y, Iwakuma T, Takahashi M, Otsuki A, Ichimura S (1983) Measurement of photosynthetic production of a marine phytoplankton population using a stable ^{13}C isotope. *Mar Biol* 73:31–36
- Hamasaki K (2006) Comparison of bromodeoxyuridine immunoassay with tritiated thymidine radioassay for measuring bacterial productivity in oceanic waters. *J Oceanogr* 62:793–799
- Han MS, Furuya K (2000) Size and species-specific primary productivity and community structure of phytoplankton in Tokyo Bay. *J Plankton Res* 22:1221–1235
- Hansen HP, Koroleff F (1990) Determination of nutrients. In: Grasshoff K, Kremling K, Ehrhardt M (eds) *Methods of seawater analysis*, 3rd edition. Wiley-VCH, Weinheim, p 159–228
- Hansen PJ (1991) Quantitative importance and trophic role of heterotrophic dinoflagellates in a coastal pelagial food web. *Mar Ecol Prog Ser* 73:253–261
- Harrison PJ, Conway HL, Dugdale RC (1976) Marine diatoms grown in chemostats under silicate or ammonium limitation. I. Cellular chemical composition and steady-state growth kinetics of *Skeletonema costatum*. *Mar Biol* 35:177–186
- Harrison PJ, Conway HL, Holmes RW, Davis CO (1977) Marine diatoms in chemostats under silicate or ammonium limitation. III. Cellular chemical composition and morphology of three diatoms. *Mar Biol* 43:19–31
- Hashimoto N, Yamaguchi Y, Ishimaru T, Saino T (2005) Relationship between net and gross primary production in the Sagami Bay, Japan. *Limnol Oceanogr* 50: 1830–1835
- Hasle RG (1978) The inverted microscope method. In: Sournia A (ed) *Monographs on oceanographic methodology*, Vol 6, *Phytoplankton manual*. UNESCO, Paris, p 88–96
- Hasle RG, Syvertsen EE (1997) Chapter 2. Marine Diatoms. In: Tomas RC (ed) *Identifying marine phytoplankton*. Academic press, San Diego, p 5–386
- Hecky RE, Kilham P (1988) Nutrient limitation of phytoplankton in freshwater and marine environments: A review of recent evidence on the effects of enrichment. *Limnol Oceanogr* 33:796–822
- Hillebrand H, Durselen DC, Kirschtel D, Pollinger U, Zohary T (1990) Biovolume calculation for pelagic and benthic microalgae. *J Phycol* 35:403–424
- Hirano T (1969) Investigation of impact of river water withdrawal on fishery. *Agricultural Policy*

- Planning Department, Kanagawa Prefecture 9–13 (in Japanese)
- Hoegh-Guldberg O, Bruno JF (2010) The impact of climate change on the world's marine ecosystems. *Science* 328:1523–1528
- Hoge F, Lyon PE (2002) Satellite observation of chromophoric dissolved organic matter (CDOM) variability in the wake of hurricanes and typhoons. *Geophys Res Lett* 29:141–144
- Hogetsu K, Taga N (1977) Suruga Bay and Sagami Bay. In: Hogetsu K, Hatanaka M, Hanaoka T, Kawamura T (eds) *JIBP Synthesis, Productivity of Biocenoses in Coastal Regions of Japan*, Vol. 14. University of Tokyo Press, Tokyo, p 31–172
- Holm-Hansen O, Lorenzen CJ, Holmes RN, Strickland JDH (1965) Fluorometric determination of chlorophyll. *J Cons Perm Int Explor Mer* 30:3–15
- Hoover RS, Hoover D, Mitter, M, Landry MR, DeCarlo EH, Mackenzie FT (2006) Zooplankton response to storm runoff in a tropical estuary: bottom-up and top-down controls. *Mar Ecol Prog Ser* 318:187–201
- Horikoshi M (1977) Suruga Bay and Sagami Bay. In: Hogetsu K, Hatanaka M, Hanaoka T, Kawamura T (eds) *JIBP Synthesis, Productivity of Biocenoses in Coastal Regions of Japan*, Vol. 14. University of Tokyo Press, Tokyo, p 62–69
- Houde ED (1977) Food concentration and stocking density effects on survival and growth of laboratory-reared larvae of bay anchovy *Anchoa mitchilli* and lined sole *Achirus lineatus*. *Mar Ecol* 43:333–341
- Howarth RW (1988) Nutrient limitation of net primary production in marine ecosystems. *Annu Rev Ecol Syst* 19:89–110
- Hung, CC, Gong GC, Chou WC, Chung CC, Lee MA, Chang Y, Chen HY, Huang SJ, Yang Y, Yang WR, Chung WC, Li SL, Laws E (2010) The effect of typhoon on particulate organic carbon flux in the southern East China Sea. *Biogeosciences* 7:3007–3018
- Hwang JS, Costell JH, Strickler JR (1994) Copepod grazing in turbulent flow: elevated foraging behavior and habituation of escape responses. *J Plankton Res* 16:421–431
- Ismael AA (2003) Succession of heterotrophic and mixotrophic dinoflagellates as well as autotrophic microplankton in the harbor of Alexandria, Egypt. *J Plankton Res* 25:193–202
- Jacobson DM (1999) A brief history of dinoflagellate feeding research. *J Eukaryot Microbiol* 46:376–381
- Jacobson EM, Anderson DM (1986) Thecate heterotrophic dinoflagellates: feeding behavior and mechanisms. *J Phycol* 22:249–258
- Japan Aerospace Exploration Agency (2014) Moderate resolution imaging spectroradiometer. Available at: http://kuroshio.eorc.jaxa.jp/ADEOS/mod_nrt_new/ (accessed on 12

February 2014)

- Japan Meteorological Agency (2011) Meteorological Data Acquisition System (AMeDAS). www.jma.go.jp/jma/index (accessed 10 Aug 2011)
- Jeong HJ (1999) The ecological roles of heterotrophic dinoflagellates in marine planktonic community. *J Eukaryot Microbiol* 46:390–396
- Justic D, Rabalais NN, Turner RE, Dortch Q (1995) Changes in nutrient structure of river-dominated coastal waters: stoichiometric nutrient balance and its consequences. *Estuar Coast Shelf Sci* 40:339–356
- Kamatani A, Oku O, Tsuji H, Maeda M, Yamada Y (2000) The distribution and fate of nutrients in Sagami Bay. *Nippon Suisan Gakkaishi* 66:70–79 (in Japanese)
- Kanagawa Prefectural Fisheries Technology Center (2012) Hydrographic condition report. Available at: <http://www.agri-kanagawa.jp/suisoken/noaa2/noaa2.asp> (accessed on 1 September 2012)
- Kanda J, Fujiwara S, Kitazato H, Okada Y (2003) Seasonal and annual variation in the primary production regime in the central part of Sagami Bay. *Prog Oceanogr* 57:17–29
- Kao SJ, Liu KK (1997) Fluxes of dissolved and nonfossil particulate organic carbon from an Oceania small river (Lanyang His) in Taiwan. *Biogeochemistry* 39:255–269
- Kemp AES, Villareal TA (2013) High diatom production and export in stratified waters – A potential negative feedback to global warming. *Prog Oceanogr* 119:4–23
- Kjørboe T (1993) Turbulence, phytoplankton cell size and the structure of pelagic food webs. *Adv Mar Biol* 29:1–72
- Kitazato H, Shirayama Y, Naktsuka T, Fujiwara S, Shimanaga M, Kato Y, Okada Y, Kanda J, Yamaoka A, Masuzawa T, Suzuki K (2000) Seasonal phytodetritus deposition and responses of bathyal benthic foraminiferal populations in Sagami Bay, Japan: preliminary results from “Project Sagami 1996-1999”. *Mar Micropaleontol* 40:135–149
- Knutson TR, McBride JL, Chan J, Emanuel K, Holland G, Landsea C, Held I, Kossin JP, Srivastava AK, Sugi M (2010) Tropical cyclones and climate change. *Nature Geosci* 3:157–163
- Kobata T (2003) Sagami Bay, Wonder of the Sea—Topics on Food, Nature and Fishery. *Yumekoubou, Hadano*, p 331 (in Japanese)
- Kudo T (1991) Sudden increase of Japanese sardine larvae, *Sardinops melanostictus* (Temmnck et Schlegel), during the period from October to December in Sagami Bay. *Report of Kanagawa fisheries experimental station* 12:73–82 (in Japanese)
- Kuwahara VS, Ogawa H, Toda T, Kikuchi T, Taguchi S (2000a) Variability in the relative penetration of ultraviolet radiation to photosynthetically available radiation in temperate

- coastal waters, Japan. *J Oceanogr* 56:399–408
- Kuwahara VS, Ogawa H, Toda T, Kikuchi T, Taguchi S (2000b) Variability of bio-optical factors influencing the seasonal attenuation of ultraviolet radiation in temperate coastal waters of Japan. *Photochem Photobiol* 72:193-199
- Lagus A, Suomela J, Weithoff G, Heikkila K, Helminen H, Sipura J (2004) Species-specific differences in phytoplankton responses to N and P enrichments and the N:P ratio in the Archipelago Sea, northern Baltic Sea. *J Plankton Res* 26:779–798
- Larsson U, Hagström Å (1979) Phytoplankton exudate release as an energy source for the growth of pelagic bacteria. *Mar Biol* 52:199–206
- Lasker R (1975) Field criteria for the survival of anchovy larvae: the relation between inshore chlorophyll maximum layers and successful first feeding. *Fish Bull US* 73:847–855
- Lasker R, Smith PE (1977) Estimation of the effects of environmental variations on the eggs and larvae of the northern anchovy. *CalCOFI Rep* 19:128–137
- Lee S, Fuhrman J (1987) Relationships between biovolume and biomass of naturally derived marine bacterioplankton. *Appl Environ Microb* 53:1298–1303
- Lessard EJ, Swift E (1985) Species-specific grazing rates of heterotrophic dinoflagellates in oceanic waters, measured with a dual-label radioisotope technique. *Mar Biol* 87:289–296
- Levasseur ME, Therriault JC (1987) Phytoplankton biomass and nutrient dynamics in a tidally induced upwelling: the role of the $\text{NO}_3:\text{SiO}_4$ ratio. *Mar Ecol Prog Ser* 39: 87–97
- Lin I, Liu WT, Wu C, Wong GTF, Hu C, Chen Z, Liang W, Yang Y, Liu K (2003) New evidence for enhanced ocean primary production triggered by tropical cyclone. *Geophys Res Lett* 30:1718, doi:10.1029/2003GL017141
- Lin II (2012) Typhoon-induced phytoplankton blooms and primary productivity increase in the western North Pacific subtropical ocean. *J Geophys Res* 117:C03039
- Liu K, Chao S, Shaw P, Gong G, Chen C, Tang, T (2002) Monsoon-forced chlorophyll distribution and primary production in the South China Sea: observations and a numerical study. *Deep-Sea Res Part I* 49:1387–1412
- Loftus ME, Seliger HH (1976) A comparative study of primary production and standing crop of phytoplankton in a portion of the upper Chesapeake Bay subsequent to Tropical Storm Agnes. In Davis, J. (ed), *The effects of Tropical Storm Agnes on the Chesapeake Bay Estuarine System*. Chesapeake Res. Consortium Pub. no. 54. The Johns Hopkins University Press, Baltimore, p 509–521
- May RC (1974) Larval mortality in marine fishes and the critical period concept. In: Blaxter JHS (ed) *The early life history of fish*. Springer-Verlag Berlin Heidelberg, New York, p 3–19

- Meehl GA, Stocker TF, Collins WD, Friedlingstein P, Gaye AT, Gregory JM, Kitoh A, Knutti R, Murphy JM, Noda A, Raper SCB, Watterson IG, Weaver AJ, Zhao ZC (2007) Global Climate Projections. In Solomon S, Qin D, Manning M, Chen Z, Marquis M, Averyt KB, Tignor M, Miller HL (eds) *Climate Change 2007: The Physical Science Basis. Contribution of Working Group I to the Fourth Assessment Report of the Intergovernmental Panel on Climate Change*. Cambridge University Press, Cambridge, United Kingdom and New York, NY, USA
- Millero FJ (1996) *Chemical Oceanography*, 2nd ed, CRC Press, London, p 281–305
- Milutinovic S (2011) The influence of input uncertainties on remotely sensed estimates of ocean primary productivity. Doctoral dissertation. The University of Bergen, Norway
- Miyaguchi H, Fujiki T, Kikuchi T, Kuwahara VS, Toda T (2006) Relationship between the bloom of *Noctiluca scintillans* and environmental factors in the coastal waters of Sagami Bay, Japan. *J Plankton Res* 28:313–324
- Møller M, Mykkestad S, Haug A (1975) Alkaline and acid phosphatases of the marine diatoms *Chaetoceros affinis* var. *willei* (Gran) Hustedt and *Skeletonema costatum* (Grev.) Cleve. *J Exp Mar Biol Ecol* 19:217–226
- Morton SL (2000) Phytoplankton ecology and distribution at Manatee Cay, Perican Cays, Belize. *Atoll Res B* 472:125–132
- Mouritsen LT, Richardson Katherine (2003) Vertical microscale patchiness in nano- and microplankton distributions in a stratified estuary. *J Plankton Res* 25:783–797
- Nagaiwa R, Moteki M, Nohno H, Fujita K (2005) Larval and juvenile fish assemblages in surface waters at the mouth of Tokyo Bay. *La mer* 43:97–104 (in Japanese)
- Nagata T, Ogawa T, Frenette JJ, Legendre L, Vincent WF (1996) Uncoupled responses of bacterial and algal production to storm-induced mixing in Lake Biwa. *Jpn J Limnol* 57:533–543
- Nakata N, Mitani I (1979) Occurrence and distribution of eggs and larvae in Kaneda Bay, Kanagawa Prefecture. Report of Kanagawa fisheries experimental station 79-10:81–89 (in Japanese)
- Nakata N (1985) Chapter 10 Sagami Bay IV Biology. In: Coastal Oceanography Research Committee (ed) *Coastal oceanography of Japanese Island* [in Japanese]. Tokai University Press, Tokyo, p 417–427
- Newell RC, Moloney CL, Field JG, Lugas MI, Probyn TA (1988) Nitrogen models at the community level: plant-animal-microbe interactions. In: Blackburn TH, Sørensen J (eds) *Nitrogen cycling in coastal marine environments*. John Wiley & Sons Ltd, New York, p 379–414

- Nishitani G, Miyamura K, Ima I (2003) Trying to cultivation of *Dinophysis caudata* (Dinophyceae) and the appearance of small cells. *Plankton Biol Ecol* 50:31–36
- Ogura F (1975) Further studies on decomposition of dissolved organic matter in coastal seawater. *Mar Biol* 31:101–111
- Paerl HW, Pinckney JL, Fear JM, Peierls BJ (1998) Ecosystem responses to internal and watershed organic matter loading: Consequences for hypoxia in the eutrophying Neuse River Estuary, North Carolina, USA. *Mar Ecol Prog Ser* 166:17–25
- Paerl HW, Bales JD, Ausley LW, Buzzelli CP, Crowder LB, Eby LA, Fear JM, Go M, Peierls BL, Richardson TL, Ramus JS (2001) Ecosystem impacts of three sequential hurricanes (Dennis, Floyd and Irene) on the United States' largest lagoonal estuary, Pamlico Sound, NC. *Proc Natl Acad Sci USA* 98:5655–5660
- Paerl HW, Valdes LM, Adolf JE, Peierls BM, Harding LJ (2006) Anthropogenic and climatic influences on the eutrophication of large estuarine ecosystems. *Limnol Oceanogr* 51:448–462
- Parsons TR, Maita Y, Lalli CM (1984) A manual of chemical and biological methods for seawater analysis. Pergamon Press, Oxford
- Passow U (1991) Species-specific sedimentation and sinking velocities of diatoms. *Mar Biol* 108:449–455
- Price JF (1981) Upper ocean response to a hurricane. *J Phys Oceanogr* 11:153–175
- Probyn TA (1987) Ammonium regeneration by microplankton in an upwelling environment. *Mar Ecol Prog Ser* 37:53–64
- Rees AP, Joint I, Donald KM (1999) Early spring bloom phytoplankton-nutrient dynamics at the Celtic Sea Shelf Edge. *Deep Sea Res II* 46:483–510
- Ridderinkhof H (1992) On the effects of variability in meteorological forcing on the vertical structure of a stratified water column. *Cont Shelf Res* 12:25–36
- Riegman R, Flaming IA, Noordeloos AAM (1998) Sizefractionated uptake of ammonium, nitrate and urea and phytoplankton growth in the North Sea during spring 1994. *Mar Ecol Prog Ser* 173:85–94
- Roden CM, O'Mahony KW (1984) Competition as a mechanism of adaptation to environmental stress in outdoor cultures of marine diatoms. *Mar Ecol Prog Ser* 16:219–227
- Ruiz J, Macías D, Peters F (2004) Turbulence increases the average settling velocity of phytoplankton cells. *P Natl Acad Sci USA* 101:17720–17724
- Sassa C, Kawaguchi K (2006) Occurrence patterns of mesopelagic fish larvae in Sagami Bay, central Japan. *J Oceanogr* 62:143–153

- Satoh F, Hamasaki K, Toda T, Taguchi S (2000) Summer phytoplankton bloom in Manazuru Harbor, Sagami Bay, central Japan. *Plankton Biol Ecol* 47:73–79
- Sellner KG, Sellner SG, Lacouture RV, Magnien RE (2001) Excessive nutrients select for dinoflagellates in the stratified Patapsco River estuary: *Margalef* reigns. *Mar Ecol Prog Ser* 220:93–102
- Shang SL, Li FS, Wu J, Hu C and others (2008) Changes of temperature and bio-optical properties in the South China Sea in response to typhoon Lingling, 2001. *Geophys Res Lett* 35:L10602, doi:10.1029/2008GL033502
- Sherr EB, Sherr BF (2007) Heterotrophic dinoflagellates: a significant component of microzooplankton and major grazers of diatoms in the sea. *Mar Ecol Prog Ser* 352:187–197
- Shiah FK, Chung SW, Kao SJ, Gong GC, Liu KK (2000) Biological and hydrographical responses to tropical cyclones (typhoons) in the continental shelf of the Taiwan Strait. *Cont Shelf Res* 20:2029–2044
- Shibata A, Goto Y, Saito H, Kikuchi T, Toda T, Taguchi S (2006) Comparison of SYBR Green I and SYBR Gold stains for enumerating bacteria and viruses by epifluorescence microscopy. *Aquat Microb Ecol* 43:223–231
- Shuman FR, Lorenzen CJ (1975) Quantitative degradation of chlorophyll by a marine herbivore. *Limnol Oceanogr* 20:580–586
- Sigaud TCS, Aïdar E (1993) Salinity and temperature effects on the growth and chlorophyll-a content of some planktonic algae. *Braz J Oceanogr* 41:95–103
- Smayda TJ (1997) Harmful algal blooms: Their ecophysiology and general relevance to phytoplankton blooms in the sea. *Limnol Oceanogr* 42:1137–1153
- Smayda TJ, Trainer VL (2010) Dinoflagellate blooms in upwelling systems: Seeding, variability, and contrasts with diatom bloom behaviour. *Prog Oceanogr* 85:92–107
- Smith PE, Lasker R (1978) Position of larval fish in an ecosystem. *Rapp P-v Réun Cons Int Explor Mer* 173:77–84
- Smith RC (1981) Remote sensing and depth distribution of ocean chlorophyll. *Mar Ecol Prog Ser* 5:359–361
- Steward GF, Azam F (1999) Bromodeoxyuridine as an alternative to H-3-thymidine for measuring bacterial productivity in aquatic samples. *Aquat Microb Ecol* 19:57–66
- Strathmann RR (1967) Estimating the organic content of phytoplankton from cell volume or plasma volume. *Limnol Oceanogr* 12:411–418
- Strom SL, Morello TA (1998) Comparative growth rates and yields of ciliates and heterotrophic dinoflagellates. *J Plankton Res* 20:571–584

- Subrahmanyam B, Rao KH, Rao NS, Murty VSN, Sharp RJ (2002) Influence of a tropical cyclone on chlorophyll a concentration in the Arabian Sea. *Geophys Res Lett* 29: 2065, doi:10.1029/2002GL015892
- Sugawara T, Hamasaki K, Toda T, Kikuchi T, Taguchi S (2003) Response of natural phytoplankton assemblages to solar ultraviolet radiation (UV-B) in the coastal water, Japan. *Hydrobiologia* 493:17–26
- Sun L, Yang Y, Xian T, Lu Z, Fu Y (2010) Strong enhancement of chlorophyll a concentration by a weak typhoon. *Mar Ecol Prog Ser* 404:39–50
- Suzuki R, Ishimaru T (1990) An improved method of the determination of phytoplankton chlorophyll using N,N-Dimethylformamide. *J Oceanogr* 46:190–194
- Tanaka O (1953) The pelagic copepods of the Izu region. *Pub Seto Mar Biol Lab* 1:126–129
- Tang S, Chen C, Zhan H, Zhang J, Yang J (2008) An appraisal of surface chlorophyll estimation by satellite remote sensing in the South China Sea. *Int J Remote Sens* 29:6217–6226
- Tilman D, Kiesling R, Sterner R, Kilham SS, Johnson FA (1986) Green, bluegreen and diatom algae: Taxonomic differences in competitive ability for phosphorus, silicon and nitrogen. *Arch Hydrobiol* 106:473–485
- Tozzi S, Schofield O, Falkowski P (2004) Historical climate change and ocean turbulence as selective agents for two key phytoplankton functional groups. *Mar Ecol Prog Ser* 274:123–132
- Tupas L, Koike I (1991) Simultaneous uptake and regeneration of ammonium by mixed assemblages of heterotrophic marine bacteria. *Mar Ecol Prog Ser* 70:273–282
- Turner RE, Rabalais NN, Zhang ZN (1990) Phytoplankton biomass, production and growth limitations on the Huanghe (Yellow River) continental shelf. *Cont Shelf Res* 10:545–571
- Turner JT (2002) Zooplankton fecal pellets, marine snow and sinking phytoplankton blooms. *Aquat Microb Ecol* 27:57–102
- Valdes-Weaver LM, Piehler MF, Pinckney JL, Howe KE, Rossignol K, Paerl HW (2006) Long-term temporal and spatial trends in phytoplankton biomass and class-level taxonomic composition in the hydrologically variable Neuse–Pamlico estuarine continuum, North Carolina, U.S.A. *Limnol Oceanogr* 51:1410–1420
- Vargas CA, Martínez RA, Cuevas LA, Pavez MA, Cartes C, González HE, Escribano R, Daneri G (2007) The relative importance of microbial and classical food webs in a highly productive coastal upwelling area. *Limnol Oceanogr* 52:1495–1510
- Tsuchiya K, Yoshiki T, Nakajima R, Miyaguchi H, Kuwahara VS, Taguchi S, Kikuchi T, Toda T (2013a) Typhoon-driven variations in primary production and phytoplankton assemblages in

- Sagami Bay, Japan: A case study of typhoon *Mawar* (T0511). *Plankton Benthos Res* 8:74-87
- Tsuchiya K, Kuwahara VS, Yoshiki T, Nakajima R, Miyaguchi H, Kumekawa N, Kikuchi T, Toda T (2013b) Phytoplankton community response and succession in relation to typhoon passages in the coastal waters of Japan. *J Plankton Res* doi:10.1093/plankt/fbt127
- Tsunogai S, Noriki S (1988) Biological process and chemical substance in ocean. In: Nishimura M (ed) *Ocean chemistry*, Sangyo-Tosho, Tokyo, p 101–138 (in Japanese)
- Walker ND, Leben RR, Balasubramanian S (2005) Hurricane-forced upwelling and chlorophyll a enhancement within cold-core cyclones in the Gulf of Mexico. *Geophys Res Lett* 32:L18610, doi:10.1029/2005GL023716
- Walsby AE (1992) The gas vesicles and buoyancy of *Trichodesmium*. In: Carpenter EJ, Capone DG, Rueter JG (eds) *Marine Pelagic Cyanobacteria: Trichodesmium and other Diazotrophs*. Kluwer Academic Publishers, MA, p 141–161
- Webber DF, Webber MK, Roff JC (1992) Effects of flood waters on the planktonic community of the Hellshire Coast, Southeast Jamaica. *Biotropica* 24:362–374
- Webster PJ, Holland GJ, Curry JA, Chang HR (2005) Changes in tropical cyclone number, duration, and intensity in a warming environment. *Science* 309:1844–1846
- Welschmeyer NA, Copping AE, Vernet M, Lorenzen CJ (1984) Diel fluctuation in zooplankton grazing rate as determined from the downward vertical flux of pheopigments. *Mar Biol* 83:263–270
- Welschmeyer NA, Lorenzen CJ (1985) Chlorophyll budgets: Zooplankton grazing and phytoplankton growth in a temperate fjord and the Central Pacific Gyres. *Limnol Oceanogr* 30:1–21
- Wetz MS, Paerl HW (2008) Estuarine phytoplankton responses to hurricanes and tropical storms with different characteristics (trajectory, rainfall, winds). *Estuar Coast* 31:419–429
- Williams PJLeB (1998) The balance of plankton respiration and photosynthesis in the open oceans. *Nature* 394:55–57
- Yamada Y, Oouchi K, Satoh M, Tomita H, Yanase W (2010) Projection of changes in tropical cyclone activity and cloud height due to greenhouse warming: Global cloud-system-resolving approach. *Geophys Res Lett* 37:L07709, doi:10.1029/2010GL042518
- Yasuki N, Suzuki K, Tsuda A (2013) Responses of lower trophic-level organisms to typhoon passage on the outer shelf of the East China Sea: an incubation experiment. *Biogeosciences Discuss* 10:6605–6635
- Zeeman IS (1985) The effects of tropical storm Dennis on coastal phytoplankton. *Estuar Coast Shelf Sci* 20:403–418

- Zhao H, Tang D, Wang Y (2008) Comparison of phytoplankton blooms triggered by two typhoons with different intensities and translation speeds in the South China Sea. *Mar Ecol Prog Ser* 365:57–65
- Zheng MG, Tang D (2007) Offshore and nearshore chlorophyll increases induced by typhoon winds and subsequent terrestrial rainwater runoff. *Mar Ecol Prog Ser* 333:61–74
- Zhou L, Tan Y, Huan L, Huan J, Liu H, Lian X (2011) Phytoplankton growth and microzooplankton grazing in the continental shelf area of northeastern South China Sea after Typhoon Fengshen. *Cont Shelf Res* 31:1663–1671